A Study on Restoration of Fatigue Damage in Stainless Steel by High-density Pulse Current

Yongpeng TANG

A Study on Restoration of Fatigue Damage in Stainless Steel by High-density Pulse Current

Department of Mechanical Science and Engineering

Nagoya University

Yongpeng TANG

Contents

Chapter 1 Introduction

1.1 Fatigue fracture

Fatigue fracture is generally considered to be the most serious type of fracture in machinery parts because fatigue fracture can occur in normal service, without excessive overloads, and under normal operating conditions. In 2002, a placing boom on a truck-mounted concrete pump suddenly broke down at a condominium construction site in Japan. One worker who was engaged in smoothing the concrete surface was killed by the falling placing boom. The cause of the accident was investigated intensively. After macro- and micro-observations of the fracture surface were conducted, considering the broken concrete pump had been used for 12 years, it was implied that the fracture of the boom might be attributed to fatigue fracture.

Fatigue fractures occur any time in the society. Fatigue fractures are serious due to the insidious, which are frequently sneaky and can occur without warning anything to be amiss. Obviously, if service is abnormal as a result of excessive overloading, corrosive environments, or other conditions, the possibility of fatigue fracture is increased. Fatigue of material refers to the changes in properties resulting from the application of cyclic loads. Hence, the importance of fatigue is evident.

1.1.1 The definition of fatigue

Fatigue occurs when a material is subjected to repeated loading and unloading. In materials science, fatigue is the progressive and localized structural damage that occurs when a material is subjected to cyclic loading. The nominal maximum stress values are less than the ultimate tensile stress limit, and may be below the yield stress limit of the material. If the loads are above a certain threshold, microscopic cracks will begin to form at the stress concentrators. A descriptive definition of fatigue is found in the report entitled General Principles for Fatigue Testing of Metals which was published in 1964 by the International Organization for Standardization in Geneva [1]. Fatigue is defined as a term which applies to changes in properties which can occur in a metallic material due to the repeated application of stresses or strains, although usually this term applies specially to those changes which lead to cracking of failure. This description is also generally valid for the fatigue of nonmetallic materials.

The research on the deformation and fracture of materials by fatigue dates back to the nineteenth century. It is needed to note that the first systematical research on fatigue life was conducted by Wohler [2] in 1870 on the fatigue life of the chassis of train cars. Wohler investigated the material behavior under a constant loading amplitude. The behavior under specific loading spectra and for different materials has been investigated afterwards by experiments and simulations.

Fatigue damage is an important phenomenon associated with the degradation of the mechanical properties of a material due to cyclic loading and represents a fundamental aspect of the overall evaluation of the remaining life of machine parts and components in service. Approximate 80% of failure accidents in mechanical structures are caused due to the fatigue fracture, as shown in Fig. 1-1. The relative cost of these failures caused an amount of waste of the source. Consequently, it also has an effect to decrease the environmental loading from the viewpoint of reducing consumption of lifecycle energy of metal materials. For these reasons, it is essential to improve the long-time durability and reliability of material to extend fatigue lifetime of material.

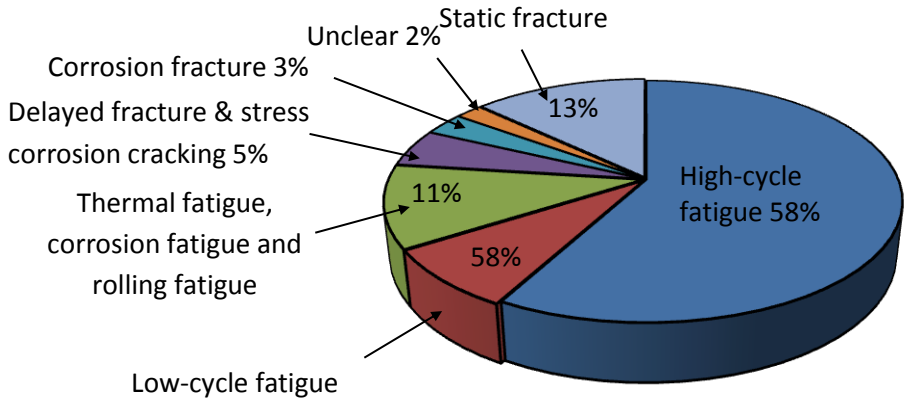

Fig. 1-1 Causes of failure accident in metal materials.

When a material is subjected to a cyclic loading, a fatigue crack nucleus can be initiated on a microscopically small scale, then followed by a crack growth to a macroscopic size, and finally creating material failure in the last cycle of the fatigue life [3]. After a microcrack has been nucleated, crack growth can still be slow in

erratic process, due to the effects of the microstructures (e.g. grain boundaries). Thus, the fatigue life is usually split into a crack initiation period and a crack propagation period. Various steps in the fatigue life are indicated in Fig. 1-2 [4]. The initiation period is supposed to include some microcrack growth, but the fatigue cracks are still too small to be visible. In the second period, the crack is growing until complete failure. Microscopic investigations have shown that fatigue crack nuclei start as invisible microcracks in slip bands [4]. Differentiating between the two periods is of great importance because several surface conditions can affect the crack initiation period, but have a negligible influence on the crack growth period. It should be noted here that fatigue prediction methods are different for the two periods. The stress concentration factor K_t is the important parameter for the prediction of crack initiation. The stress intensity factor K is used for the prediction of crack propagation.

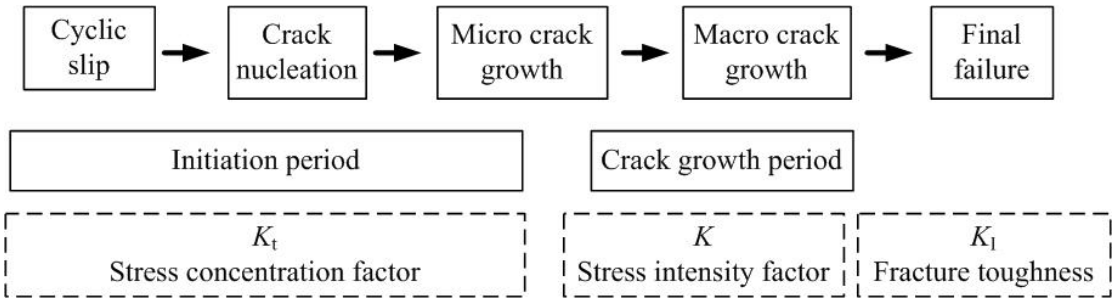

Fig. 1-2 Causes of failure accident in metal materials.

1.1.2 The physics of fatigue crack initiation

Understanding of the fatigue mechanism is essential for considering various technical

conditions which affect fatigue life, such as the material surface quality, residual stress, and environmental influence [5]. This knowledge is essential for the analysis of fatigue properties of an engineering structure. Fatigue prediction can only be evaluated when fatigue is understood as a crack initiation process followed by a crack growth period. For this reason, understanding of the physics of fatigue crack initiation is a prerequisite for this study.

During fatigue cyclic loading, slip irreversibility and accumulation exist in a material. At the defect level, slip irreversibilities are a result of dislocations: annihilating, cross-slipping, penetrating precipitates, transmitting through grain boundaries, and piling-up. These slip irreversibilities are the early signs of damage during fatigue cyclic loading. To accommodate the irreversible slipping processes, the dislocations subsequently form low-energy, stable structures and increasing dislocation density during cyclic forward and reverse loading. The result leads to strain localization in a small region within the materials, i.e. persistent slip bands (PSBs) and dislocation cells and bundles.

Strain localization is a precursor to crack initiation. It is important to focus on experimental observations of strain localization. The classical fatigue damage with respect to localization of strain leads to fatigue crack initiation. Strain accumulates primarily through dislocation motion. Upon forward and reverse loading, slip moves in distinct paths within each cycle, in which the slip processes are not fully reversible.

Slip irreversibilities and the arrangements of dislocations in low energy configurations define the unique nature of fatigue and the existence of PSBs. PSBs

represent a critical mechanism of fatigue crack initiation in metallic materials. Therefore, due to their importance in the fatigue loading process, it is necessary to carry out analysis of both slip irreversibilities and low energy configuration defect structures. This fundamental understanding is necessary to study persistent slip bands in metals and alloys including the appropriate characterization, theory, and modeling. From this fundamental knowledge both micromechanical and crystal plasticity models can be used to predict crack initiation.

1.2 Effect of electric current on fatigue behavior

In the past fifty years, the applications of electric current, as an instantaneous high energy input method, have been widely developed in the fields of materials science and engineering. It has been found that the application of electric current can have significant effects on the improvement of mechanical properties of metals, such as plastic deformation, recrystallization and fatigue behavior [6-12].

Moreover, some studies have proposed that electric current has an effect on the fatigue behavior. Karpenko et al. [13] found that the low cycle fatigue life of low carbon steel increased with the application of continuous pulses. Conrad et al. [14-16] demonstrated that current pulses increased the fatigue life of copper. Additionally, Hosoi et al. [17] observed a temporary delay effect on crack propagation by healing a fatigue crack with a controlled high-density electric current field. S.G. Qiao et al. [18] found that the fatigue damage of aluminum alloys induced by tensile test can be partly

healed by electropulsing and recrystallization phenomenon. H.Q Lin et al. [19] analyzed the effects of pulse current stimulation on the thermal-fatigue-crack propagation and the delaying of crack propagation. Although previous studies have increased the fatigue life of metallic materials by applying an electric current, the effect of electric current on the crack initiation has not been investigated till now.

Xiao et al. [20] studied the effect of current pulsing on persistent slip bands in fatigued copper single crystals. They found that the treatment by electropulsing made the PSBs vanish locally and proposed that the locally vanishing of the PSBs may decrease the possibility of fatigue crack initiation. However, there no evidence was shown in their report. Generally, the PSBs play an important role in the fatigue crack initiation [1]. These interfaces between the PSBs and the matrix serve as preferential sites for fatigue crack initiation. Therefore, the effect of the healing of slip bands on the delaying of fatigue crack initiation based on the application of electric current was evaluated in this study. In addition, Xiao et al. [20] thought that the locally vanishing of the PSBs is due to the effect of thermal compressive stress on dislocation induced by electropulsing. However, the effect of electron wind force may also affect the motion of dislocation which has been reported in Reference [21-25]. Hence, the mechanism of dislocation restoration by the application of electric current was studied in detail in this research. Moreover, strain accumulates primarily through dislocation motion and accumulation during fatigue loading process [26]. The strain hardening occurs with the increase of strain accumulation [27, 28]. However, the effect of electric current on the strain and hardness has not been reported. Hence, the

evaluation of recovered residual strain and strain hardening based on the application of electric current were studied in this research.

During the fatigue loading process, the primary emphasis is that the fatigue crack initiation is caused by accumulation of micro-defects, such as dislocations [29-31] in the material. Therefore, Konovalov et al. [32-34] studied the evolution of dislocation substructures in fatigue loaded stainless steel by electropulsing. They found that dislocation substructures were changed by the electropulsing treatment. They concluded that the change of dislocation substructures was the reason for the improvement of fatigue lifetime. He et al. [35] also observed the effect of electropulsing on decreasing dislocation density. However, the quantitative evaluation of the changed dislocation density due to the effect of applied electric current has been few studied up to now. Therefore, effect of electric current on the dislocation density was quantitatively measured. Furthermore, the relationship between the dislocation density and the fatigue crack initiation was established proposed based the fatigue crack initiation model.

Through the study of the effect of electric current on fatigue behavior, it was found the effect of electric current can improve the fatigue strengthen. However, the effect of electric current on fatigue damage is necessary to investigate in more detail. It is essential to clarify the mechanism of the effect of electric current. Therefore, it can be concluded that the delaying fatigue crack initiation due the electric current is an important way to extend the fatigue lifetime. In the microstructure, it is important to elucidate the evolution of dislocation structure due to the effect of electric current.

This is the basis to build the relationship between the dislocation density and the delaying fatigue crack initiation.

1.3 Research Contents

Fatigue is a principal mode of damage in accidents involving failure of metallic equipment. Thus, the prevention of fatigue fractures in metal materials is an effective way to prolong their service life. To improve fatigue strength, various surface engineering techniques have been developed, such as high-frequency quenching, carburizing, nitriding and shot peening. Pretreatment on the material surface is effective for the suppression of crack initiation. However, once a fatigue crack is initiated during service, the reliability of the structure is severely impaired and the mentioned methods are inefficient in delaying the progress of fatigue failure. The durability and reliability of material have been seriously destroyed. Therefore, to improve long-term durability and reliability of material is a critical issue to extend the safe service life of metal material.

Hence, the ability to heal the fatigue damage caused by fatigue crack initiation during service and recover the fatigue strength at the healed zone would be very desirable in terms of structural integrity. The primary emphasis is relating the fatigue crack initiation to the microstructure of the material.

Therefore, the aim of this study is to give an effective way to extend the fatigue lifetime of material by high-density pulse current (HDPC). The development of this

technique will bring a dramatic improvement in the long-term reliability of structures, with the effect of reducing their maintenance costs and the environmental load.

In this study, the effect of HDPC on the restoration of fatigue damage in stainless steel is investigated. The healing effect on the fatigue crack initiation is evaluated by a curve of the cyclic stress versus the cycle to failure (*S*-*N*). Furthermore, the timing effect of applied current on fatigue crack initiation is investigated experimentally.

To elucidate the effect of HDPC on the delaying fatigue crack initiation, the mechanism of the delaying effect was investigated, from the viewpoint of the physics. In addition, because the interfaces between the PSBs and the matrix serve as preferential sites for fatigue crack initiation, the relief evolution of slip bands was quantitatively measured by atomic force microscope (AFM). On the other hand, when fatigue cracks emanate from notches, the initial growth of the nascent cracks can be significantly influenced by the plastic deformation occurring at the root of the notch. Thus, the character of plastic strain and Vickers microhardness (HV) at the root of the notch was investigated. The mechanism of delaying fatigue crack initiation was analyzed from the viewpoint of the restoration of fatigue damage.

Furthermore, it is necessary to investigate the effect of applied HDPC on the damaged microstructure of material. In the microstructure, the evolution of the dislocation structure was observed by transmission electron microscopy (TEM). To quantitatively evaluate the effect of HDPC on the dislocation structure, the dislocation density was measured by the section line method. The dislocation structures were also investigated in order to examine the effect of HDPC on fatigue damage recovery.

To build the relationship between the delaying fatigue crack initiation and the dislocation structure, the model of fatigue damage parameter was proposed based on the fatigue crack initiation model in which the accumulation of the dislocation density was considered. The proposed model was evaluated against experimental data and the predication of the delaying effect on the fatigue crack initiation was demonstrated.

1.4 Thesis Organization

This dissertation aims to establish a method to delay the fatigue failure. In this study, the application of HDPC was carried out to restore the fatigue damage. Furthermore, the mechanism of healing effect is discussed. The delaying effect of the crack initiation due to the application of HDPC is evaluated by the fatigue crack initiation model in which the accumulation of the dislocation density was considered.

Chapter 1 is the introduction of the research background, such as the fatigue fracture and fatigue crack initiation. Furthermore, the motivation of this study was represented. Meanwhile, the method to delay the fatigue fracture was reviewed. The application of HDPC on the mechanical properties of metals was discussed.

Chapter 2 introduces the experimental material, equipment, condition, procedure, the preparation of TEM sample. The experimental method which is used to evaluate the healing effect due to the application of HDPC was also described.

In chapter 3 we represent the results of HDPC on fatigue behavior. To evaluate the healing effect on delaying fatigue crack initiation, the fatigue crack initiation was

evaluated by a curve of the cyclic stress versus the cycle to failure (*S*-*N*), with and without the application of HDPC. Furthermore, the timing effect of applied HDPC was investigated. The healing of fatigue damage was addressed to explain the mechanism of delaying effect. The relief evolution of slip bands was quantitatively measured by AFM, and the distribution of residual strain at the root of the notch was observed by the digital image correction (DIC) method. Additionally, the strain hardening around the notch tip was evaluated by the HV measurement.

Chapter 4 describes the dislocation structures before and after the application of HDPC. Furthermore, the dislocation densities before and after the application of HDPC were compared. The effect of HDPC on the dislocation structures was analyzed in order to explain the physical mechanism of healing effect.

In chapter 5, the delaying effect on the crack initiation due to the application of HDPC was evaluated by the fatigue crack initiation model in which the accumulation of the dislocation density was considered. The relationship between the delaying fatigue crack initiation and the dislocation density was established. The model of fatigue damage parameter was proposed based on the fatigue crack initiation model. The proposed model was evaluated against experimental data.

Chapter 6 is the conclusion of this thesis. The important results were summarized.

References:

[1] S. Suresh, Fatigue of materials, Cambridge University Press, (1991).

[2] R.I. Stephens, A. Fatemi, R.R. Stephens, H.O. Fuchs, Metal fatigue in engineering, Wiley Interscience, (2001).

[3] D.S. Michael, The physics of fatigue crack initiation, Int. J. Fatigue, 57 (2013) 58-72.

[4] J. Schijve, Fatigue of structures and materials, Springer, Second Edition (2008).

[5] J.A. Ewing, J.C. Humfrey, The fracture of metals under repeated alternations of stress, Phil. Trans. Roy. Soc., A, 200 (1903) 241–250.

[6] Y.Z. Zhou, R.S. Qin, S.H. Xiao, Reversing effect electropulsing on damage of 1045 steel, J. Mater. Res., 15 (2000) 1056-1061.

[7] Z.Y. Zhou, Z. You, G.H. He, B.L. Zhou, The healing of quenched crack in 1045 steel under electropulsing, J. Mater. Res., 16 (2000) 17-19.

[8] Y.Z. Zhou, J.D. Guo, M. Gao, G.H. He, Crack healing in a steel by using electropulsing technique, Mater. Lett., 58 (2004) 1732-1736.

[9] H. Song, Z.J. Wang, T.J. Gao, Effect of high density electropulsing treatment on formability of TC4 titanium alloy sheet, Trans. Nonferrous Met. Soc. China, 17 (2007) 87-92.

[10] Z.J. Wang, H. Song, Effect of high density electropulsing on microstructure and mechanical properties of cold rolled TA15 titanium alloy sheet, J. Alloys Compd.,

470 (2009) 522-530.

[11] Z.J. Wang, H. Song, Effect of electropulsing on anisotropy behavior of cold rolled commercially pure titanium sheet, Trans. Nonferrous Met. Soc. China, 19 (2009) 409-413.

[12] H. Song, Z.J. Wang, Microcrack healing and local recrystallization in predeformed sheet by high density electropulsing, Mater. Sci. Eng. A, 490 (2008) 1-6.

[13] G.V. Karpenko, O.A. Kuzin, V.I. Tkachev, V.P. Rudenko, The effect of electric current on the low-cycle fatigue of steels, Sov. Phys. Dokl., 21 (1976) 159-160.

[14] H. Conrad, J. White, W.D. Cao, X.P. Lu, A.F. Sprecher, Effect of electric current pulses on fatigue characteristics of polycrystalline copper, Mater. Sci. Eng. A, 145 (1991) 1-12.

[15] W.D. Cao, H. Conrad, On the effect of persistent slip band (PSBs) parameters on fatigue life, Fatigue Fract. Eng. Mater. Struct., 15 (1992) 573-531.

[16] Z.H. Lai, C.X. Ma, H. Conrad, Cyclic softening by high density electric current pulses during low cycle fatigue of alpha-titanium, Scripta Mett. Mater., 15 (1992) 527-532.

[17] A. Hosoi, T. Nagohama, Y. Ju, Fatigue crack healing by a controlled high density electric current field, Mater. Sci. Eng. A, 533 (2012) 38-42.

[18] S.R. Qiao, Y.L. Li, Y. Li, C.Y. Zhang, Damage healing of aluminum alloys by D.C. electropulsing and evaluation by resistance, Rare Metal. Mater. Eng., 38 (2009) 570-573.

[19] H.Q. Lin, Y.G. Zhao, Z.M. Gao, L.G. Han, Effects of pulse current stimulation on the thermal fatigue crack propagation behavior of CHWD steel, Mater. Sci. Eng. A, 478 (2008) 93-100.

[20] S.H. Xiao, et al., The effect of high current pulsing on persistent slip bands in fatigued copper single crystals, Mater. Sci. Eng. A, 332 (2002) 351-355.

[21] A.F. Sprecher, S.L. Mannan, H. Conrad, On the mechanisms for the electroplastic effect in metals, Acta Metall. Mater., 34 (1986) 1145-1162.

[22] S.W. Nam, et al., Electrical win force-driven and dislocation template amorphization in phase-change nanowires, Science, 336 (2012) 1561-1566.

[23] K.M. Klimov, G.O. Shnyrev, I.I. Novikov, Electroplasticity of metals, Soviet Phys. Dokl., 19 (1975) 787-788.

[24] V. Ya. Kravchenko, Effect of directed electron beam on moving dislocations, Soviet Phys. Jetp, 24 (1967) 1135-1142.

[25] A.M. Roshchupkin, V.E. Miloshenko, V.E. Kalinin, Effect of electrons on the motion of dislocations in metals, Soviet Phys. Solid St., 21 (1979) 435-438.

[26] D. Ye, Z. Wang, An approach to investigate pre-nucleation fatigue damage of cyclically loaded metals using Vickers microhardness tests, Int. J. Fatigue, 23 (2001) 85-91.

[27] D.Y. Ye, D.J. Wang, P. An, Characteristics of the change in the surface microhardness during high cycle fatigue damage, Mater. Chem. Phys., 44 (1996) 179-181.

[28] D.Y. Ye, X.Y. Tong, L.J. Yao, X.X. Yin, Fatigue hardening/softening behavior

investigated through Vickers microhardness measurement during high-cycle fatigue, Mater. Chem. Phys., 56 (1998) 199-204.

[29] H. Mughrabi, Dislocation wall and cell structures and long-range internal stresses in deformed metal crystals, Acta Mater., 31 (1983) 1367-1379.

[30] J.R. Hancock, J.C. Grosskreutz, Mechanisms of fatigue hardening in copper single crystals, Acta Mater., 17 (1969) 77-97.

[31] C. Laird, P. Charsley, H. Mughrabi, Low-energy dislocation structures produced by cyclic deformation, Mater. Sci. Eng. A, 81 (1986) 433-450.

[32] S.V. Konovalov, A.A. Atroshkina, Y.F. Ivanov, V.E. Gromov, Evolution of dislocation substructures in fatigue loaded and failed stainless steel with the intermediate electropulsing treatment, Mater. Sci. Eng. A, 527 (2010) 3040-3043.

[33] O.V. Sosnin, et al., Control of austenite steel fatigue strength, Int. J. Fatigue, 27 (2005) 1186-1191.

[34] O.V. Sosnin, et al., The structural-phase state changes under the pulse current influence on the fatigue loaded steel, Int. J. Fatigue, 27 (2005) 1221-1226.

[35] G.H. He, et al., Investigation of thermal expansion measurement of brass strip H62 after high current density electropulsing by the CCD technique, Mater. Sci. Eng. A, 292 (2000) 183-188.

Chapter 2 Experimental Approach

2.1 Experimental material

The SUS316 stainless steel is an austenitic chromium nickel stainless steel containing molybdenum. The chemical composition is shown in Table 2-1. The molybdenum gives SUS316 better overall corrosion resistant properties, particularly higher resistance to pitting and crevice corrosion in chloride environments, and provides increased strength at elevated temperatures.

Table 2-1 Chemical composition of the stainless steel SUS316 (wt.%)

C	Si	Mn	P	S	Ni	Cr	Mo	Fe
0.05	0.43	1.3	0.028	0.03	10.1	17.09	2.01	Balance

The mechanical properties of SUS316 are shown in Table 2-2. It has excellent forming characteristics. It is readily formed into a variety of parts for applications in the industrial, architectural, and transportation fields. The SUS316 stainless steel also has outstanding welding characteristics. The austenitic structure also gives SUS316 excellent toughness. The SUS316 stainless steel has a very broad of application within industry due to its corrosion-resistant properties. Most of the structural

applications occur in the chemical and power engineering industries. These applications include an extremely diversified range of uses. Typical uses include furnace parts, heat exchangers, jet engine parts, chemical equipment, parts exposed to marine atmospheres and tubing. Especially, the nuclear energy sector makes a lot of use of stainless steel. The SUS316 stainless steel was selected as the primary candidate material for the mercury container vessel of the spallation neutron source [1]. It was widely used in the nuclear industry. Core and secondary parts of most reactor types in service today are built from the stainless steel, as are reprocessing plants and research reactors. The nuclear decommissioning and waste storage industry are also prime users of high quality stainless for different types of transport or storage canisters and boxes. The reliability and durability of the structure depend on the strength of materials. Therefore, it is essential to find an effective way to improve the fatigue strength of stainless steel.

Table 2-2 Mechanical properties of SUS316

Yield stress [MPa]	Tensile strength [MPa]	Elongation [%]	Reduction of area [%]	Young's modulus [GPa]	Poisson's ratio	Hardness [HBW]
300	573	47	76	197	0.29	161

Hence, the SUS316 austenite stainless steel was used as the experimental material in this study. The SUS316 austenite stainless steel is one of the most classical stainless steels. Metallographic observations showed that the average linear intercept grain size

is approximate 75 μm in the initial state as shown in Fig. 2-1.

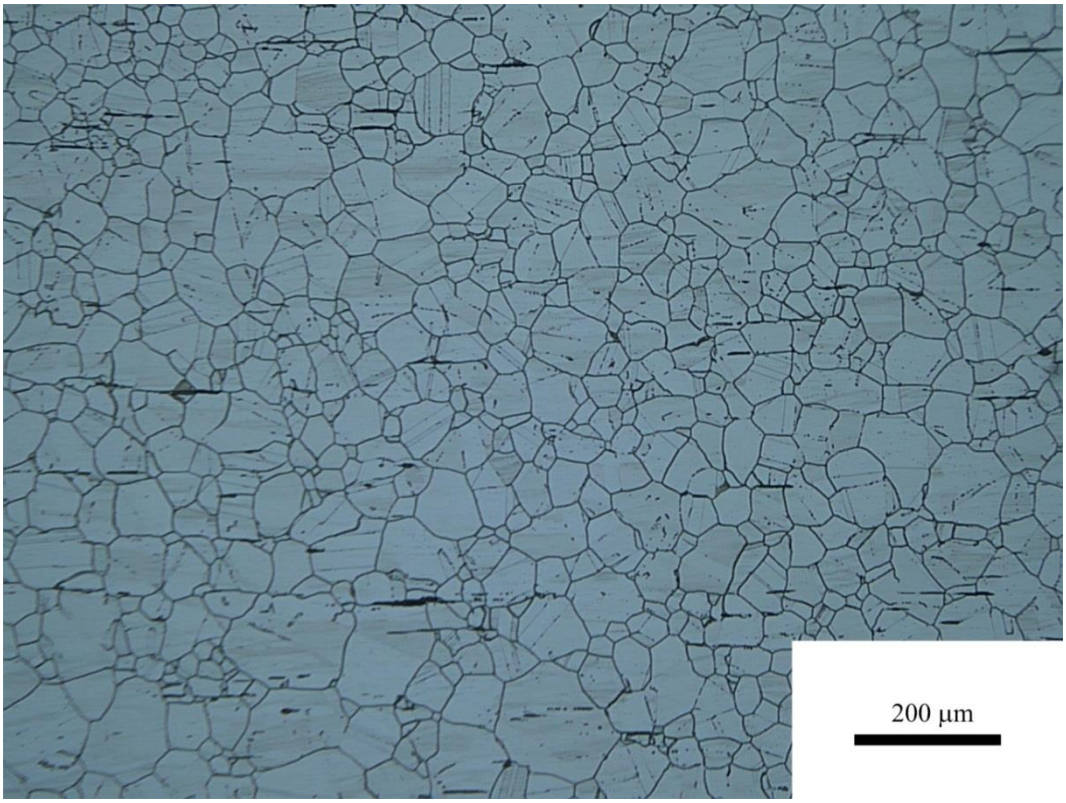

Fig. 2-1 Optical micrograph of the microstructure of SUS316 in original state.

2.2 Fatigue Experiments

2.2.1 Preparation of specimen

According to the ASTM standard test method for notch fatigue test, a notch was introduced in the dumbbell-shaped specimen at the center of one side, as shown in Fig. 2-2. The length and root radius of the notch were 2 mm and 0.15 mm, respectively.

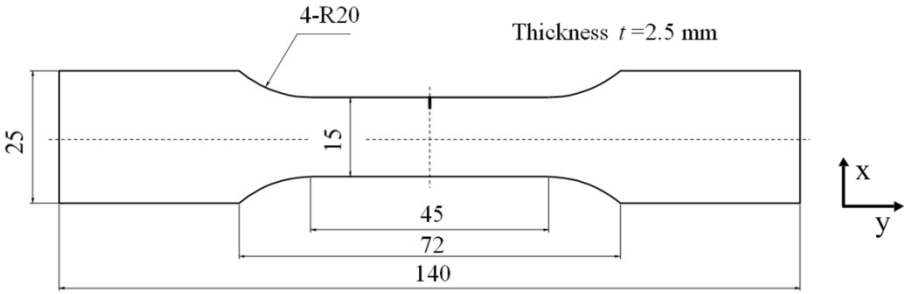

Fig. 2-2 Schematic of specimen (unit: mm).

The theoretical stress concentration factor, K_t, is defined as the ratio between the peak stress at the root of the notch and the nominal stress which would be present if a stress concentration did not occur. The stress concentration factor, K_t, is the important parameter for the prediction of fatigue crack initiation. The geometric parameters to determine the stress concentration factor are shown in Fig. 2-3. The stress concentration factor K_t was obtained by the following Eq. 2-1 [2].

$$K_t = C_1 + C_2\left(\frac{l}{H}\right) + C_3\left(\frac{l}{H}\right)^2 + C_4\left(\frac{l}{H}\right)^3, \qquad (2\text{-}1)$$

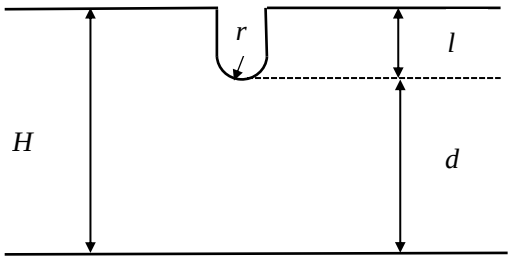

Fig. 2-3 The geometric parameters to determine the stress concentration factors.

where, r=0.15 mm is the radius of the notch tip, l=2 mm the length of the notch, H=15 mm the width of the specimen, and d=13 mm the ligament length.

When $2.0 \leq \frac{l}{r} \geq 20.0$,

$$C_1 = 0.953 + 2.136\sqrt{\frac{l}{r}} - 0.005\frac{l}{r}, \quad (2\text{-}2)$$

$$C_2 = -3.255 - 6.281\sqrt{\frac{l}{r}} + 0.068\frac{l}{r}, \quad (2\text{-}3)$$

$$C_3 = 8.203 + 6.893\sqrt{\frac{l}{r}} + 0.064\frac{l}{r}, \quad (2\text{-}4)$$

$$C_4 = -4.851 - 2.793\sqrt{\frac{l}{r}} - 0.128\frac{l}{r}. \quad (2\text{-}5)$$

Fig. 2-4 The mirror-surface of a specimen after mechanical polishing.

Thus, according to Eqs. 2-1 - 2-5 [2], the stress concentration factor was K_t=5.8. The specimens were prepared by wire cutting, and the specimens were treated with a stress relief annealing at 1173 K for 10 min to remove the residual stresses caused by the machining process.

Following annealing treatment, the surface of the specimen was polished with emery papers with grain numbers of #400, #800, #1200, #1500 and #2000, respectively. Then, the specimen was polished to a mirror surface by buffing with alumina powder with a grain diameter of 1.0 μm, 0.30 μm and 0.05 μm, respectively. The final polishing was with colloidal silica suspension (OP-U suspension). The mirror-surface of specimen (Fig. 2-4) was obtained after the mechanical polishing on the polishing machine (MARUMOTO STRUERS S5629), as shown in Fig. 2-5.

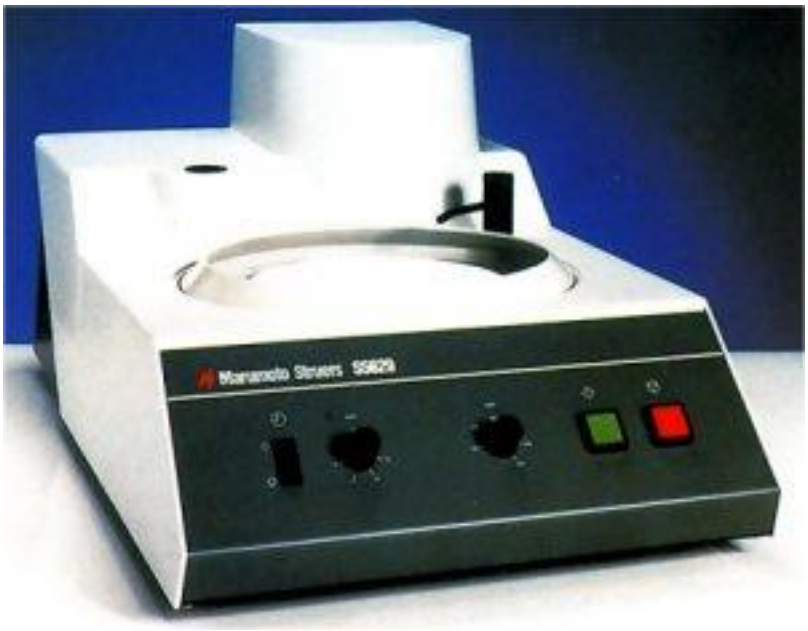

Fig. 2-5 The mechanical polishing machine.

2.2.2 Fatigue test

In this study, to evaluate the healing effect due to the application of HDPC on fatigue damage, the tensile fatigue tests were carried out. Tensile fatigue tests under a controlled load with a hydraulic-driven testing machine (SHIMADAZU 4830) were carried out at room temperature in laboratory air, as shown in Fig. 2-6. The fatigue tests were conducted at a stress ratio of R=0.05 and a frequency of f=10 Hz. The process of microcrack initiating was monitored by optical microscope (KEYENCE VH-2100R) in real time as shown in Fig. 2-7.

Fig. 2-6 The hydraulic-driven testing machine.

The specimens were separated into two groups after a certain cyclic loading. One group underwent the application of HDPC, whereas the other group did not. The specimen was then removed from the fatigue testing machine. After the application of HDPC, the specimen was reset on the fatigue testing machine and the fatigue testing was continued until the occurrence of fatigue crack initiation.

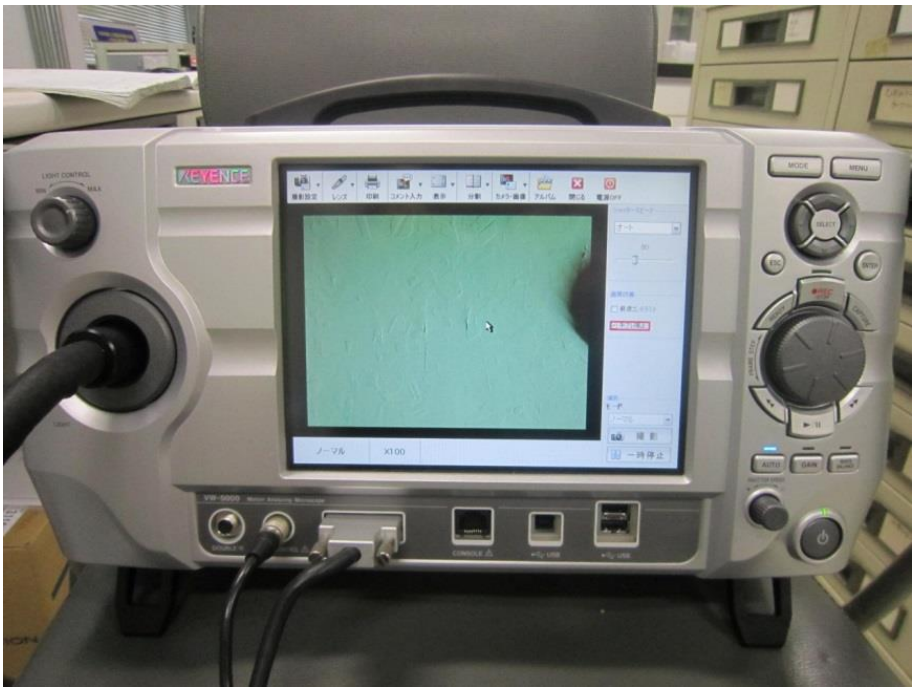

Fig. 2-7 The fatigue test was monitored by optical microscope in real time.

2.3 Application of high-density pulse current

2.3.1 Equipment of the pulse current

The high-density pulse current was applied after the fatigue tests using a

transistor-type power source (MIYACHI MDA-8000B). Chromium copper with a 5 mm diameter was used as the electrodes. The change of the distance between the two electrodes is available. In this study, the distance between the two electrodes is 1.3 mm. The two electrodes were connected to the side of the specimen, straddling the notch, as shown in Fig. 2-8. This transistor-type power source could supply the maximum voltage 30 V and maximum electric current 9990 A. The minimum time of duration is 0.01 msec. In this study, the electric current treatment consisted of a pulse of 3 kA for 0.5 ms.

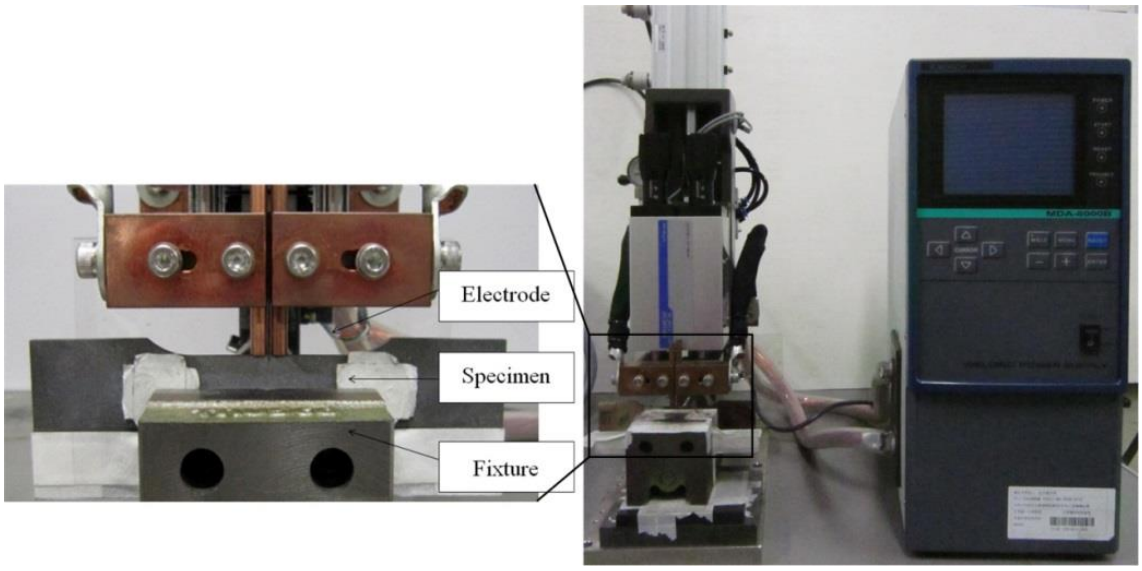

Fig. 2-8 Specimen and electrodes used for the application of HDPC.

Comparing the traditional application of electric current [3-6], the electric current was applied to the specimen with near contact electrodes in this study. Therefore, the

electric current density was much high around the crack tip. An example of the distribution of electric current density simulated by COMSOL is shown in Fig. 2-9.

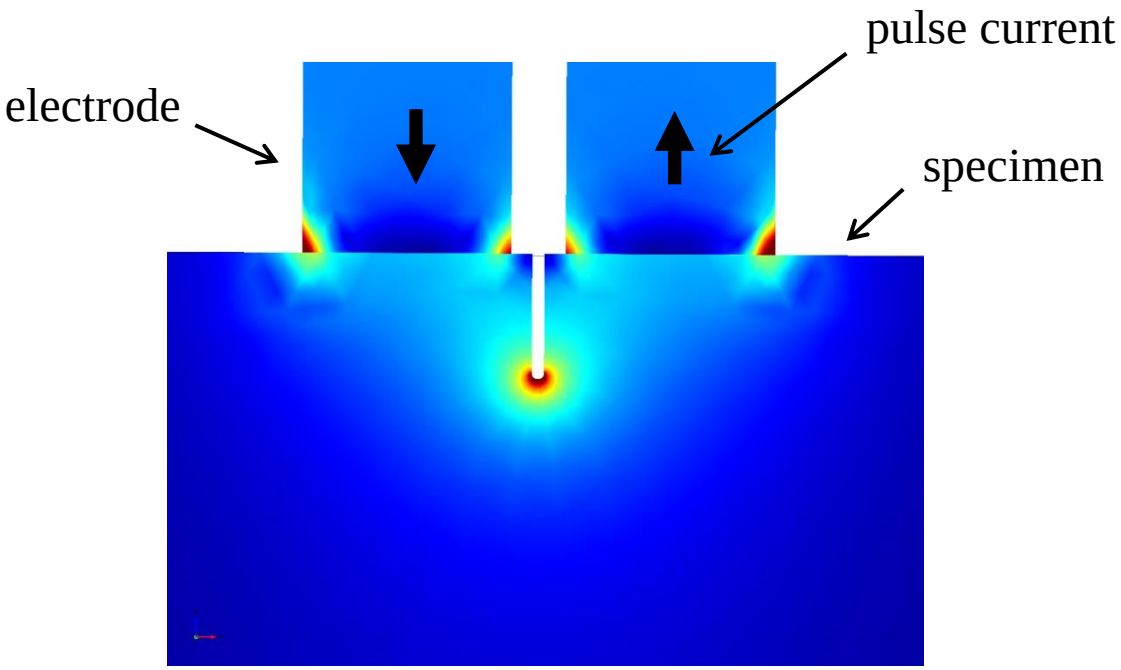

Fig. 2-9 Simulation of distribution of current density around the notch tip by COMSOL.

2.3.2 Conditions of HDPC

Due to the varying maximum net stress, the number of cycles used for the applied current was varied. Here, four test conditions were conducted and for each condition three specimens were used. The detailed conditions of the applied pulse current are shown in Table 2-3. The results of delaying effect of HDPC for fatigue crack initiation with varying maximum n et stress were shown in section 3.1. To evaluate the healing effect due to the application of HDPC, the healing of fatigue damage including the

slip bands, the residual strain and the strain hardening were investigated at the maximum net stress of 115 MPa, as shown in section 4.1.

Table 2-3 Fatigue test and current applying test

	Group A		**Group B**		**Group C**		**Group D**	
Maximum net stress, σ_{max} [MPa]	115		139		162		185	
Stress ratio, *R*	0.05		0.05		0.05		0.05	
Application of current [A]	without	3000	without	3000	without	3000	without	3000
Number of cycles to apply current, *N* [cycle]		2.0×10^5		9.0×10^4		5.0×10^4		1.5×10^4
Pulse duration [ms]		0.5		0.5		0.5		0.5

2.3.3 Electric current conditions for fatigue crack initiation at maximum net stress of 115 MPa

The timing effect of the application of HDPC on fatigue crack initiation was investigated under the test condition of maximum net stress of σ_{max}=115 MPa. Fatigue tests were carried out under the three kinds of conditions as shown in Table 2-4. The specimens were separated into two groups after a certain cyclic loading. One group underwent the application of HDPC, whereas the other group did not. Under each condition four specimens were used. The high-density pulse current was applied at fatigue loading cycles 1.0×10^5 and 2.0×10^5, respectively. The delaying effect is shown in Chapter 4.

Table 2-4 Test conditions of fatigue and applied current

	Group E	**Group F**	**Group G**
Maximum net stress, σ_{max} [MPa]	115	115	115
Stress ratio, R	0.05	0.05	0.05
Application of current [A]	without	3000	3000
Number of cycles for applied current, N [cycle]		1.0×10^5	2.0×10^5
Pulse duration [ms]		0.5	0.5

2.4 Evaluation of healing effect

2.4.1 Delaying fatigue crack initiation

The effect of HDPC on the *S-N* curve is investigated. The fatigue crack initiation was evaluated through the number of cycles at different maximum net stress. Under each condition, i.e. different stress levels, with and without the application of HDPC, respectively, three specimens were tested. Here, fatigue crack initiation was defined as the number of fatigue cycles when a surface crack reaches 25 μm as shown in Fig. 2-10. The process of microcrack initiating was monitored by in-situ observation with optical microscopy (OM) on the specimen surface. Since the fatigue crack initiation was evaluated based on the observation of surface crack on one side surface, the crack leading edge around the center or another side surface of the specimen may have a different value with the evaluated one, i.e. the crack may have a larger propagation

inside the specimen or only be a surface crack. In addition, the notch tip and the side surface conditions were the same for the specimens with and without the application of HDPC.

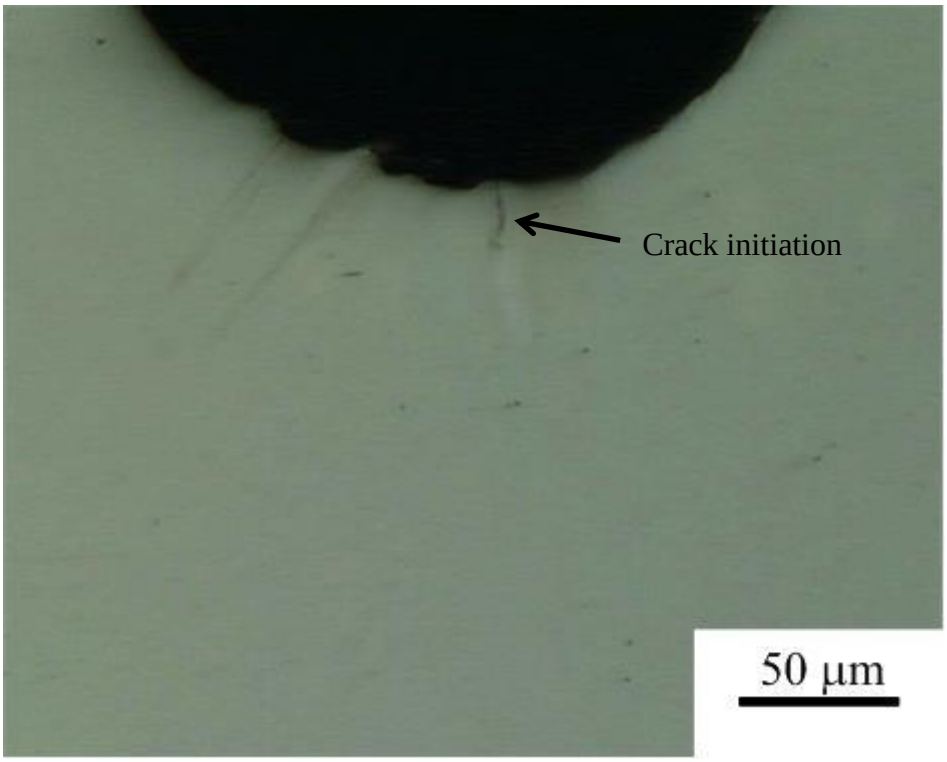

Fig. 2-10 The image of the definition of fatigue crack initiation.

2.4.2 Observation of slip bands with atomic force microscope

Nanotechnologies are believed to bring revolutionary impact on many aspects of science and engineering. One of the most promising tools for the nanotechnology is scanning probe microscopes. Among many types of scanning probe microscopes, AFM is now attracting a great deal of imaging surfaces of solid with the resolution of

0.01 nm. The accurate geometry of solid surface can be reliably obtained by using data analysis software. AFM evidence of surface relief has been widely used for fatigue crack initiation [7-9].

The nucleation of fatigue cracks represents an important stage in the damage evolution in cyclically loaded materials. In homogeneous materials without appreciable macroscopic defects the surface of the material plays a prominent role in fatigue crack nucleation, and the majority of fatigue cracks starts from the surface. If macroscopic defects are present, then the free surface-forming boundary between the defect and the matrix can also be a site of crack nucleation. The localization of the cyclic plastic strain in PSBs is now accepted as a general and very important feature of cyclic straining in crystalline materials, and represents the first signs of fatigue damage.

PSBs play an important role in basic research on fatigue [10, 11]. It is well known that there are abrupt changes of the dislocation density and distribution between the PSBs and matrix. One may then expect these interfaces to serve as preferential sites for fatigue crack nucleation. Materials suffer severe damage once a fatigue crack nucleates. This kind of damage is unavoidable during the processing and application of materials. To evaluate the effect of HDPC on the slip bands, the relief evolution of slip bands was observed by AFM before and after the application of HDPC under the test condition of maximum net stress of σ_{max}=115 MPa.

2.4.3 Measurement of residual strain by digital image correlation method

To analyze the change of residual strain due to the application of HDPC, the digital image correlation (DIC) method was used to investigate the residual strain before and after the application of HDPC. The application of computer-based image acquisition and deformation measurements was first proposed by Peters and Ranson in material systems [12]. The changes in images can be described by the same continuum concepts that govern the deformation of small areas on a surface. An approach was proposed to relate measurable image deformations to object deformations. For the field of experimental mechanics, these original concepts have been refined and incorporated into numerical algorithms to extract object deformations from an image sequence [13-19]. The resulting algorithms and software have been used successfully to obtain surface deformations in a wide variety of applications [20–32].

Image analysis software can be used consistently and repeatedly to obtain surface deformations with an accuracy of ±0.01 pixels or better for in-plane displacement components. This accuracy has been established using the VIC-2D software based on a wide range of experimental and simulation studies [33].

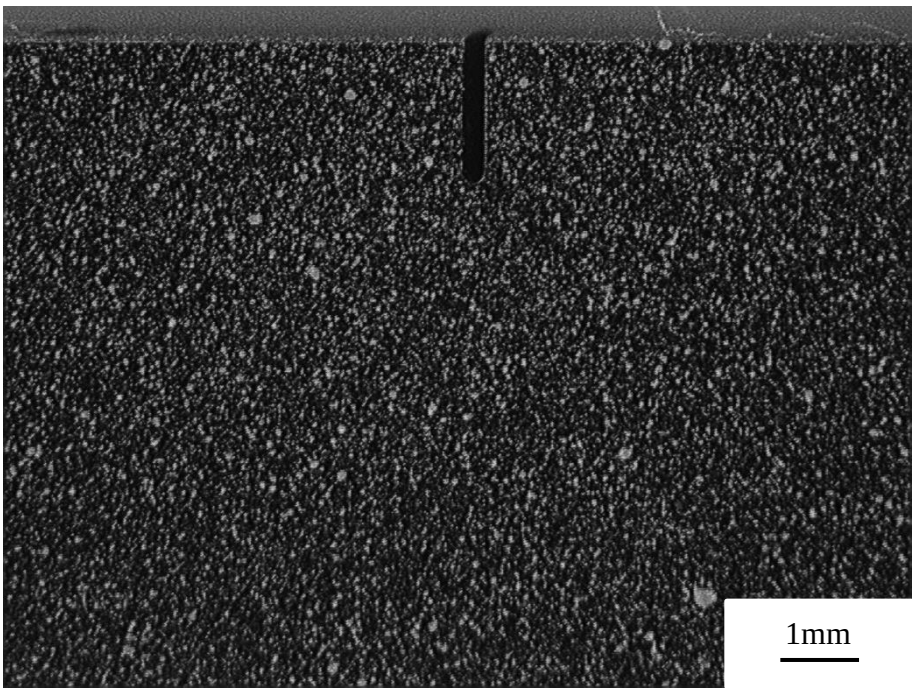

Fig. 2-11 Distribution of spray paint on the original surface of a specimen.

To analyze the change of residual strain due to the application of HDPC by the DIC method, spray paint was distributed uniformly on the original surface of the specimens, as shown in Fig. 2-11. According to the experimental fatigue data in Table 2-3, the high-density electric current was applied after 2.0×10^5 fatigue cycles at a maximum net stress of σ_{max}=115 MPa. The morphology of the spray coating on the specimen surface during the three processes, namely, before the fatigue tests, after the fatigue tests and after the application of the HDPC, was recorded by an optical microscope with a 1600×1200 pixel spatial resolution. In this study, 25×25 pixel subsets and linear subset shape functions were used to perform the correlation process and to obtain the center-point displacement field. A step size of two pixels was used

during the correlation process, resulting in 600×500 pairs of displacement data at each load step. To determine whether the strain of out-of-plane displacement would affect the measurements, separate mechanical measurements were performed. Since the predicted strain of out-of-plane motions is sufficiently small ($\varepsilon_{rr}=4.0\times10^{-5}$), it was neglected in the deformation measurements of the present experiment. The distribution of residual strain around the vicinity of the notch tip was evaluated, which is shown in section 3.4.2.

2.4.4 Measurement of microhardness

Microhardness testing is a well-accepted means of assessing various mechanical properties (flow stress, fracture stress, Young's modulus, fracture toughness, etc.) of thin layers and engineered surfaces. It has been very extensively used for practical applications as well as for scientific research due to its simplicity, convenience, non-destructiveness and direct correlation with service performance [34-36].

In this study, the method for measuring microhardness is used to investigate the fatigue damage evolution at the surface of cyclically loaded metal. According to the concept of continuum damage mechanics, the variation of strain hardening during cyclic loading is associated with the evolution of fatigue failure [37, 38]. Hence, the variable pre-nucleation fatigue damages before and after the application of HDPC were investigated by the microhardness measurement.

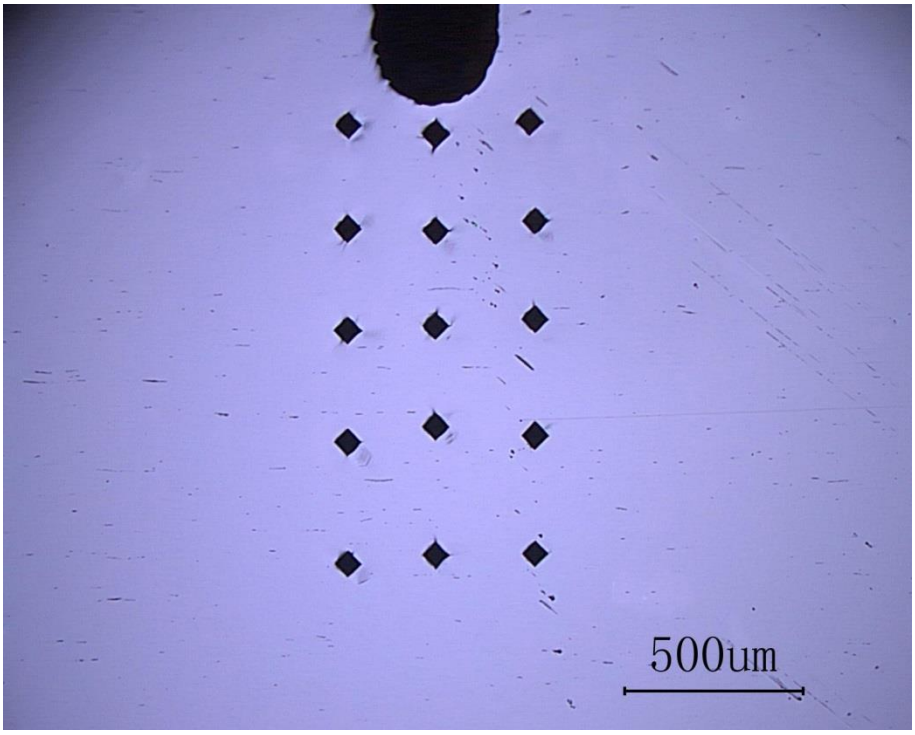

Fig. 2-12 Measurement of Vickers mircohardness.

According to experimental fatigue data, the high-density pulse current was applied after loading cycles of 2.0×10^5 at a maximum net stress was σ_{max}=115 MPa. The Vickers microhardness (HV) was measured before and after the application of HDPC at the same position of the two surfaces of the specimen (Fig. 2-12) with Vickers mircohardness tester (Fig. 2-13). All microhardness measurements were taken using a standard procedure of loading at 0.5 kg.

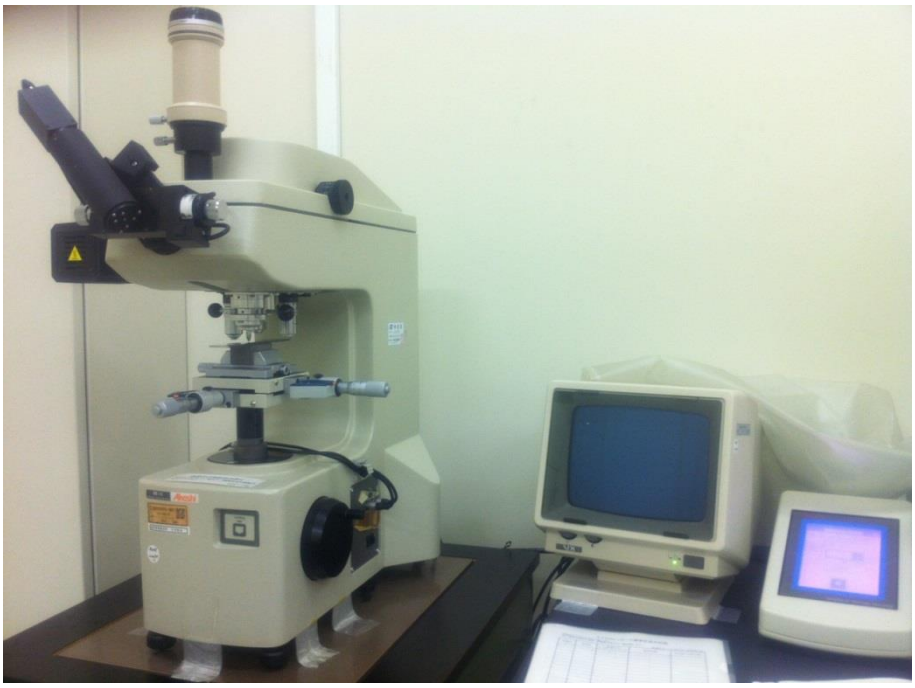

Fig. 2-13 Vickers mircohardness tester.

2.4.5 Transmission electron microscopy observation

TEM constitutes arguably the most efficient and versatile tools for the characterization of materials. TEM is a microscopy technique whereby a beam of electrons is transmitted through an ultra-thin specimen, interacting with the specimen as it passes through. An image is formed from the interaction of the electrons transmitted through the specimen. The image is magnified and focused onto an imaging device to be detected by a sensor such as a CCD camera, as shown in Fig. 2-14 [39].

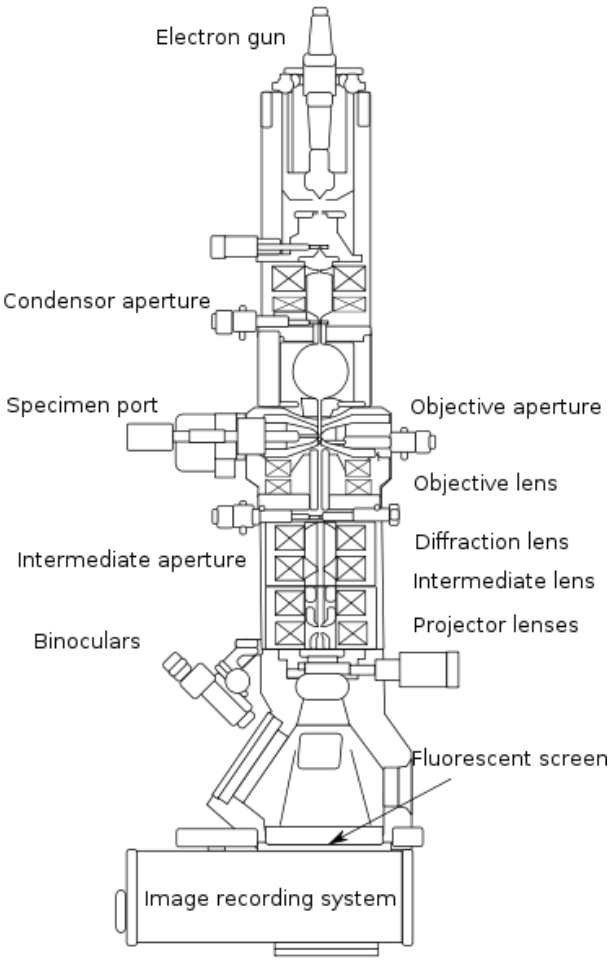

Fig. 2-14 Layout of optical components in a basic TEM [39].

TEMs are capable of imaging at a significantly higher resolution than light microscopes, owing to the small de Broglie wavelength of electrons. This enables the user of instrument to examine fine detail-even as small as a single column of atoms, which is tens of thousands times smaller than the smallest resolvable object in a light microscope. TEM forms a major analysis method in a range of scientific fields, in both physical and biological sciences. TEMs find application in cancer research, virology, materials science as well as pollution, nanotechnology, and semiconductor

research.

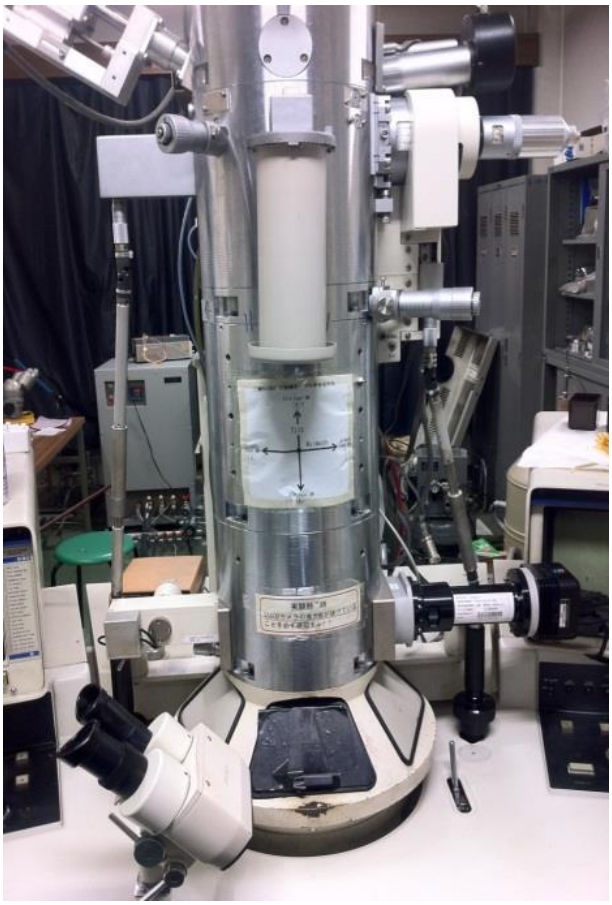

Fig. 2-15 Transmission electron microscopy (HITACHI H-800).

In this study, the TEM HITACHI H-800 was used to observe the dislocation structure, as shown in Fig. 2-15. The surface of thin foils was mechanically polished to thickness of 100 μm, and then was electropolished with a double jet apparatus. Because the sample surface layers affected by mechanical grinding were fully removed by the subsequent electropolishing, the preparation procedure for this standard TEM sample can effectively preserves the original material structure.

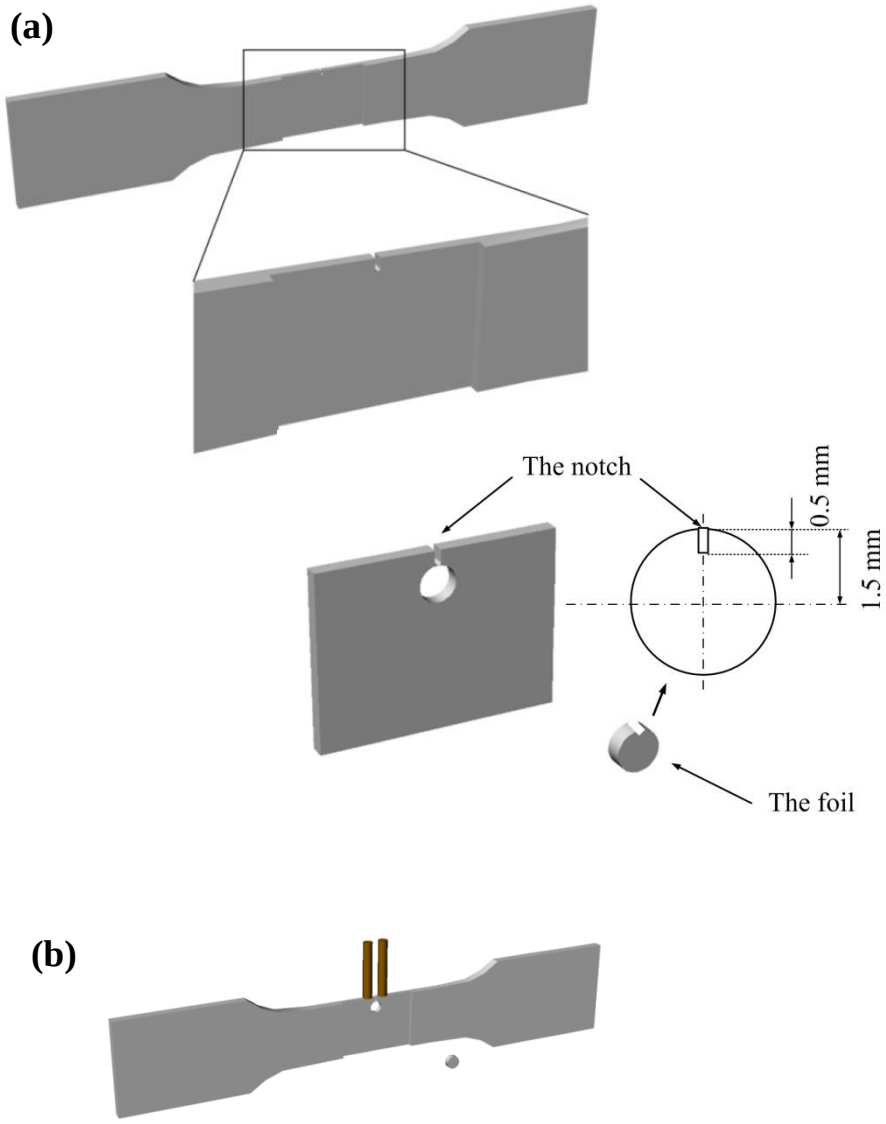

Fig. 2-16 Preparation for TEM sample (a) before and (b) after application of HDPC.

To observe the dislocation structure, thin foils for TEM observation were cut from the same position from the vicinity of the notch tip by wire cutting before and after the application of HDPC. The thin foils with the diameter of 3 mm were cut from the fatigue test specimen as shown in Fig.2-16. The distance between the center of thin foil and the tip of notch is 1.0 mm. Then the foil was electropolished with a double jet

apparatus. Since it is difficult to get a hole exactly at the center of the TEM foil during the electropolished process, three samples were prepared for either condition with and without the application of HDPC.

2.4.6 Measurement of the temperature

The application of HDPC causes a high-speed heating. To clarify the Joule heating effect on the healing of the fatigue damage, the increase of the temperature was investigated. The temperature rise at the root of the notch tip was measured by the thermocouple temperature measurement equipment (LOGER GL900), as shown in Fig. 2-17. The equipment is a high-speed recording device for the simultaneous measurements of temperature. The fast sampling rate is 10 μs.

Fig. 2-17 The equipment of temperature measurement (LOGER GL900).

In this study, the electric current treatment consisted of a pulse of 3 kA for 0.5 ms. Therefore, the increase of the temperature due to the application of HDPC can be recorded simultaneously.

References:

[1] T.S. Byun, N. Hashimoto, K. Farrell, Temperature dependence of strain hardening and plastic instability behaviors in austenitic stainless steels, Acta Mater., 17 (1969) 77-97.

[2] D. Pilkey, Stress concentration factors, Wiley-Interscience, (1997).

[3] G.V. Karpenko, O.A. Kuzin, V.I. Tkachev, V.P. Rudenko, The effect of electric current on the low-cycle fatigue of steels, Sov. Phys. Dokl., 21 (1976) 159-160.

[4] H. Conrad, J. White, W.D. Cao, X.P. Lu, A.F. Sprecher, Effect of electric current pulses on fatigue characteristics of polycrystalline copper, Mater. Sci. Eng. A, 145 (1991) 1-12.

[5] W.D. Cao, H. Conrad, On the effect of persistent slip band (PSBs) parameters on fatigue life, Fatigue Fract. Eng. Mater. Struct., 15 (1992) 573-531.

[6] Z.H. Lai, C.X. Ma, H. Conrad, Cyclic softening by high density electric current pulses during low cycle fatigue of alpha-titanium, Scripta Mett. Mater., 15 (1992) 527-532.

[7] J. Polak, J. Man, K. Obrtlik, AFM evidence of surface relief formation and models of fatigue crack nucleation, Int. J. Fatigue, 25 (2003) 1027-1036.

[8] J. Man, K. Obrtlik, J. Polak, Study of surface relief evolution in fatigued 316L austenitic stainless steel by AFM, Mater. Sci. Eng. A, 351 (2003) 123-132.

[9] J. Man, M. Petrenec, K. Obrtlik, J. Polak, AFM and TEM study of cyclic slip localization in fatigued ferritic $X_{10}CrA_{124}$ stainless steel, Acta Mater., 52 (2004) 5551-5561.

[10] H. Mughrabi, The cyclic hardening and saturation behavior of copper single crystals, Mater. Sci. Eng., 33 (1978) 207-223.

[11] S. Suresh, Fatigue of materials, Cambridge University Press, (1998).

[12] W.H. Peters, W.F. Ranson, Digital imaging techniques in experimental stress analysis, Opt. Eng., 21 (1982) 427-432.

[13] M.A. Sutton, W.J. Wolters, W.H. Peters, W.F. Ranson, S.R. McNeill, Determination of displacements using an improved digital correlation method, Image Vis. Comput., 1 (1983) 133-139.

[14] W.H. Peters, Z.H. He, M.A. Sutton, W.F. Ranson, Two-dimensional fluid velocity measurements by use of digital speckle correlation techniques, Exp. Mech., 24 (1984) 117-121.

[15] J. Anderson, W.H. Peters, M.A. Sutton, W.F. Ranson, T.C. Chu, Application of digital correlation methods to rigid body mechanics, Opt. Eng., 22 (1984) 738-742.

[16] T.C. Chu, W.F. Ranson, M.A. Sutton, W.H. Peters, Applications of digital image correlation techniques to experimental mechanics, Exp. Mech., 25 (1985) 232-245.

[17] M.A. Sutton, S.R. McNeill, J. Jang, M. Babai, The effects of subpixel image restoration on digital correlation error estimates, Opt. Eng., 10 (1988) 870-877.

[18] M.A. Sutton, M. Cheng, S.R. McNeill, Y.J. Chao, W.H. Peters, Application of an optimized digital correlation method to planar deformation analysis, Image Vis. Comput., 4 (1988) 143-150.

[19] M.A. Sutton, H.A. Bruck, S.R. McNeill, Determination of deformations using digital correlation with the Newton-Raphson method for partial differential corrections, Exp. Mech., 29 (1989) 261-267.

[20] M.A. Sutton, J.L. Turner, T.L. Chae, H.A. Bruck, Full field representation of discretely sampled surface deformation for displacement and strain analysis, Exp. Mech., 31 (1991) 168-177.

[21] S.R. McNeill, W.H. Peters, M.A. Sutton, W.F. Ranson, A Least square estimation of stress intensity factor from video-computer displacement data, Proceeding of the 12th Southeastern Conference of Theoretical and Applied Mechanics, (1984) 188-192.

[22] M.A. Sutton, H.A. Bruck, T.L. Chae, J.L. Turner, Experimental investigations of three-dimensional effects near a crack tip using computer vision, Int. J. Fract., 53 (1991) 201-228.

[23] G. Han, M.A. Sutton, Y.J. Chao, A study of stable crack growth in thin SEC specimens of 304 stainless steel, Eng. Fract. Mech., 52 (1995) 525-555.

[24] G. Han, M.A. Sutton, Y.J. Chao, A study of stationary crack tip deformation fields in thin sheets by computer vision, Exp. Mech., 34 (1994) 357-369.

[25] B.E. Amstutz, M.A. Sutton, D.S. Dawicke, Experimental study of mixed mode I/II stable crack growth in thin 2024-T3 aluminum, ASTM STP 1256 Fatigue Fract., 26 (1995) 256-273.

[26] J. Liu, M.A. Sutton, J.S. Lyons, Experimental characterization of crack tip deformations in alloy 718 at high temperatures, ASME J. Eng. Mater. Technol., 20 (1998) 71-78.

[27] M.A. Sutton, Y.J. Chao, J.S. Lyons, Computer vision methods for surface deformation measurements in fracture mechanics, ASME Method. Fract., 176 (1993) 123-133.

[28] J.S. Epstein, Experimental techniques in fracture, Wiley VCH, (1993).

[29] J.S. Lyons, J. Liu, M.A. Sutton, Deformation measurements at 650 ˚C with computer vision, Exp. Mech., 36 (1996) 64-71.

[30] M.A. Sutton, Y.J. Chao, Measurement of strains in a paper tensile specimen using computer vision and digital image correlation-Part 2: Tensile specimen test system, Tappi J., 71 (1988) 173-175.

[31] P.K. Rastogi, D. Inaudi, Trends in optical non-destructive testing and inspection, Elsevier, (2000).

[32] P.K. Rastogi, Topics in applied physics, Springer, (2000).

[33] M.A. Sutton, J.H. Yan, V. Tiwari, H.W. Schreier, J.J. Orteu, The effect of out-of-plane motion on 2D and 3D digital image correlation measurements, Opt. Eng., 46 (2008) 746-757.

[34] Y.U. Milman, B.A. Galanov, S.I. Chugunova, Plasticity characteristic obtained

through hardness measurement, Acta Metall. Mater., 41 (1993) 2523-2532.

[35] D.Y. Ye, D.J. Wang, P. An, Characteristics of the change in the surface microhardness during high cycle fatigue damage, Mater. Chem. Phys., 44 (1996) 179-181.

[36] D.Y. Ye, X.Y. Tong, L.J. Yao, X.X. Yin, Fatigue hardening/softening behavior investigated through Vickers microhardness measurement during high-cycle fatigue, Mater. Chem. Phys., 56 (1998) 199-204.

[37] D.Y. Ye, Z. Wang, An approach to investigate pre-nucleation fatigue damage of cyclically loaded metals using Vickers microhardness tests, Int. J. Fatigue, 23 (2001) 85-91.

[38] K. Zeng, E. Soderlund, A.E. Giannakopoulos, D.J. Rowcliffe, Controlled indentation: A general approach to determine mechanical properties of brittle materials, Acta. Mater., 44 (1996) 1127-1141.

[39] D.B. Williams, C.B. Carter, Transmission electron microscopy, Plenum Press, (1996).

Chapter 3 Effect of high-density pulse current on fatigue behavior

3.1 Introduction

The initiation of fatigue cracks represents an important stage in the fatigue damage evolution in loaded materials. Fatigue crack initiation is a consequence of cyclic slip. It implies cyclic plastic deformation. Specially, when fatigue cracks emanate from notches, the initial growth of the nascent cracks can be significantly influenced by the plastic deformation occurring at the root of the notch. The classical fatigue experiments were respect to localization of strain as a precursor to crack initiation. Due to the physics of the fatigue crack initiation, the recovery of residual strain was quantitatively evaluated with the DIC method to investigate the effect of HDPC on healing of the fatigue damage.

On the surface of the specimen, PSBs represent a critical mechanism of crack initiation in materials. These interfaces between the PSBs and the matrix serve as preferential sites for fatigue crack initiation. Microscopic investigations have shown that fatigue crack nuclei start as invisible microscracks in slip bands. Thus, for understanding the delaying effect of the application of HDPC on the fatigue crack initiation, to know the slip bands topography and its change is essential. The locally

vanishing of the PSBs can decrease the possibility of fatigue crack initiation [1]. Thus, the relief evolution of the slip bands was quantitatively evaluated by AFM in this chapter. The residual strain at the root of notch was quantitatively evaluated by the DIC method before and after the application of HDPC. Additionally, to evaluate the effect of HDPC on strain hardening, the microhardness was measured around the root of notch tip. The delaying effect on the fatigue crack initiation is evaluated by a curve of the cyclic stress versus cycles to reach the fatigue crack initiation (*S*-*N*). The mechanism of the HDPC on delaying fatigue crack initiation was analyzed in this chapter.

3.2 Effect of high-density pulse current on the *S*-*N* curve

To evaluate the delaying effect of HDPC on the fatigue crack initiation, the *S*-*N* curves with and without the application of HDPC were investigated. The effect of HDPC on the *S*-*N* curves is shown in Fig. 3-1. The fatigue crack initiation was evaluated through the number of cycles at different maximum net stress.

As shown in Fig. 3-1, it is found that fatigue crack initiation was delayed after the application of HDPC. The delaying effect tends to increase with the decrease of maximum net stress. The application of HDPC is more effective at the lower stress, especially, at the lowest stress (maximum net stress of σ_{max}=115 MPa). Therefore, it is thought that the stress concentration factor will also affect the delaying effect and small K_t may have a high delaying effect. For this stress value, with the current

application the crack initiation occurred at an average of 2.9×10^5 cycles, with a maximum of 3.2×10^5 cycles. Without the current application the crack initiation occurred at an average of 2.3×10^5 cycles. The average increase in the number of cycles due to the healing effect exceeds 26%, but is limited to 13% at the high stress of σ_{max}=162 MPa. The increase in the number of cycles was shown in detail, as shown in Table 3-1. The results indicate that the application of HDPC delay fatigue crack initiation [2].

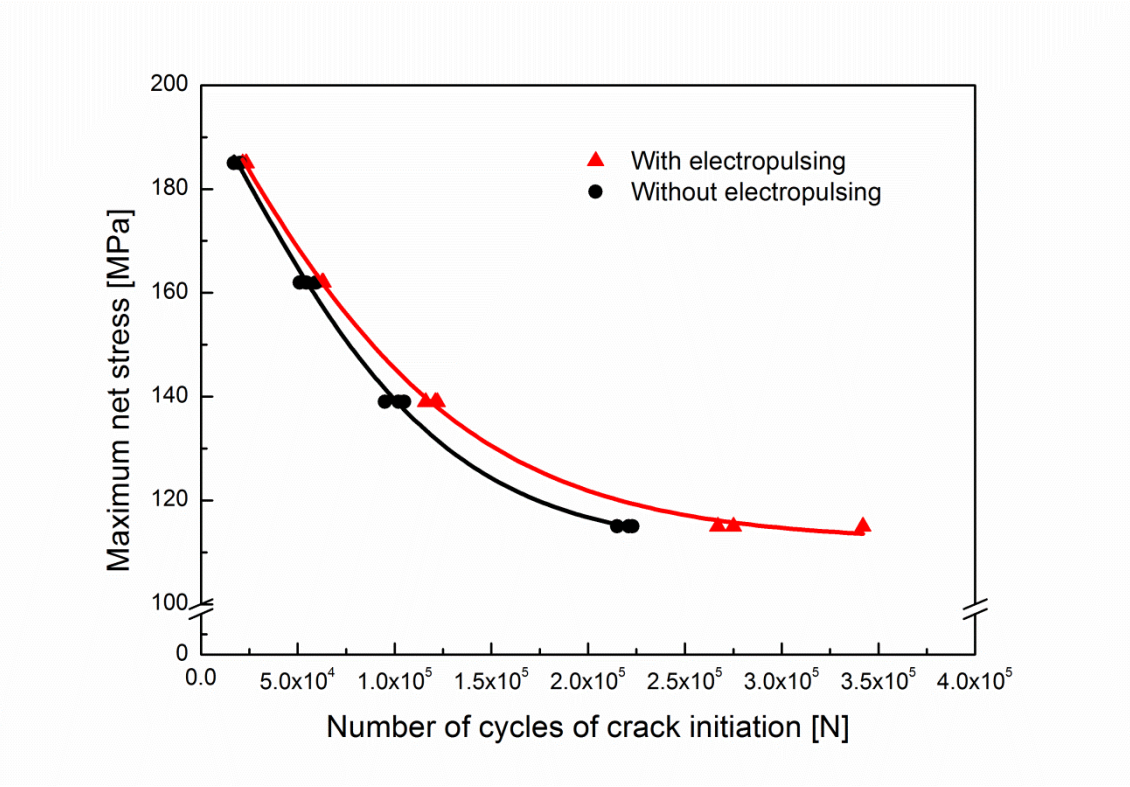

Fig. 3-1 *S-N* curves of stainless steel with and without electric current.

Table 3-1 Increased fatigue crack initiation due to the application of HDPC

	Group A		**Group B**		**Group C**		**Group D**	
Maximum net stress, σ_{max} [MPa]	115		139		162		185	
Stress ratio, R	0.05		0.05		0.05		0.05	
Application of current [A]	without	3000	without	3000	without	3000	without	3000
Number of cycles to apply current, N [cycle]		2.0×10^5		9.0×10^4		5.0×10^4		1.5×10^4
Pulse duration [ms]		0.5		0.5		0.5		0.5
Average cycles number of initiation, N [cycle]	2.3×10^5	2.9×10^5	1.0×10^5	1.2×10^5	5.5×10^4	6.2×10^4	1.9×10^4	2.3×10^4
Increased fatigue crack initiation life [%]		26		20		13		21

3.3 Delaying effect on fatigue crack initiation at maximum net stress 115 MPa

In section 3.2 we have found the delaying fatigue crack initiation due to the application of HDPC. Furthermore, the delay effect tends to increase with the decrease of maximum net stress. The maximum delaying effect is up to 26% at a maximum net stress of σ_{max}=115 MPa. Because of an inhomogeneous stress distribution, a stress concentration occurs at the surface due to the stress concentration factor K_t=5.8. Additionally, the fatigue limit depends on the mean stress of cyclic load. Thus, to evaluate the delaying effect when the HDPC was applied at different fatigue loading cycles, the fatigue crack initiation at a maximum net stress of σ_{max}=115 MPa

was investigated [3].

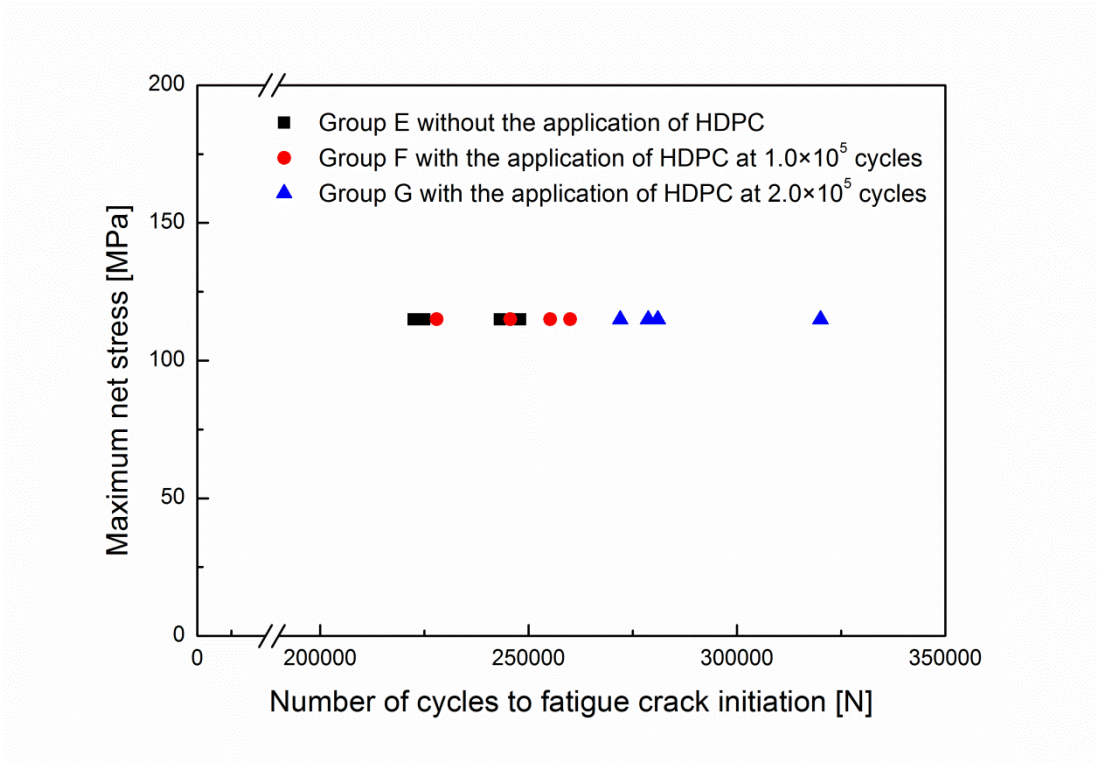

Fig. 3-2 Relationship between the maximum net stress and the number of cycles of fatigue crack initiation, with and without the application of HDPC.

Figure 3-2 shows the fatigue life based on the fatigue crack initiation at a maximum net stress of σ_{max}=115 MPa. When the HDPC was not applied, the crack initiation was observed at an average of 2.34×10^5 cycles as shown in Table 3-2. It was found that fatigue crack initiation was extended after the application of HDPC. When the high-density pulse current was applied at 2.0×10^5 cycles, the fatigue crack initiation was observed at an average of 2.93×10^5 cycles and the maximum of 3.2×10^5cycles. The number of cycles increased 26.3% on average due to the application of HDPC. However, when the high-density pulse current was applied at 1.0×10^5 cycles, the fatigue crack initiation occurred at an average of 2.47×10^5 cycles. The increased

number of cycles is limited to 6.5% on average. The results indicate that the application of HDPC delays fatigue crack initiation, and the delaying effect was different depending on the timing of the application of HDPC. It is thought that the healing effect on fatigue damage was different when the high-density pulse current was applied at different loading cycles. To elucidate the varying healing effect on fatigue damage, the dislocation was evaluated by TEM in Chapter 4.

Table 3-2 Increased fatigue crack initiation due the application of HDPC at the different loading cycles

	Group E	**Group F**	**Group G**
Maximum net stress, σ_{max} [MPa]	115	115	115
Stress ratio, R	0.05	0.05	0.05
Application of current [A]	without	3000	3000
Number of cycles for applied current, N [cycle]		1.0×10^5	2.0×10^5
Pulse duration [ms]		0.5	0.5
Average cycles number of initiation, N [cycle]	2.34×10^5	2.47×10^5	2.93×10^5
Increased fatigue crack initiation life [%]		6.5	26.3

3.4 Healing effect of high-density pulse current on the fatigue damage

3.4.1 Observation of slip bands

The relief evolution of slip bands was investigated before and after the application of HDPC. Figure 3-3 shows the topography of the specimen surface observed by AFM.

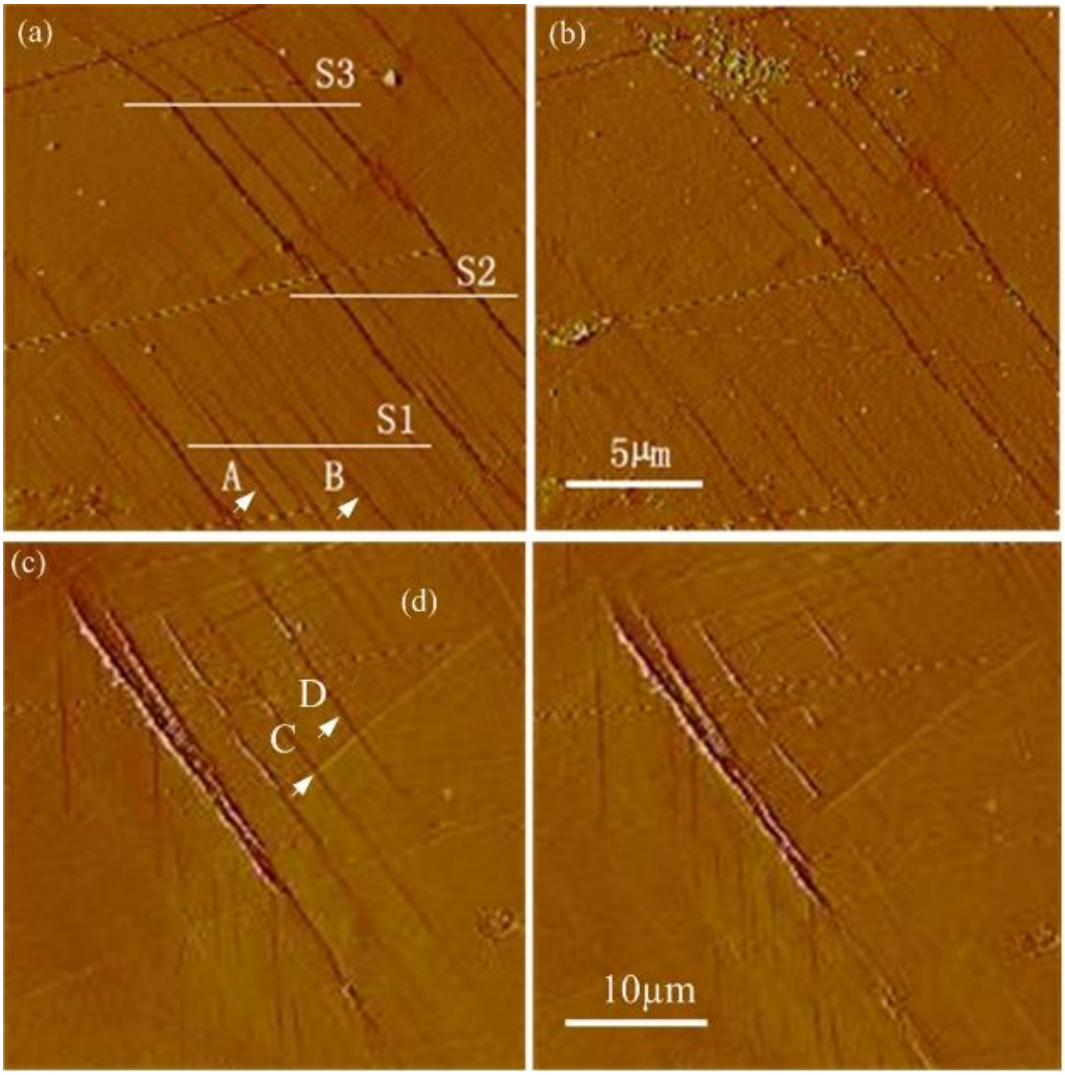

Fig. 3-3 AFM micrographs of the surface relief: (a) before and (b) after the application of HDPC; (c) before and (d) after the application of HDPC with high magnification.

The characteristics of the slip bands after fatigue loading 2.0×10^5 cycles at a maximum net stress of σ_{max}=115 MPa were shown in Fig. 3-3 (a) and (c). The

characteristics of the slip bands at the same site were compared after the application of HDPC, as shown in Fig. 3-3 (b) and (d). High magnification of the characteristics of the slip bands before and after the application of HDPC were shown in Fig. 3-3 (c) and (d). It was observed that the height of slip bands decrease after the application of HDPC. The slip bands A, B, C and D disappeared after the application of HDPC [3].

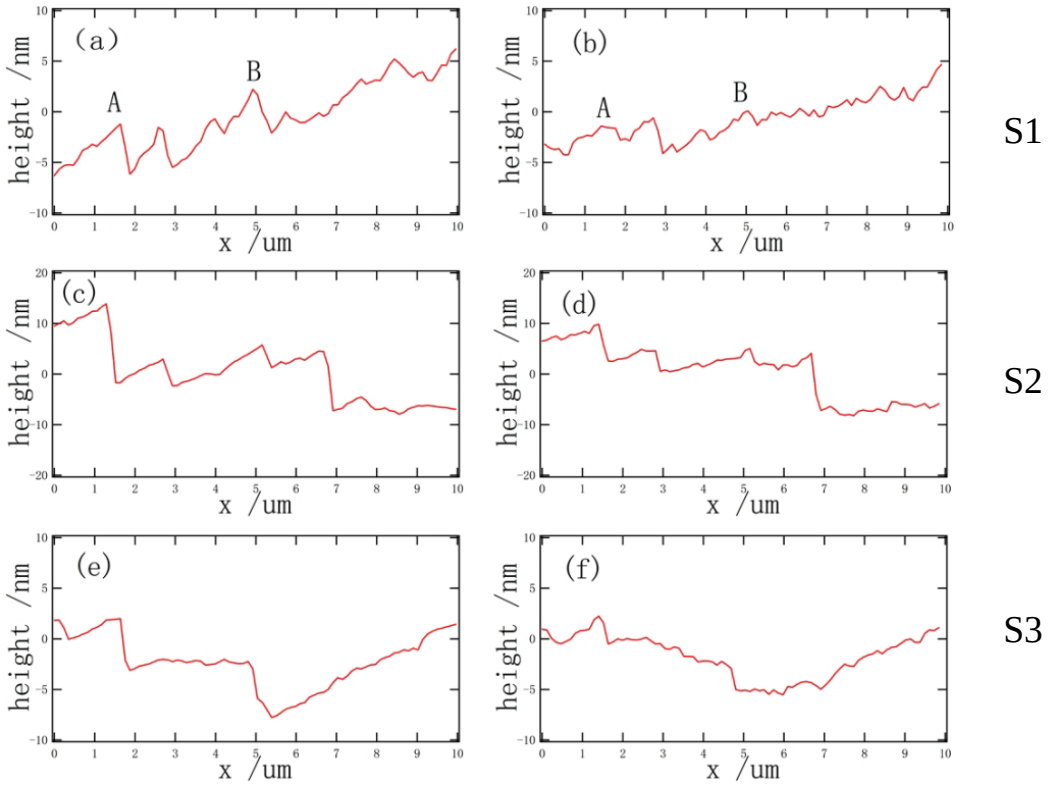

Fig. 3-4 Profiles of surface height in three different lines in Fig. 3-2 (a): (a) before and (b) after the application of HDPC for line S1; (c) before and (d) after the application of HDPC for line S2; (e) before and (f) after the application of HDPC for line S3.

Figure 3-4 shows the characteristic of surface relief profiles on the three different lines of S1, S2, S3 shown in Fig. 3-3 (a). After the application of HDPC, it was found

that the height of slip bands was decreased. It is noted that the slip bands were healed easily when the height of slip bands was smaller than 10 nm. It is indicated that the local disappearance of slip bands and the decrease of slip height are due to the application of HDPC.

3.4.2 Residual strain evaluation

The distribution of the strain at the root of the notch tip was measured by DIC method. The strains were measured by comparing the displacement states of the surface before and after the fatigue tests. After the fatigue tests, the displacement was recorded in unloading state. Hence, the strain distribution obtained by the DIC method is the residual strain in this study.

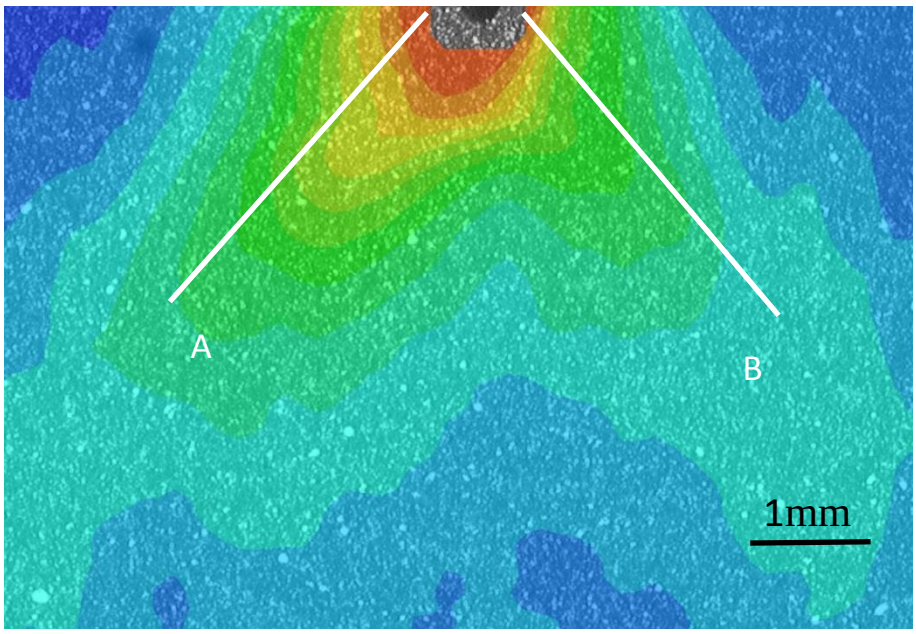

Fig. 3-5 Distribution of residual strain ε_{yy} around notch after the application of HDPC.

Figure 3-5 presents the distribution of residual strain after the fatigue loading 2.0×10^5 cycles at a maximum net stress of σ_{max}=115 MPa. It was found that the residual strain, ε_{yy}, which is parallel to the tensile direction distributed around the notch tip, gradually decreased with increasing distance from the notch tip. Because the residual strain, ε_{xx}, is perpendicular with the tensile direction and the value of ε_{xx} is 10 times smaller than ε_{yy} after the fatigue test, only the change of ε_{yy} before and after the application of HDPC is discussed here [2].

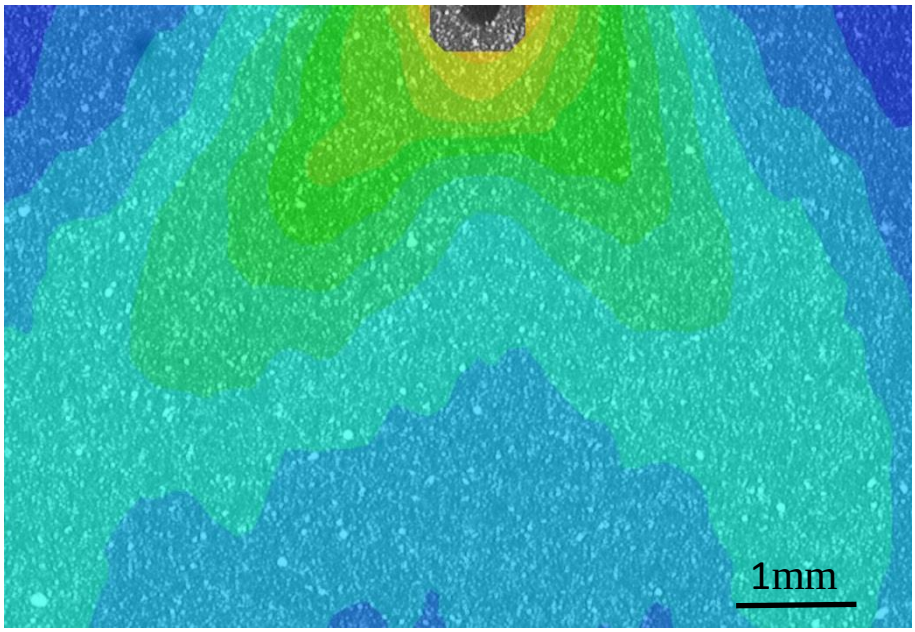

Fig. 3-6 Distribution of residual strain ε_{yy} around the notch tip after the application of HDPC.

Figure 3-6 presents the changed residual strain after the application of HDPC. The distributed concentration of ε_{yy} decreased after the application of HDPC. The plastic zone at the root of the notch tip became smaller. Meanwhile, it was concluded that the

residual stress concentration relaxed with the recovery of residual strain. Additionally, the recovery of residual strain can also be proved by the observation of local disappear of slip bands and the decrease of the slip height as described in section 3.4.1.

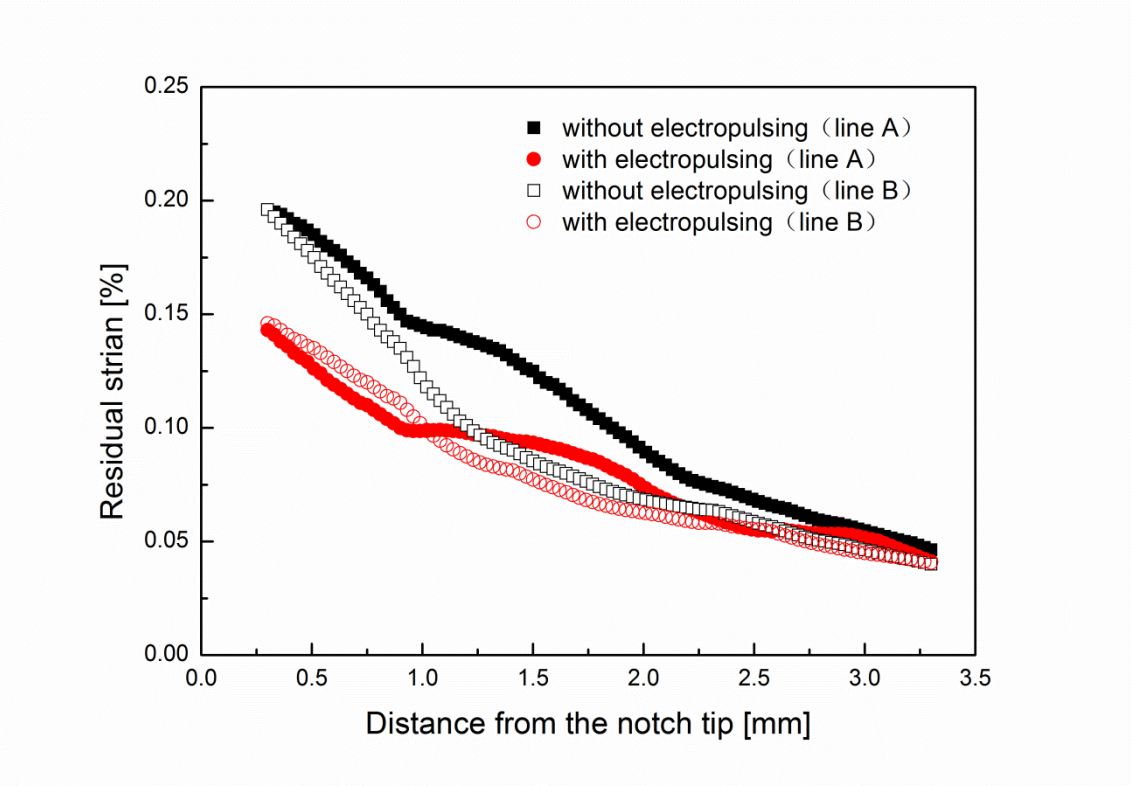

Fig. 3-7 Values of ε_{yy} measured at the positions on lines A and B shown in Fig. 3-4.

To evaluate the recovery effect due to the application of HDPC, the values of ε_{yy} were evaluated quantitatively with the DIC method. Figure 3-7 presents the measured results before and after the application of HDPC at the positions on lines A and B, as shown in Figs. 3-5. It was observed that ε_{yy} around the notch tip had recovered partially after the electric current was applied. When the value of ε_{yy} was above 0.1%

after the fatigue test, ε_{yy} had recovered up to 25.3% on average. However, the recovery ratio is limited to an average of 9.7% at the position where ε_{yy} was less than 0.1% after the fatigue test. It was found that the recovery effect due to the application of HDPC was affected by the value of residual strain before the application of HDPC.

3.4.3 Measurement of Vickers microhardness

Figure 3-8 shows the values of HV, plotted against the distance from the notch tip. Two specimens with the same conditions were measured. Each data point represents the average of three test values, and the error bars indicate the total range of the individual measured values.

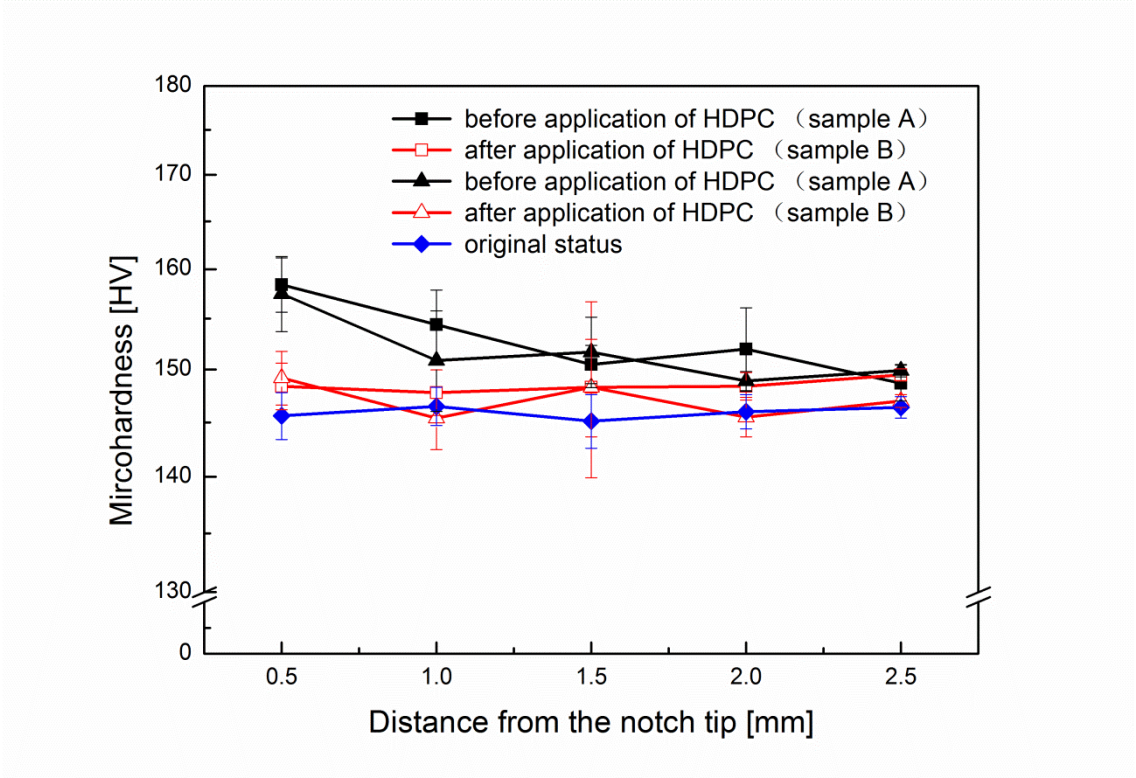

Fig. 3-8 Variation of HV before and after the application of HDPC.

Two features of Fig. 3-8 are noted. First, the HV near the notch tip is higher than that far from the tip, which indicates that HV increases within the plastic zone after cyclic loading. Second, after the application of HDPC, the increased HV due to the cyclic loading decreased to the nominal hardness as shown in Fig. 3-8. This result demonstrates that the strain hardening caused by the cyclic loading was recovered by application of HDPC.

3.5 Analysis of the delaying effect based on the restoration of fatigue damage

3.5.1 Healing of slip bands

In homogeneous materials without appreciable macroscopic defects the surface of the material plays a prominent role in fatigue crack initiation. The majority of fatigue cracks start from the surface. If macroscopic defects including inclusions, holes and non-coherent precipitates are present, then the free surface-forming boundary between the defect and the matrix can also be a site of crack nucleation [4]. Ewing and Humfrey [5] reported the localized surface damage and the initiation of fatigue cracks in the areas of pronounced surface relief. The studies of extrusion and intrusion appearance on the surface of fatigued metals inspired further interest in the mechanisms of fatigue crack initiation [6]. Forsyth et al. proposed that the slip bands consist of extrusions and intrusions, which are developed on the initially flat surface

where emerging PSBs. They are believed to be the critical precursor to the nucleation of fatigue cracks.

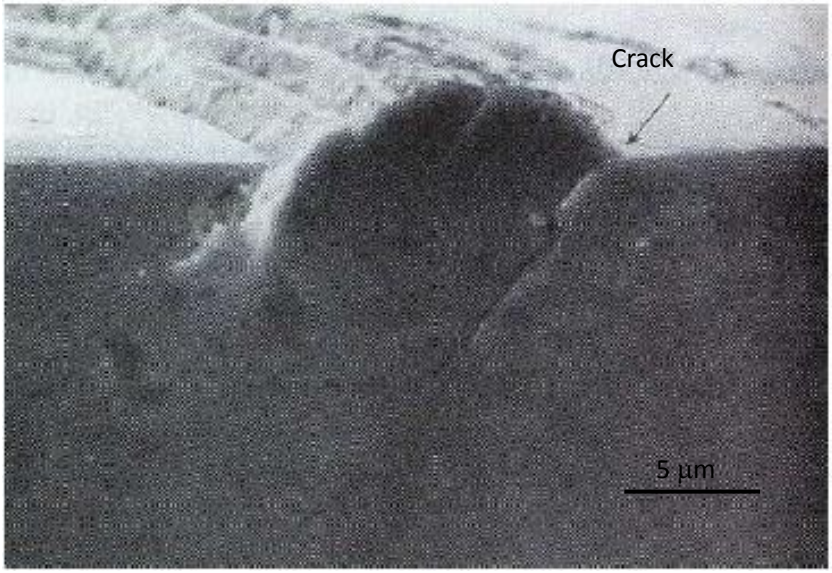

Fig. 3-9 Fatigue crack initiation at a PSB matrix interface in Cu crystal [4].

It is well known that there are abrupt changes of the dislocation density and distribution between the PSBs and matrix. The interface between the PSBs and matrix is a plane of discontinuity across. One may then expect these interfaces to serve as preferential sites for fatigue crack nucleation, as shown in Fig. 3-9 [4]. Concomitant interferometric observations of the test specimen revealed that the strains within the PSBs are highly inhomogeneous and localized at the PSB-matrix interface. These results imply that fatigue crack initiation is strongly biased by the roughening of the surface (Fig. 3-10). Materials suffer severe damage once a fatigue crack nucleates. This kind of damage is unavoidable during the processing and application of materials. Therefore, the slip bands play an important role in basic research on fatigue behavior.

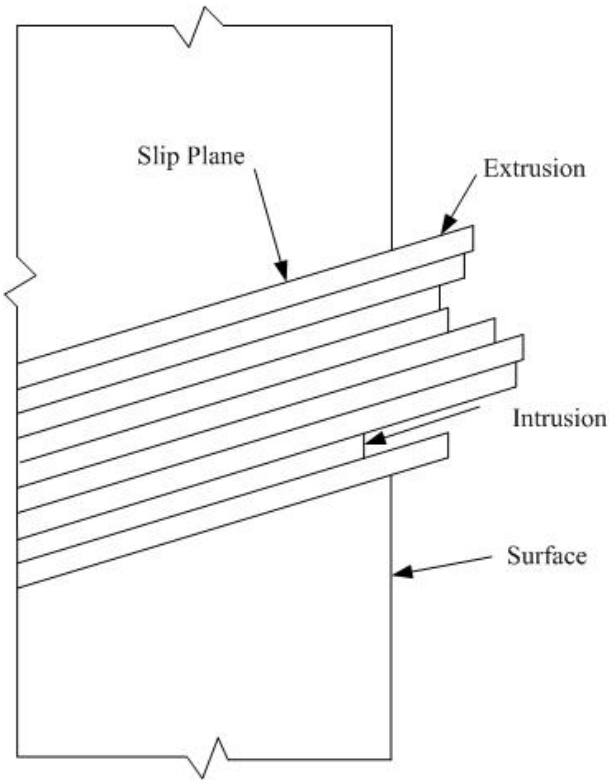

Fig. 3-10 The roughening of the surface due to the PSBs.

After the application of HDPC, the local disappear of slip bands and the decrease of the height of slip bands give the evidence for the delaying effect on the fatigue crack initiation. These interfaces between the PSBs and the matrix serve as preferential sites for fatigue crack initiation. Microscopic investigations have shown that fatigue crack nuclei start as invisible microscracks in slip bands. The locally vanishing of the PSBs can decrease the possibility of the fatigue crack initiation. It is an important reason for the delaying effect of fatigue crack initiation.

3.5.2 Recovery of residual strain

The localization of the cyclic strain in slip bands is now accepted as a general and very important feature of cyclic straining in materials, and represents the first signs of fatigue damage. Phenomenological approaches based on the recovery of residual strain and the delaying fatigue crack initiation were obtained directly from the present experiment.

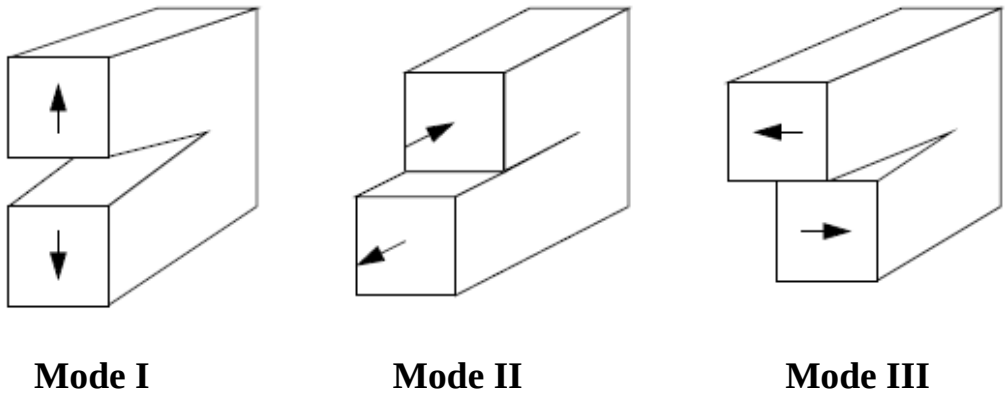

Fig. 3-11 Standard fracture modes.

When fatigue cracks emanate from notches, the initial growth of the nascent cracks can be significantly influenced by the plastic deformation occurring at the root of the notch. For the model I tensile fatigue test (Fig. 3-11), the effect of plasticity on the near-tip fields is directly evident in Fig. 3-12 [7].

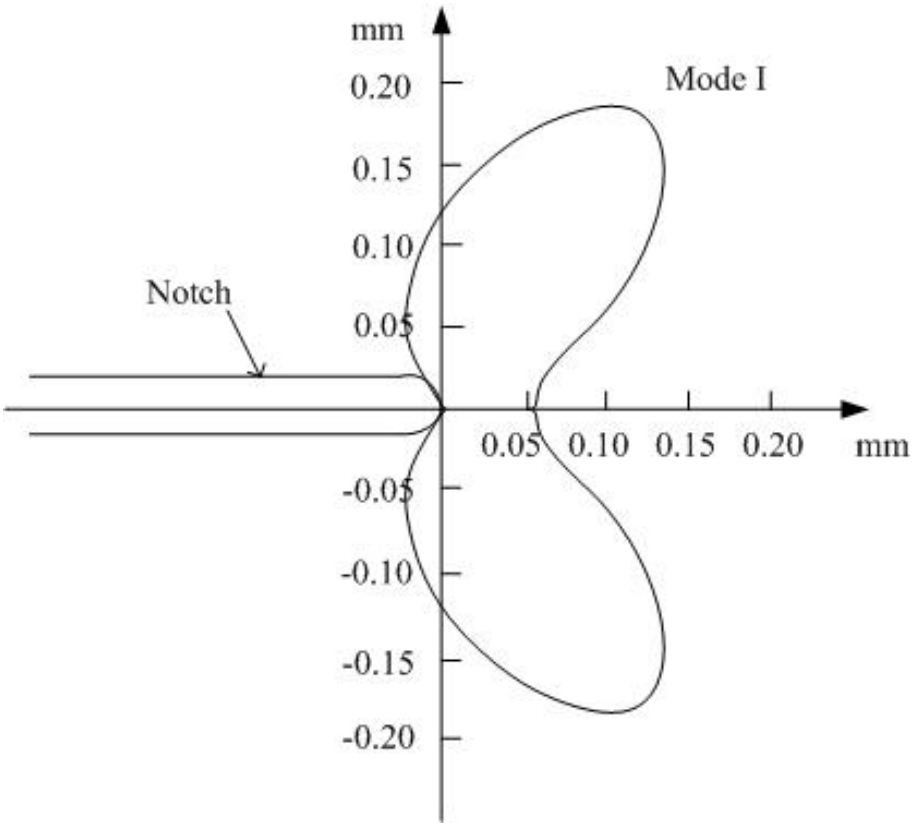

Fig. 3-12 The plastic zone ahead of the notch in model I fatigue test [7].

The measurement result of a plastic zone created by the fatigue loading has been shown in Fig. 3-5. It was found that the experimental results were corresponding to the model I analysis. It is known that fatigue damage is conditioned by the cyclic-plastic deformation [8-9]. The recovery of residual strain indicates the decrease of the fatigue damage. Thus, the recovery of residual strain has an effect on the temporary retardation of fatigue crack initiation.

3.5.3 Vickers microhardness tests

Measurement of microhardness has been given to quantify the damage, whereas a great deal of experimental evidence has proved that the fatigue damage in these stages is primarily related to the occurrence and development of localized plastic-strain concentration at or near the surface of materials during cycling [10-12]. In other words, it is feasible to investigate the pre-nucleation fatigue damage, i.e. fatigue damage in the stages prior to micro-crack nuclei, from the pre-nucleation degradation of material properties and microstructures within the surface layers under cyclic loading.

On the other hand, using the effective stress concept and the strain equivalence hypothesis [13], the stress-strain relationship coupled with damage represents the deterioration of the material properties and microstructures due to the loading forces. Damage values in the surface grains increase continuously after a certain number of cycles thereby inducing the process of microhardness increasing. Therefore, it can be inferred from the above analysis that the damage variable defined on the basis of the variation of Vickers microhardness during cycling can well reveal some characteristics of fatigue damage evolution and distribution, particularly in the stages prior to nucleation of fatigue crack initiation. Consequently, after the application of HDPC, the decrease of microhardness within the plastic zone results the delaying fatigue crack initiation.

3.6 Effect of other factors on fatigue crack initiation

3.6.1 Stress concentration factor K_t

In this study, the notch fatigue test was carried out. The stress concentration factor, K_t, is the important parameter for the prediction of crack initiation. Thus, the K_t will also has an effect on delaying crack initiation. The value of K_t=5.8 used in this study has been shown in section 2.2.1. Actually, in case of low K_t, the fatigue crack initiation period will occupy the most of fatigue life. However, in the case of high K_t the crack propagation period will control the total fatigue life. Although the value of K_t = 5.8 is high in this study, the experimental results show that the application of HPDC can delay the fatigue crack initiation. Therefore, it is thought that the stress concentration factor will also affect the delaying crack initiation and the lower K_t may have a high delaying effect. Additionally, to study the delaying crack initiation under the condition of high K_t, the recovery of fatigue damage was investigated under the lower mean stresses.

3.6.2 Thickness of specimen

In this study, the specimens with thickness of 2.5 mm only were used to investigate the delaying crack initiation by application of HDPC. It is possible to realize the delaying crack initiation for specimens with different thicknesses by application of

HDPC with different electric current density. For the increased thickness, the applied electric current density to the material will be decreased. Therefore, it is possible to increase the electric current density to obtain the same delaying effect for the large thickness specimens.

3.7 Summary

In this chapter, the effect of HDPC on the fatigue behavior was investigated. The fatigue crack initiation was delayed successfully by the application of HDPC. The delaying effect was different depending on the timing of the application of HDPC. The reason of the delaying fatigue crack initiation was due to the restoration of fatigue damage. To clarify the effect of HDPC on the healing of fatigue damage, on the surface of specimen, the slip bands were observed. Furthermore, the residual strain and microhardness at the root of the notch tip were also evaluated. It was found that the residual strain was recovered after the application of HDPC. It implies the relaxation of the stress concentration around the notch. The strain hardening was also recovered. In addition, the locally disappearance of slip bands and the decrease of the height of slip bands were found. The locally disappear of slip bands can decrease the possibility of fatigue crack initiating.

References:

[1] S.H. Xiao, et al., The effect of high current pulsing on persistent slip bands in fatigued copper single crystals, Mater. Sci. Eng. A, 332 (2002) 351-355.

[2] Y.P. Tang, A. Hosoi, Y Morita, Y. Ju, Restoration of fatigue damage in stainless steel by high-density electric current, Int. J. Fatigue, 56 (2013) 69-74.

[3] Y.P. Tang, A. Hosoi, Y. Iwase, Y. Ju, Effect of high-density electric current on the microstructure and fatigue crack initiation of stainless steel, Mater. Trans., 54 (2013) 2085-2092.

[4] J. Polak, J. Man, K. Obrtlik, AFM evidence of surface relief formation and models of fatigue crack nucleation, Int. J. Fatigue, 25 (2003) 1027-1036.

[5] J.A. Ewing, J.W.C. Humfrey, The fracture of metals under repeated alternations of stress, Phil. Trans. R. Soc., 200 (1903) 241-250.

[6] P.J. Forsyth, Exudation of material from slip bands at the surface of fatigued crystals of aluminium - copper alloy, Nature, 171 (1953) 172-173.

[7] S. Suresh, Fatigue of materials, Cambridge University Press, (1998).

[8] M. Klesnil, P. Lukas, Fatigue of metallic materials, Elsevier, (1980).

[9] B.I. Sandor, Undamentals of cyclic stress and strain, University of Wisconsin press, (1972).

[10] D.Y. Ye, D.J. Wang, P. An, Characteristics of the change in the surface microhardness during high cycle fatigue damage, Mater. Chem. Phys., 44 (1996)

179-181.

[11] D.Y. Ye, X.Y. Tong, L.J. Yao, X.X. Yin, Fatigue hardening/softening behavior investigated through Vickers microhardness measurement during high-cycle fatigue, Mater. Chem. Phys., 56 (1998) 199-204.

[12] D. Ye, Z. Wang, An approach to investigate pre-nucleation fatigue damage of cyclically loaded metals using Vickers microhardness tests, Int. J. Fatigue, 23 (2001) 85-91.

[13] J.L. Chaboche, Continuous damage mechanics - A tool to describe phenomena before crack initiation, Nucl. Eng. Des., 64 (1981) 233-247.

Chapter 4 Effect of high-density pulse current on dislocation

4.1 Introduction

To investigate the effect of HDPC on fatigue behavior, we had demonstrated the restoration of fatigue damage in the Chapter 3. The delaying fatigue crack initiation was realized by the application of HDPC. The healing of the slip bands was found. The residual strain and the strain hardening were recovered within the plastic zone at the root of notch. In this chapter, to clarify the mechanism of healing effect due to the application of HDPC, the effect of HDPC on the microstructure was investigate at the atom level.

In the microstructure, dislocations have been found experimentally to play a fundamental role for fatigue crack initiation. During the cyclic loading process, the accumulation process of fatigue damage can be qualitatively analyzed by means of the evolution features of the dislocation structures. Additionally, in the formation of slip bands, the dislocation mechanics play an important role in the fatigue response of the material. The localization of strain as a precursor to fatigue crack initiation accumulates primarily through the dislocation motion. As the hardness is structurally sensitive and related closely to the intrinsic structural factors of the material at the

submicroscopical level, it is strongly affected by the distribution of dislocations. Therefore, it is necessary to investigate the effect of HDPC on the dislocation structure.

The evolution of dislocation substructures in fatigue loaded stainless steel by electropulsing has been studied previously [1-4]. They found that dislocation substructures were changed by the electropulsing treatment. However, the quantitative evaluation of the effect of HDPC on dislocation has been few studied up to now. The relationship between the dislocation structure and the crack initiation is still unclear. Therefore, to clarify the mechanism of healing effect on fatigue damage, the dislocation structures before and after the application of HDPC were investigated by transmission electron microscopy in this chapter.

4.2 Effect of high-density pulse current on dislocation structure

The typical dislocation structures were investigated by the observation of TEM to evaluate the effect of HDPC on the dislocation structure. Three samples were observed under each condition. Figure 4-1 shows the TEM photographs of the typical dislocation structures. Only a few dislocations were observed in the original material, as shown in Figs. 4-1 (a) and (b). The dislocation density is very low in the original state [5].

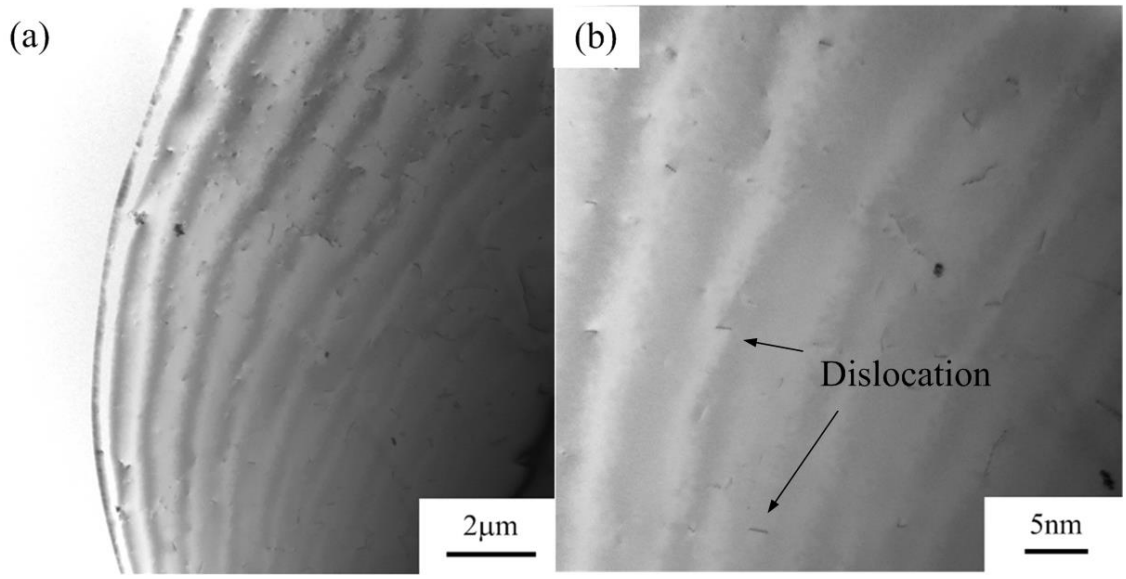

Fig. 4-1 Typical TEM images of dislocation structure before the fatigue test: (a) original material; (b) high magnification.

To observe the evolution of dislocation structure during the cyclic loading process, the dislocation structure was observed after 1.0×10^5 cycles and 2.0×10^5 cycles, respectively. With the increase of cyclic loading, it was found that local high-density dislocation structures, such as dislocation lines and pile-ups, were formed based on the observation of TEM in [011] beam direction, as shown in Figs. 4-2 (a) and (b), and Figs. 4-3 (a) and (b). Dislocation density increases with the increase of loading cycles. A large amount of dislocation slips were observed at 2.0×10^5 cycles, as shown in Figs. 4-3 (a) and (b). The dislocation structures developed under cyclic loading are similar as those reported in other literatures for the stainless steel [6-8].

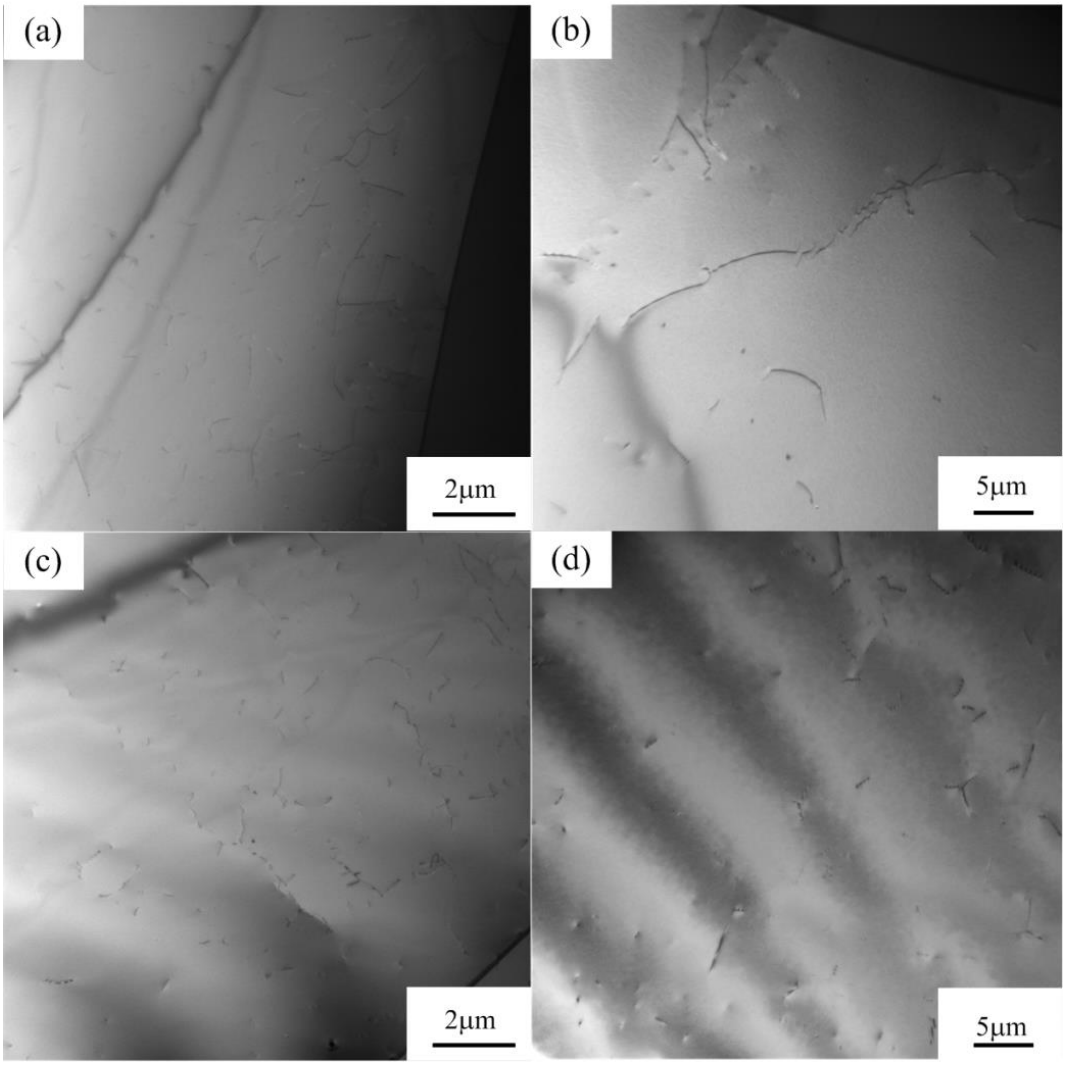

Fig. 4-2 Typical TEM images of dislocation structure: (a) low magnification after 1.0×10^5 cycles; (b) high magnification after 1.0×10^5 cycles; (c) low magnification after the application of HDPC; (d) high magnification after the application of HDPC.

To investigate the effect of HDPC on the dislocation, the dislocation structure was observed after the application of HDPC, as shown in Figs. 4-2 (c) and (d), and Figs. 4-3 (c) and (d), under identical diffracting conditions. It was found that the dislocation pile-ups disappeared after the application of HDPC. When the fatigued specimen

underwent an application of HDPC, the density of dislocations was observed becoming much lower than that without the application of HDPC, due to less tightly bound dislocations in the various walls or cell boundaries. The lower dislocation density verifies that electrical stimulation has an effect on the disappearance of dislocations [5]. The effect of HDPC on the decrease of dislocation density was quantitatively analyzed in the section 4.3.

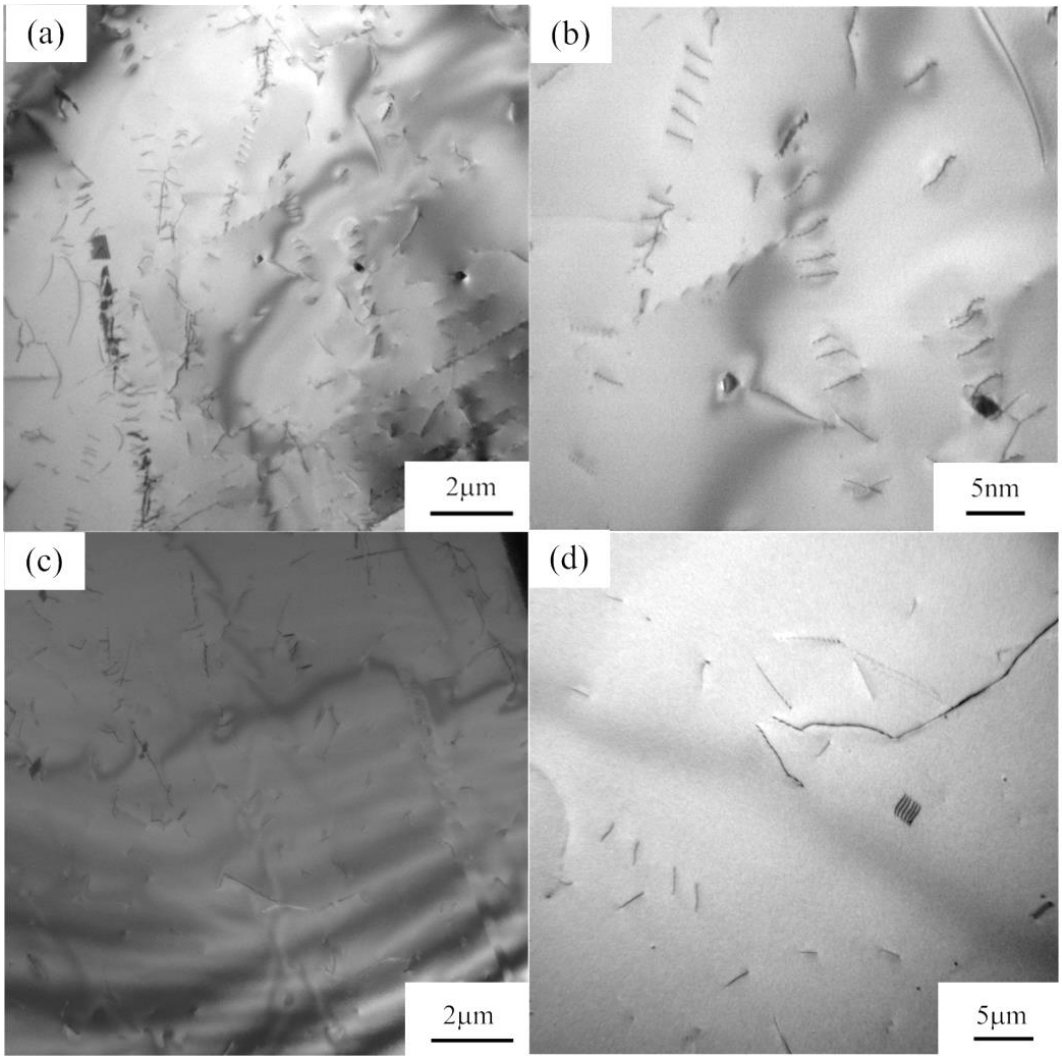

Fig. 4-3 Typical TEM images of dislocation structure: (a) low magnification after 2.0×10^5 cycles; (b) high magnification after 2.0×10^5 cycles; (c) low magnification

after the application of HDPC; (d) high magnification after the application of HDPC.

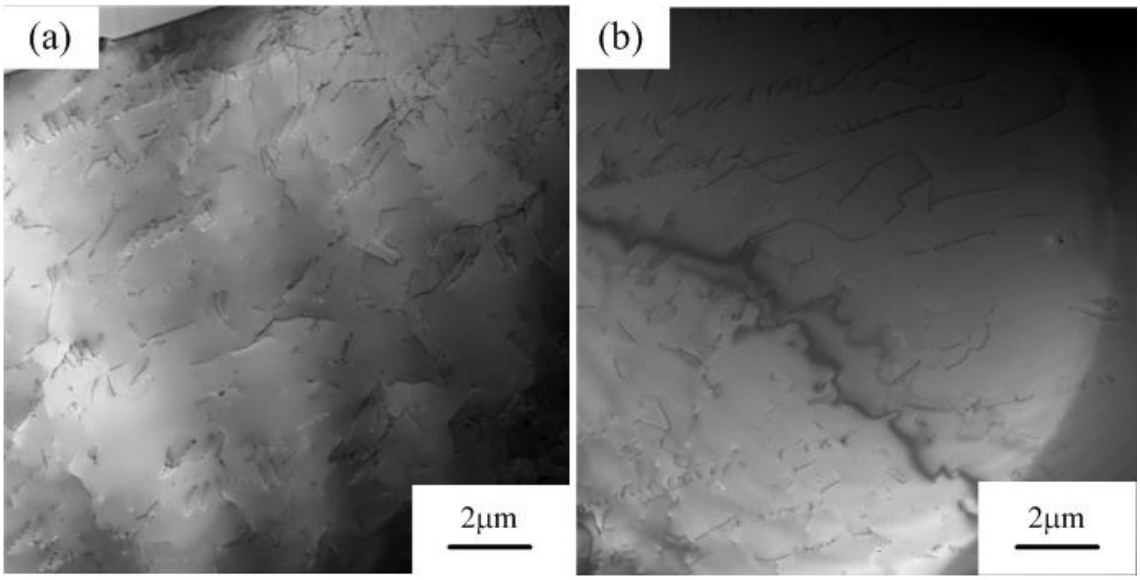

Fig. 4-4 Typical TEM images of dislocation structure: (a) reached crack initiation without the application of HDPC; (b) reached crack initiation after the application of HDPC at 2.0×10^5 cycles.

Figure 4-4 (a) and (b) show the dislocation structures with and without the application of HDPC when the fatigue crack initiation occurs at 2.34×10^5 and 2.93×10^5 cycles, respectively. When the fatigue crack initiation occurs, a large number of dislocation pile-ups accumulate at the grain boundary, and the dislocation density is very high. The dislocation distribution with the application of HDPC is similar with that without the application of HDPC. To analyze the multi-application of HDPC on the delaying crack initiation, the dislocation structure after the multi-application of HDPC was observed as shown in Fig. 4-5 (a) and (b). Figure 4-5

(a) is the dislocation distribution after the second time to apply HDPC at 2.5×10^5 cycles and (b) is the dislocation distribution after the third time to apply HDPC at 3.0×10^5 cycles, before the crack initiation. The electric current density and the duration time of HDPC is the same as that of the first time application. The quantitatively evaluation of the dislocation density is shown in section 4.3.2.

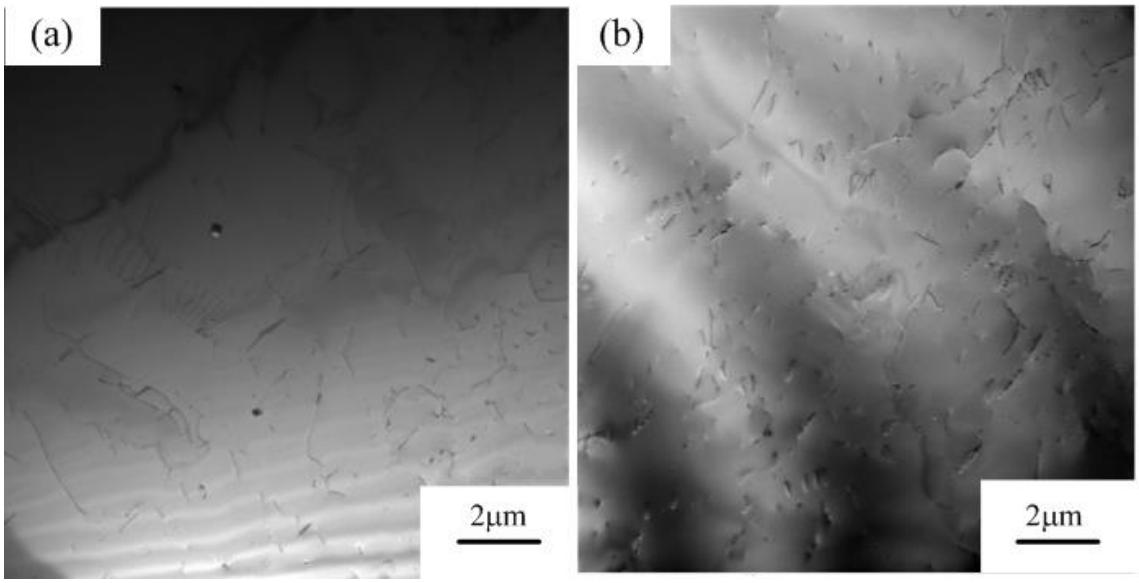

Fig. 4-5 Typical TEM images of dislocation structure: (a) after the second time to apply HDPC at 2.5×10^5 cycles; (b) after the third time to apply HDPC at 3.0×10^5 cycles.

4.3 Quantitative evaluation of dislocation density

4.3.1 Measurement of dislocation density

Dislocation density has been measured by the section line method with the correlation for dislocation invisibility [9, 10]. Scanning lines were drawn horizontally and vertically over observed pictures and the number of intersection points of them with dislocations were counted. For each image, a total of 20 scanning lines were plotted as ten vertical lines and ten horizontal lines to form a squared grid, as shown in Fig. 4-6. The dislocation density, *D*, can be expressed as the ratio of the number of intersection points, *N*, to the multiplication of the total length of the lines, *L*, and foil thickness, *t*:

$$D = \frac{N}{Lt}. \qquad (4\text{-}1)$$

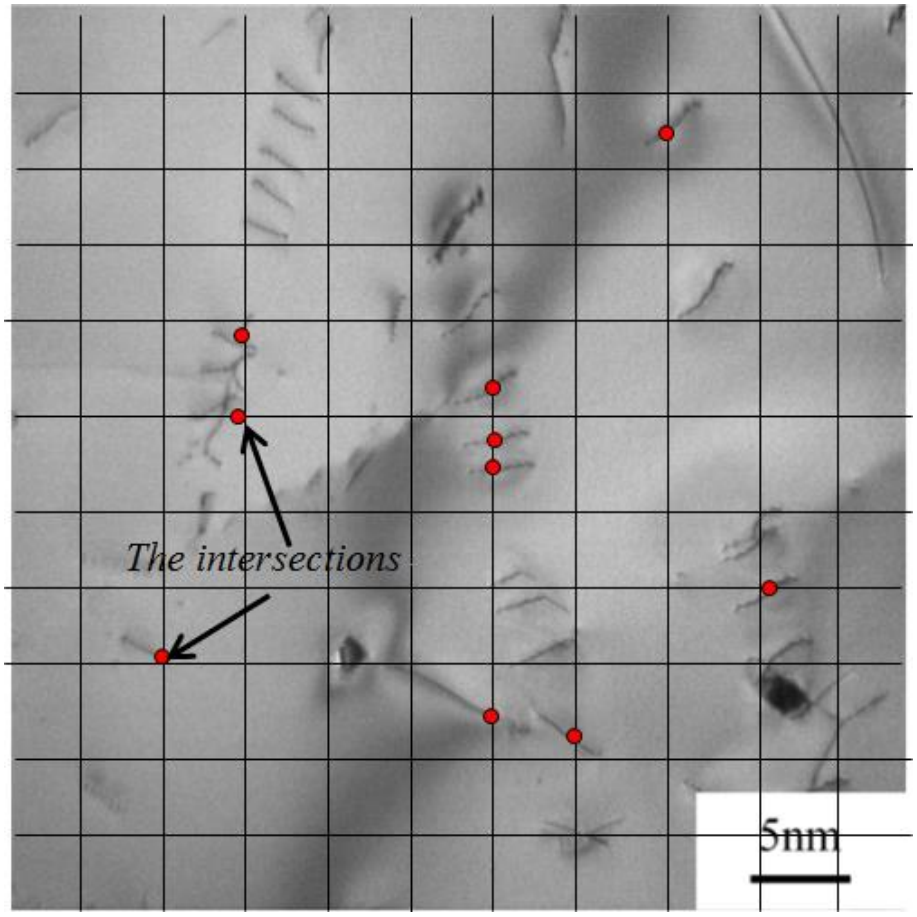

Fig. 4-6 The vertically and horizontally scanning lines in the TEM images.

The accuracy of the dislocation density measurements determined with the formula depends on the precise measurement of the foil thickness which is determined by a convergent beam electron diffraction technique [11]. Kelly et al. [12] showed that the thickness can be measured by the convergent beam electron diffraction technique with the accuracy of 5%.

A second method was used to check the reliability of the dislocation density results obtained from the section line method. In this method, the dislocation density was measured by manually tracing and measuring the total length of the dislocation line, L_t, within selected TEM images using Image J software, which is a much more tedious task to perform compared with the section line method. The total dislocation density, D, was calculated using the following relationship [13]

$$D = \frac{L_t}{At}, \qquad (4\text{-}2)$$

where A is the imaged foil area. The difference in the measured densities using these two techniques was found to be minimal compared with other errors that were present during the measurement. For this reason the section line method was considered to be sufficient for the dislocation density measurements.

4.3.2 Analysis the dislocation density before and after the application of high-density pulse current

The dislocation densities of the original state, and at 1.0×10^5 cycles and 2.0×10^5 cycles loadings were measured, respectively. To investigate the effect of HDPC on dislocations, the dislocation densities after the application of HDPC at 1.0×10^5 cycles and 2.0×10^5 cycles were also evaluated, respectively. The dislocation density was concluded on the basis of the observation of the three samples for either condition with and without the application of HDPC. The dislocation distribution highly influences the qualitative estimation of dislocation density. To decrease the error of the qualitative estimation of dislocation density, ten areas around the hole of the specimen were observed under each condition in the present study.

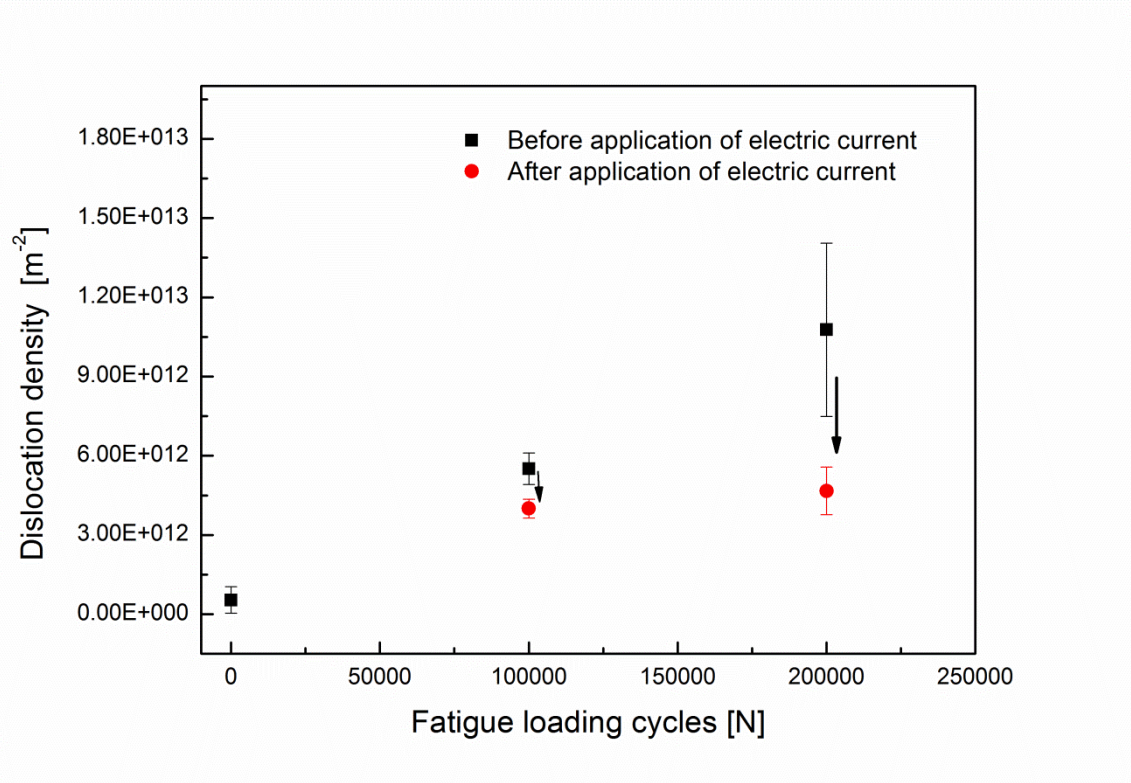

Fig. 4-7 Dislocation densities before and after the application of HDPC.

The dislocation density of the original state is 1.38×10^{9} m^{-2} in average. As shown in Fig.4-7, the dislocation density is very low. The dislocation density at 1.0×10^{5} cycles before the application of HDPC is 5.51×10^{12} m^{-2} in average. Dislocation density increases with the increase of loading cycles. A large amount of dislocation lines were observed at 2.0×10^{5} cycles. Dislocation density increased up to 1.08×10^{13} m^{-2} on average.

On the other hand, it is noted that dislocation density decreased to 4.67×10^{12} m^{-2} on average when the electric current was applied at 2.0×10^{5} cycles. When the high-density pulse current was applied at 1.0×10^{5} cycles, dislocation density is decreased to 4.0×10^{12} m^{-2} on average. The results show that the delaying effect of HDPC on fatigue crack initiation is related to the decrease of dislocation density.

In addition, when fatigue crack initiation occurs at 2.34×10^{5} cycles without the application of HDPC (Fig. 4-4 (a)), the dislocation density was measured to be 1.21×10^{13} m^{-2} in average. On the other hand, for the occurrence of crack initiation at 2.93×10^{5} cycles with the application of HDPC at 2.0×10^{5} cycles (Fig. 4-4 (b)), the dislocation density was measured to be 1.18×10^{13} m^{-2} in average. Moreover, for the multi-application of HDPC, when the high-density pulse current was applied at 2.5×10^{5} and 3.0×10^{5} cycles, respectively, the dislocation densities were measured to be 6.65×10^{12} m^{-2} and 8.35×10^{12} m^{-2} in average.

4.4 The Mechanism of healing effect on dislocation

4.4.1 Electron wind force

The idea that the electrons in a metal exert a drag on dislocations, as shown in Fig. 4-8, especially those moving at high speeds at very low temperatures, is now generally accepted [14]. The drift electrons in a metal may assist dislocations in overcoming obstacles to their motion. The drift electrons can exert a push or wind on dislocations, in contrast to a drag. That moving electrons in a metal crystal may interact with the dislocations therein was first reported by Troitskii and Lichtman in 1963 [15]. They found during electron irradiation of Zn single crystals undergoing plastic deformation that occurred a significant decrease in the flow stress and an improvement in ductility when the electron beam was directed along the slip plane.

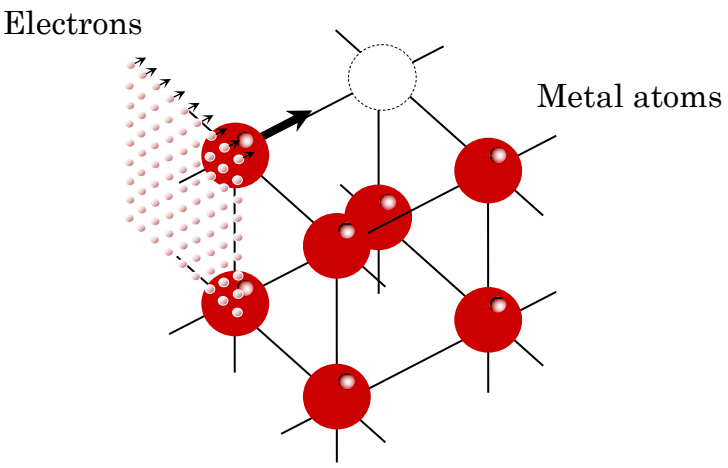

Fig. 4-8 A schematic showing the electron wind force.

The ideas that drift electrons can influence the generation and motion of dislocations led Troitskii and other scientists to conduct an extensive series of investigations into the influence of direct electric current pulses on the mechanical properties of metals.

The electric current can exert a drag on dislocations as the electrons collide with atoms. The force is named electron wind force and it is proportional to current density [16]. Williams et al. [17] verified the electron wind force exerting on the motion of nanoscale structures by experiment. The structures can be moved by the electron wind force back and forth when the direction of the current was changed. S.W. Nam et al. [18] studied the effect of electric pulses on the crystalline-to-amorphous phase change in a single crystalline nanowire memory device by in situ transmission electron microscopy. They found that electrical pulses produce dislocations in crystalline nanowire, which become mobile and glide in the direction of hole-carried motion.

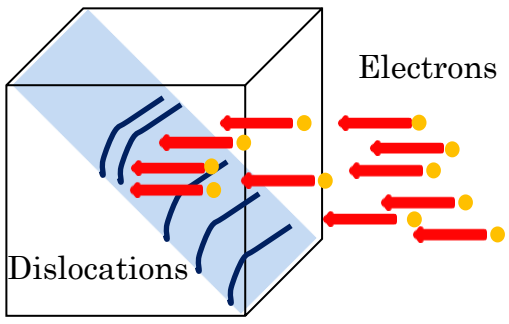

Fig. 4-9 A schematic showing the electron wind force on dislocation.

In this study, it is considered that the electric wind force can exert a drag on dislocations as the electrons collide with atoms when electric current was applied upon unloading as shown in Fig. 4-9. The electron drag coefficient, B_e [14], is given by the following expression

$$(f/l) = \tau b = B_e v_d , \qquad (4\text{-}3)$$

where (f/l) is the force per unit length acting on the dislocation, τ is the resolved shear stress, b the Burgers vector and v_d the dislocation velocity. B_e can be determined for metals by a number of methods, including ultrasonic attenuation, dislocation velocity and the decrease in flow stress associated with the normal to superconducting transition and values in the range of 10^{-6}~10^{-3} have been reported. The more recent considerations suggest that B_e is of the order of 10^{-5} [19-21].

4.4.2 Decrease of dislocation density by high-density pulse current

The opposite parallel dislocations have an effect on each other at a distance. They attract each other since glide moving them together would reduce the energy. Moreover, the extended strain fields would begin to cancel even before annihilation. Edge dislocations of opposite sign are elastic dipoles of opposite sign and would attract like analogous electrical dipoles. When the opposite dislocations are not on the same slip plane they attract but can only move under special circumstances. The movement of dislocations toward each other and their final annihilation is an

important mechanism of recovery effect.

Dislocations have been found experimentally to play a fundamental role for fatigue crack initiation [22-25]. Even prior to macro-scale plasticity, dislocations get generated during cyclic loading, which cluster and form channel-vein structures and later on ladder-like structures. Ladder-like structures are found inside persistent slip bands which carry most of the plastic deformation and lead to surface roughness, in the form of so-called ex-, in- and protrusions. Especially during reverse loading, the newly generated dislocations may glide back, with the two dislocations of opposite sign approaching each other. They annihilate when the distance between them is less than a critical distance. This distance is a material parameter and is taken to be 6*b* commonly. Annihilation also occurs when two dislocations of opposite sign from different dislocation pairs approach each other. In this case, the other dislocations of those pairs are taken to recombine to form a new dislocation pair. Furthermore, dislocations can leave the grain at the free surface, leaving behind a step of the height equal to *b*. The geometrical change at the surface is not taken into account. According to St. Venant's principle [26], the size of the area influenced by the surface step is on the order of the surface step, i.e. *b*. This area is very small compared to the grain size. Furthermore, this area is at the free surface. The driving forces on the dislocations are dominated by the shear stress, which pulls the dislocations out of the crystal. However, the step produced by them increases and with it the area influenced by the surface roughness when more dislocations move out at the free surface.

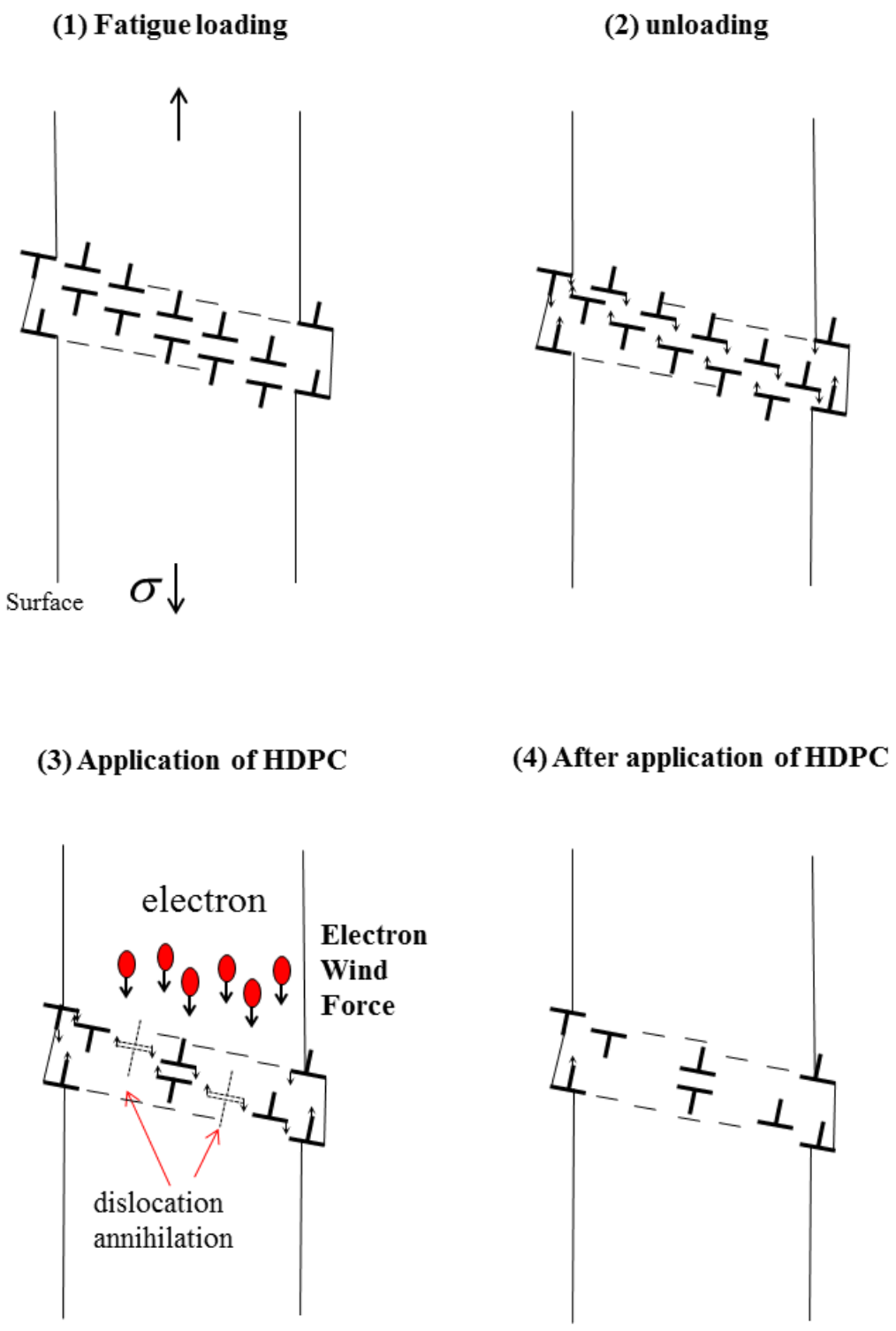

Fig. 4-10 A schematic showing the electron wind force on dislocation motion.

During fatigue loading process, once dislocations are nucleated, they glide away from the source and more dislocations get generated. With the motion and accumulation of dislocation, the dislocation density increased as shown in the Fig. 4-10 (1). When decreasing the applied stress, some dislocations glide back and annihilate each other. During the cyclic fatigue loading, the total strain energy of dislocation is minimized in the system upon unloading or minimum loading as shown in Fig. 4-10 (2). Hence, dislocations with opposite signs are activated to reverse slip on an adjacent plane [27]. The movement and annihilation of dislocations is an important mechanism of the recovery effect of fatigue damage. The annihilation of dislocations reduced the dislocation density.

When the high-density pulse current was applied upon unloading, the electric current can exert a drag on dislocations as the electrons collide with atoms. Therefore the electron wind force is one of the important reasons for the improved reverse of dislocations as shown in Fig. 4-10 (3). On the basis of experimental results, the reverse of dislocations leads to uniform distribution and low density of dislocations. Thus, after applied electric current, dislocation density was decreased due to the annihilation of dislocation dipoles as shown in Fig. 4-10 (4).

4.4.3 Joule heating effect

The application of HDPC causes a high-speed heating. To clarify the Joule heating effect on the healing of the fatigue damage, the increase of the temperature was

investigated. The temperature rise at the root of the notch tip was measured by the thermocouple temperature measurement equipment (LOGER GL900). The measured result was shown in Fig. 4-11. Thermal distribution around the notch due to the application of HDPC was approximately 230 ℃. Since the increased temperature is relative low, it is thought that the joule heating is a side effect in this study. Zhou et al. [28] also compared the dislocation densities under the treatments of electropulsing and annealing. It was found that the dislocation density in the electropulsed treatment is lower than that in the annealed treatment. Moreover, it was suggested that the effect of heating on the mobility of the dislocation is limited.

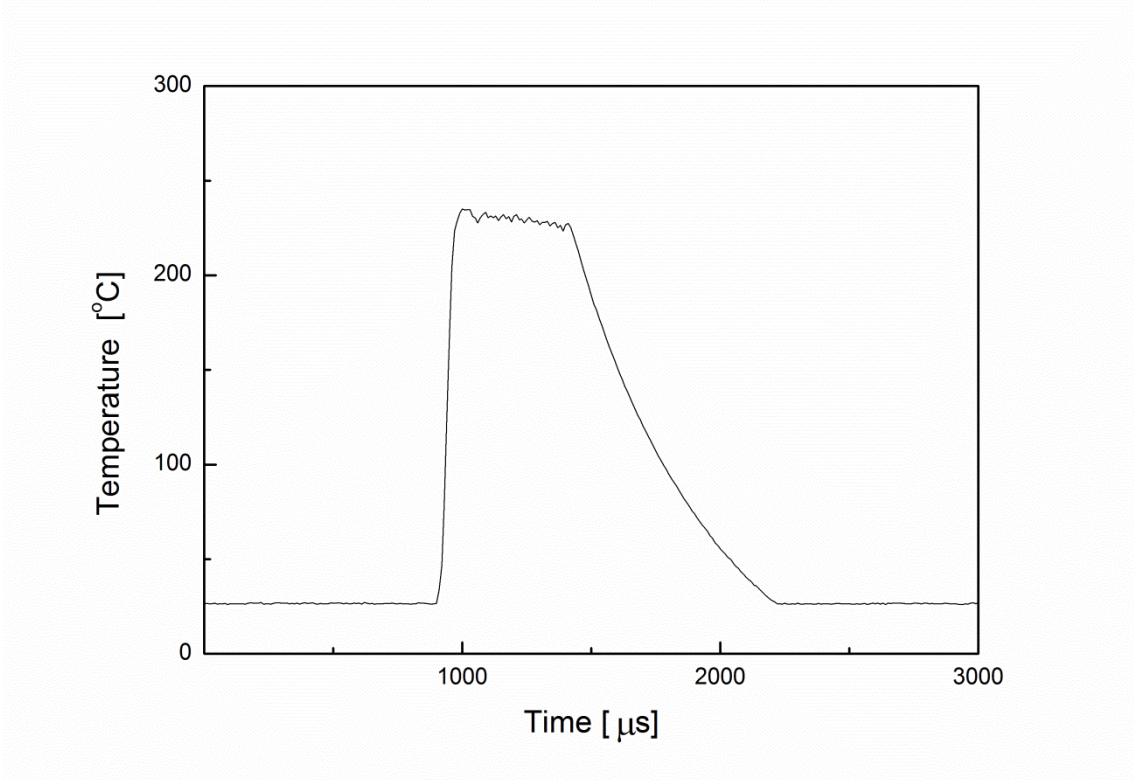

Fig. 4-11 The temperature rise due to the application of HDPC.

4.5 The Mechanism of healing effect on fatigue damage

To explain the reason of healing effect on the fatigue damage, the healing effect was discussed by analysis of the healing of slip bands, recovery of residual strain and strain hardening. The physics of the slip bands is the essential to explain the mechanism of healing slip bands.

Figure 4-12 shows the vacancy-dipole models for explaining the nucleation of slip bands. The nucleation of slip bands at the beginning stage of cyclic saturation is also accompanied by the formation of extrusions. This surface roughening appears to be instigated when the average dislocation distance in the fatigued matrix approaches the annihilation distance for dislocations. The first specific model proposed by Essmann et al. [29] ascribes the formation of static extrusions to super-saturation of vacancies in the PSBs. The random slip produces the notch peak geometry that is the source of fatigue crack initiation [30]. They developed a comprehensive model for surface roughening and crack nucleation on the basis of the hypothesis that the annihilation of the dislocations within the slip band is the origin of slip irreversibility.

The mechanisms proposed by Essmann et al. [29] can be described by the following sequence of events, as shown in Fig. 4-12. Dislocation structures that are generated at Franck-Read sources, *S*, are terminated by mutual annihilation before the reversal of strain. The annihilation of vacancy-type dipoles, as shown in Fig. 4-12 (a), is the dominant point defect generation process. If two screw dislocations of opposite

sign, left hand screw, S_{LH}, and right hand screw, S_{RH}, glide in the PSB channels, they will annihilate each other by cross slip when the distance between this pair of dislocations becomes less than a critical spacing, y_s. Similarly, a dipole consisting of edge dislocations of opposite sign will annihilate to form a vacancy if the spacing of the edge dislocations, y_e, becomes less than the critical spacing.

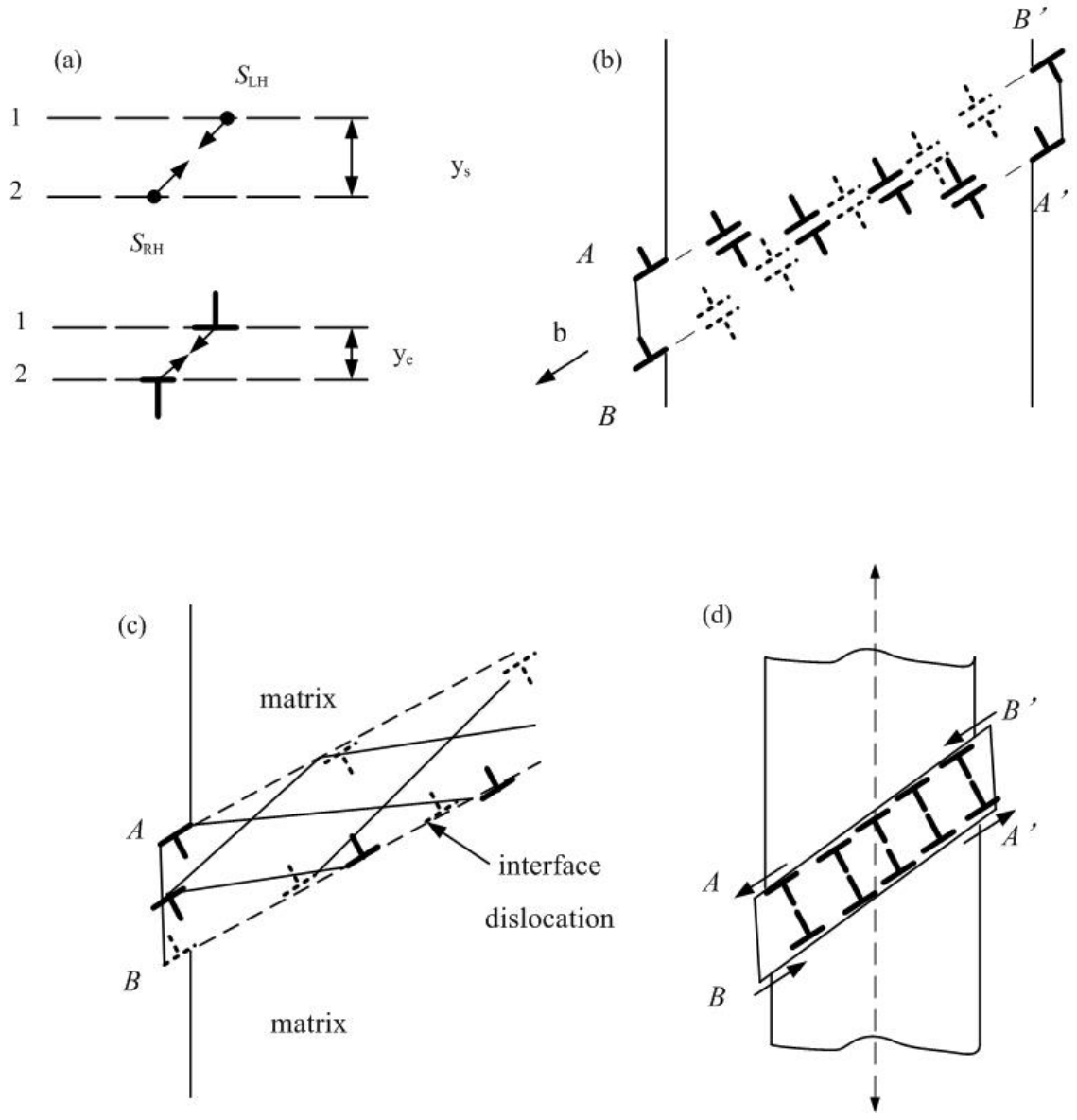

Fig. 4-12 (a) Descriptions of the critical annihilation distance for screw and

edge dislocations. (b) Mechanism of extrusion formation by combined glide and dislocation annihilation. (c) Irreversible slip in the slip bands creating effective interfacial dislocations which put the slip bands in a state of compression. (d) The combined effects of applied stresses and internal stresses.

Dislocations moving during the tensile portion of the fatigue cycle are denoted by solid symbols and those moving during the compression portion by dotted symbols. During tensile loading process, the slip is transmitted across the specimen by the sequence of microscopic processes extending from *A* to *A'*. At the locations where the edge dislocations are annihilated, the plane on which up slip is dominant is changed because of the annihilation process. Therefore, the effective slip plane *A-A'* is not parallel to the primary Burgers vector *b*, but is slightly inclined to *b*. Slip steps are created at surface locations *A* and *A'* during the tensile portion of fatigue loading.

On reversing the strain into compression, slip steps are formed at *B* and *B'* by similar process. The steps *A-B* and *A'-B'* thus constitute an extrusion [26]. If interstitial-type dipoles, rather than vacancy-type dipoles, are considered, then intrusions, rather than extrusions, form by a process analogous to that described in Fig. 4-12 (b). The extrusion in Fig. 4-12 (b) ceases to grow when the concentration of vacancies formed by edged dislocation annihilation attains a saturation value, within the slip band. At saturation, the effective slip plane no longer deviates from ***b*.** While Fig. 4-12 (b) illustrates the formation of extrusions by two microscopic slip processes,

Fig. 4-12 (c) schematically shows this phenomenon for the situation involving the superposition of multiple slip processes. The path *X*-*Y* denotes the glide of a combined slip process aided by annihilation, just as in Fig. 4-12 (b).

For the sake of clarity, the other paths are merely represented by straight lines. These lines join edge dislocations which have either survived the annihilation process and arrived at the free surface or have been deposited at the PSB-matrix interface. These latter interface dislocations have the same sign and give rise to internal stresses [26]. Thus, the net result of the irreversible slip process after one cycle is a row of edge dislocations at the PSB-matrix interface. The extra half planes of atoms of these edge dislocations face into the PSBs.

The arrangement of interface dislocations in Fig. 4-12 (c) leads to an elastic compressive stress within the slip bands acting along *b* and to a tensile stress in the matrix adjoining the slip bands [26]. The combined effect of the applied stress and the internal stress produced by the interface dislocations is schematically shown in Fig. 4-12 (d). The bigger arrows denote the internal stress arising from the mutual repulsions of the interface dislocations. The smaller arrows refer to the stress resolved in the direction of the PSBs due to the far field axial load, which reverses sign during every half fatigue cycle. Thus, *A* and *A'* serve as stress concentration points in tensile loading where the internal stress and the applied stress combine to produce high local stresses. *B* and *B'* are stress concentrating sites during compression where the two stresses oppose each other.

As shown in Fig. 4-12, the slip bands were formed during cyclic loading. In the

formation of slip bands, the dislocation motion plays an important role in the fatigue response of the material. Figure 4-12 shows the glide of dislocation within the slip bands. As a consequence, the slip lines appeared in several favorably oriented crystals on the surface of the material. After the application of HDPC, the results reveal that the annihilation of dislocations induced the uniform distribution and low density of dislocations. For the early stage of extrusions with height less than 10 nm, it results that the destroyed slip system leads to the decrease of extrusion height and made the extrusions vanish locally. However, if the new surface of extrusion is oxidized, it is difficult to reverse the height of extrusion by applied the electric current. It is thought that the recovery of dislocation pile-ups takes an effect to heal the initial extrusion.

The discovery of dislocations and their role in plastic deformation of crystalline materials led to the first models of extrusion and intrusion formation [31]. However, the discovery of the role of cyclic strain localization, the identification of specific dislocation structures of the PSBs led to more accurate models of surface relief formation and fatigue crack nucleation. The evidence on point defect formation in cyclic straining and their migration [32, 33] suggested the important role of vacancies or interstitials in the formation of the surface relief.

The locally disappear of slip bands and the decrease of slip height may be due to the decrease of local strain concentration at the interface of slip bands and matrix. The relationship between the local strain, ε_l, for an individual slip bands and its height h was given as [34, 35]

$$\varepsilon_l = kh\varepsilon_p, \qquad (4\text{-}4)$$

where k is a constant, ε_p is the average plastic strain. It suggested that the relaxation of local strain concentration reduces the reverse of slip bands. The recovery of residual strain corresponds to the locally disappear of slip bands and the decrease of slip height.

Fatigue crack initiation is a consequence of cyclic slip. It implies cyclic plastic deformation. Fatigue occurs at stress amplitudes below the yield stress. At such a low stress level, plastic deformation is limited to a small number of grains of the material. This microplasticity preferably occurs in grains at the material surface because of the lower constraint on slip. A slip step implies that a rim of new material will be exposed to the environment. The fresh surface material will be immediately covered by an oxide layer in most environments. Another significant aspect is that slip during the increase of the load also implies some strain hardening in the slip bands. As a consequence, upon unloading a larger shear stress will be present on the same slip band, but now in the reversed direction. Reversed slip will thus preferably occur in the same slip band. If fatigue would be a fully reversible process, the fatigue fracture will never occur. Two reasons why it cannot be fully reversible are as follows. First, the oxide monolayer cannot simply be removed from the slip step. Secondly, strain hardening in the slip bands is also not fully reversible. After the application of HDPC, the recovery of strain hardening can have an assistant effect on the reverse of slip

bands.

On the other hand, strain accumulates primarily through dislocation motion resulting in slip within the grains of the polycrystalline aggregate. Upon forward and reverse loading, slip moves in distinct paths within each cycle, in which the slip processes are not fully reversible. Slip irreversibilities and the arrangements of dislocations in low energy configurations define the unique nature of fatigue and the existence of PSBs. As the hardness is structurally sensitive and related closely to the intrinsic structural factors of the tested specimen at the submicroscopical level [36, 37], it is strongly affected by the distribution of dislocations. Graca and Nix determined the relationship between the hardness and the dislocation density [38, 39]. They found that the HV depends on the statistically stored dislocation density. Therefore, it can be inferred from the above analysis that the recovery of residual strain and strain hardening were due to the recovery of dislocation including the decrease of dislocation density and the disappear of dislocation pile-ups.

4.6 Summary

In the microstructure, the decrease of the dislocation density was quantitatively evaluated to further understand the mechanism of the healing effect of fatigue damage due to the application of HDPC. After the application of HDPC, the partial disappearance of the dislocation pile-ups was found. It was analyzed that the decrease of dislocation density was due to the dislocation annihilation. When the HDPC was

applied upon unloading, the reverse glide of dislocation was improved due to the effect of the electron wind force. In addition, the application of high-density pulse current causes a high-rate heating. The temperature rise around the notch tip was relative low. Therefore, it is thought that joule heating is a side effect.

References:

[1] S.V. Konovalov, A.A. Atroshkina, Y.F. Ivanov, V.E. Gromov, Evolution of dislocation substructures in fatigue loaded and failed stainless steel with the intermediate electropulsing treatment, Mater. Sci. Eng. A, 527 (2010) 3040-3043.

[2] O.V. Sosnin, et al., Control of austenite steel fatigue strength, Int. J. Fatigue, 27 (2005) 1186-1191.

[3] O.V. Sosnin, et al., The structural-phase state changes under the pulse current influence on the fatigue loaded steel, Int. J. Fatigue, 27 (2005) 1221-1226.

[4] G.H. He, et al., Nvestigation of thermal expansion measurement of brass strip H62 after high current density electropulsing by the CCD technique, Mater. Sci. Eng. A, 292 (2000) 183-188.

[5] Y.P. Tang, A. Hosoi, Y. Iwase, Y. Ju, Effect of high-density electric current on the microstructure and fatigue crack initiation of stainless steel, Mater. Trans., 54 (2013) 2085-2092.

[6] O.V. Sosnin, et al., Control of austenite steel fatigue strength, Int. J. Fatigue, 27

(2005) 1186-1191.

[7] S.V. Konovalov, A.A. Atroshkina, Y.F. Ivanov, V.E. Gromov, Evolution of dislocation substructures in fatigue loaded and failed stainless steel with the intermediate electropulsing treatment, Mater. Sci. Eng. A, 527 (2010) 3040-3043.

[8] C. Gaudin, X. Feaugas, Cyclic creep process in AISI 316L stainless steel in terms of dislocation patterns and internal stresses, Acta Mater., 52 (2004) 3097-3110.

[9] D.M. Norfleet, D.M. Dimiduk, S.J. Polasik, M.D. Uchic, M.J. Mills, Dislocation structures and their relationship to strength in deformed nickel microcrystals, Acta Mater., 56 (2008) 2988-3001.

[10] M.S. Pham, C. Solenthaler, K.G. Janssens, S.R. Holdsworth, Dislocation structure evolution and its effects on cyclic deformation response of AISI 316L stainless steel, Mater. Sci. Eng. A, 528 (2011) 3261-3269.

[11] D.B. Williams, C.B. Carter, Transmission electron microscopy, Plenum Press, (1996).

[12] P.M. Kelly, A. Jostsons, R.G. Blake, The determination of foil thickness by scanning transmission electron microscopy, Phys. Status Solidi A, 31 (1975) 771-780.

[13] T. Kruml, V. Paidar, J.L. Martin, Dislocation density in Ni3, Intermetallics, 8 (2000) 729-736.

[14] J.M. Galligan, Electrons, dislocations and low-temperature plastic deformation, Scripta Metal., 18 (1984) 643-653.

[15] O.A. Troitskii, V.I. Likhtman, Anisotropy of the effect of electron-beam and

irradiation on the deformation process of zinc single crystals in the brittle state, Dokl. Akad. Nauk SSR, 148 (1963) 332-334.

[16] A.F. Sprecher, S.L. Mannan, H. Conrad, On the mechanisms for the electroplastic effect in metals, Acta Metall. Mater., 34 (1986) 1145-1162.

[17] C. Tao, W. G. Cullen, E. D. Williams, Visualizing the electron scattering force in nanostructures, Science, 328 (2010) 736-740.

[18] S.W. Nam, et al., Electrical wind force-driven and dislocation template amorphization in phase-change nanowires, Science, 336 (2012) 1561-1566.

[19] K.M. Klimov, G.O. Shnyrev, I.I. Novikov, Electroplasticity of metals, Soviet Phys. Dokl., 19 (1975) 787-788.

[20] V. Ya. Kravchenko, Effect of directed electron beam on moving dislocations, Soviet Phys. Jetp, 24 (1967) 1135-1142.

[21] A.M. Roshchupkin, V.E. Miloshenko, V.E. Kalinin, Effect of electrons on the motion of dislocations in metals, Soviet Phys. Solid St., 21 (1979) 435-438.

[22] M.D. Sangid, The physics of fatigue crack initiation, Int. J. Fatigue, DOI information: dx.doi.org/10.1016/j.ijfatigue.2012.10.009.

[23] S. Brinckmann, E.V. Giessen, A discrete dislocation dynamics study aiming at understanding fatigue crack initiation, Mater. Sci. Eng. A, 387-389 (2004) 461-464.

[24] S. Brinckmann, E.V. Giessen, A fatigue crack initiation model incorporating discrete dislocation plasticity and surface roughness, Int. J. Fract., 148 (2007) 155-167.

[25] S. Brinckmann, On the role of dislocations in fatigue crack initiation, (1974).

[26] S. Suresh, Fatigue of materials, Cambridge University Press, (1991).

[27] T. Mura, Y. Nakasone, A theory of fatigue crack initiation in solids, J. Appl. Mech., 57 (1990) 1-6.

[28] Y. Z. Zhou, S. H. Xiao, J. D. Guo, Recrystallized microstructure in cold worked brass produced by electropulsing treatment, Mater. Lett., 58 (2004) 1948-1951.

[29] U. Essmann, U. Gosele, H. Mughrabi, A model of extrusions and intrusions in fatigued metals I. Point defect production and growth of extrusions, Phil. Mag. A, 44 (1981) 405-426.

[30] K. Differt, U. Essmann, H. Mughrabi, A model of extrusions and intrusions in fatigued metals II. Surface roughening by random irreversible slip, Phil. Mag. A, 54 (1986) 237-258.

[31] O. Devereux, A.J. McEvily, R.W. Staehle, Corrosion fatigue: chemistry, mechanics and microstructure, National Association of Corrosion Engineers, (1972).

[32] J. Polak, The effect of intermediate annealing on the electrical resistivity and shear stress of fatigued copper, Scripta Metall., 4 (1970) 761-764.

[33] J. Polak, Resistivity of fatigued copper single crystals, Mater. Sci. Eng., 89 (1987) 35-43.

[34] W.D. Cao, H. Conrad, On the effect of persistent sip band (PSB) parameters on fatigue life, Fatigue Fract. Eng. Mater. Struct., 15 (1992) 573-531.

[35] H. Conrad, J. White, W. D. Cao, X. P. Lu, A. F. Sprecher, Effect of electric

current pulses on fatigue characteristics of polycrystalline copper, Mater. Sci. Eng. A, 145 (1991) 1-12.

[36] M. Klesnil, P. Lukas, Fatigue of metallic materials, Elsevier, (1980).

[37] B.I. Sandor, Undamentals of cyclic stress and strain, University of Wisconsin Press, (1972).

[38] Y.U. Milman, B.A. Galanov, S.I. Chugunova, Plasticity characteristic obtained through hardness measurements, Acta Metall. Mater., 41 (1993) 2523-2532.

[39] D.Y. Ye, D.J. Wang, P. An, Characteristics of the change in the surface microhardness during high cycle fatigue damage, Mater. Chem. Phys., 44 (1996) 179-181.

Chapter 5 Evaluation of the delaying effect of fatigue crack initiation

5.1 Introduction

Fatigue is characterized by a series of forward and reverse loading. The primary emphasis is the relationship between the fatigue crack initiation and the microstructure of material [1-5]. Irreversible slip leads to dislocation motion on a slip plane and dislocation pile–ups. Dislocation density increased with the accumulation of dislocation pile-ups. According to the classical dislocation dipole model proposed by Tanaka and Mura [6-14], dislocations nucleate and glide in the slip bands under forward and reverse loading. Tanaka and Mura envisioned that fatigue crack initiation occurs by the accumulation of dislocation dipoles during strain cycling [6-8]. When the stored strain energy of accumulated dislocations reaches a critical value, the fatigue crack occurs.

To investigate the effect of HDPC on the delay of fatigue crack initiation, the dislocation structures before and after the application of electric current were investigated by transmission electron microscopy in chapter 4. Dislocation density was quantitatively characterized before and after the application of HDPC. In this chapter, the delaying effect of the crack initiation based on the application of HDPC

was evaluated by the fatigue crack-initiation model in which the accumulation of the dislocation density was considered. The relationship between the delaying fatigue crack initiation and the decrease of dislocation density due to the application of HDPC was established.

5.2 Tanaka and Mura model

5.2.1 Dislocation models of fatigue crack initiation

Current fatigue crack initiation models are formulated based on either stress or strain. For uniaxial cyclic loading, fatigue crack initiation in metals can be described in terms of the stress-life (S-N_f) approach *via* the relation [15]

$$\sigma_a = \sigma_f N_f^{\alpha}, \qquad (5\text{-}1)$$

where σ_a is the stress amplitude, σ_f is the fatigue strength coefficient, N_f is the number of cycles to failure, and α is the fatigue strength exponent. Failure is usually defined as fatigue fracture of the specimens, but can also be defined as initiation of a fatigue crack to a certain length or depth. In the strain-life approach, the plastic strain range ($\Delta \varepsilon_p$) is related to the cycles to failure according to the Coffin-Manson relation, given by [16, 17]

$$\frac{\Delta\varepsilon_p}{2} = \varepsilon_f N_f^{\beta}, \qquad (5\text{-}2)$$

where ε_f is the fatigue ductility coefficient, and β is the fatigue ductility exponent. Both phenomenological models are well known, but either contains parameters that describe the role of microstructure in the fatigue-crack initiation process or the fatigue life.

To explain fatigue crack initiation or combine dislocation structuring and crack initiation, several models in the literature had been studied [18]. These models can be divided into two groups. On the one hand, the continuum based models treat the dislocations not individually but as an average over a region [19]. On the other hand, the models are based on discrete dislocation or discrete slip plane events [20]. The latter is to indicate experimental observations by a sequence of physical mechanisms.

Mott et al. [21] proposed one of the first models in 1958. It is suggested that vacancies are generated below the surface as a result of the production of extrusions. Because he found more extrusions than intrusions on the surface, it was concluded that vacancies accumulate inside. Consequently, these clusters of vacancies then grow and form cracks underneath the surface. Antonopoulos et al. [22] proposed a model based on the vacancy dipoles, which are more likely to form than interstitial dipoles. The formation energy of the vacancy dipoles is lower than that of interstitials. Due to the difference in formation energy, interstitials are thought to be much earlier to escape than vacancies. Furthermore, it is concluded that there would be twice as many vacancies as interstitials in the PSBs during fatigue. Finally, the results of the dislocation dipole are a super vacancy dipole and then placed at the end of the wall due to the adding up the dislocation dipoles in a PSBs wall. A row of super

dislocations along the PSBs-matrix interface were formed. Antonopoulos et al. proposed that the configuration leads to tension normal to the PSB-matrix interface in the slip bands. Moreover, the volume increase due to the growth of protrusions from the density of vacancy dipoles were calculated, which are corresponding to the values measured in experiments [22].

Essmann et al. [23] observed the pre-dominance of vacancy over interstitial dipoles and proposed the sequence of events. A dislocation pair *A*-*B* nucleate, the dislocation *A* glides to the surface of the grain and produces a surface step while dislocation *B* stays inside the bulk. Meanwhile, another dislocation pair is generated on an adjacent glide plane. Dislocation *C* of the newly generated dislocation pair is forming a vacancy dipole with dislocation *B*. Thus, a band of dislocation dipoles forms due to the similar process including the gliding and formation of vacancy dipoles [18].

It is noted that the dislocations on the PSBs-matrix interface in the Essmann model are changed in sign compared to the Antonopoulos model. However, the extrusion in the both models developed on both sides of the crystal. These extrusions are as the result of the vacancy dipoles which develop in the slip bands [18]. Moreover, Essmann et al. [23] proposed that vacancies are diffusing along the dislocation loops through diffusion to the matrix which surrounds the slip bands. It is argued that this effect leads to the growth of protrusions at elevated temperatures. The diffusion is impossible and the growth of protrusions is restricted at lower temperatures. Repetto et al. [24] reported constitutive rules for the vacancy generation and corresponding volumetric expansion inside the slip bands at elevated temperatures.

Additionally, they included the diffusion of vacancies into the matrix and found that the protrusion would grow and confirmed the results of the shape of the protrusion by the simulation and experiments [18]. On one side of the protrusion, Repetto et al. [24] found that according to the models of Antonopoulos et al. and Essmann et al., the free surface forms an acute angle with the protrusion. It is concluded that fatigue crack initiation is due to the stress singularity arising from this acute angle. Differt et al. [25] captured the small extrusion and intrusion within a protrusion based on the statistical irreversibility of slip.

Brown et al. [26] reported the dislocation distribution at the PSB-matrix interface as Antonopoulos. However, a different way was used in their study of the dislocation distribution. According to the dislocation distribution, they analyzed the stress at the free surface and in the material. Neumann [27] proposed a model according to the activation of two slip systems. In the first tensile stroke slip planes *A* and *B* get active and the material opens up. In the compression phase the dislocations glide back. However, both side of the evolving crack touch macroscopically like ordinary pieces of metal, it is difficult to totally heal the material. Therefore, a crack has initiated along slip plane *A* to the intersection with slip plane *B* [18].

It was found that all these models were based on the assumption that there are more vacancy dipoles than interstitial dipoles in the slip bands. Some researchers looked forward to investigate the change in electrical resistivity of metals during fatigue to investigate the dipole formation. Johnson et al. [28], Helgeland [29], Eikum et al. [30], Polak [31] and Kromp et al. [32, 33] found that the number of defects point increase

during fatigue loading cycles. Unfortunately, the number of vacancies were still not quantified with respect to interstitials. However, if most of the defects are assumed to be vacancies, the number of vacancies in those experiments is corresponding to the values predicted by Antonopoulos et al. [20] and Essmann et al. [23], which are based on the size of the protrusion [18].

Fatigue crack initiation is often associated with the formation of persistent slip bands [34-37]. These slip bands are produced by random irreversible slip on surface grains that leads to surface roughening, the formation of extrusions and intrusions and eventually to fatigue crack initiation within the slip bands. A crack nucleation criterion based on the formation of a critical notch depth by random slip in slip bands was proposed by Cheng and Laird [38]. This criterion, which is essentially identical to the Coffin-Manson relation [16, 19], has the form given by [39]

$$\frac{\Delta\gamma_p}{2} N_i^{\alpha} = C \qquad (5\text{-}3)$$

for metals subjected to a plastic shear strain range ($\Delta\gamma_p$). The number of fatigue cycles to crack initiation is N_i, and C is a constant. The value of the exponent α is 0.78, which was obtained by relating the slip offsets in the slip bands to the applied strain amplitude. Statistical considerations of plastic strain accumulation in a localized slip bands led to a value of 0.5 for α. In an earlier article, Saxena and Antolovich [40] demonstrated that the parameter of α in Cu-Al alloys varied from 0.5 to 1; this variation was related to the stacking fault energy and to the slip morphology. Thus, there is experimental evidence and a general consensus that the value of α ranges

from 0.5 to 1 [39], depending on the plastic strain localization process. Although it originated from consideration of slip bands formation by irreversible random slip, Eq. 5-3 by itself does not provide any insight into the role of microstructure in the crack initiation process.

More fatigue crack initiation models incorporate microstructural parameters in a direct and explicit manner. In a series of three articles, Tanaka and Mura proposed dislocation models for treating fatigue crack initiation at slip bands [6-8]. Tanaka and Mura envisioned that fatigue crack initiation occurs by the accumulation of dislocation dipoles during strain cycling. For crack initiation along a slip band, the dislocation dipole accumulation model is given by [6]

$$(\Delta\tau - 2k)N_i^{1/2} = [\frac{8\mu W_s}{\pi a}]^{1/2}, \qquad (5\text{-}4)$$

where $\Delta\tau$ is the shear stress range, k is the friction stress of dislocation, μ is the shear modulus, $2a$ is the grain size, and W_s is the specific fracture energy per unit area along the slip bands. For crack initiation at a grain boundary, Eq. 5-4 still applies, but the term W_s is replaced by the specific fracture energy per unit area of grain boundary (W_G). Several modifications of the basic model have also been made by Mura and co-workers, which are described in a series of articles [8-13, 39]. The fatigue crack initiation model developed by Venkataraman et al. [9, 39] incorporates a surface energy term (γ_s) and a slip irreversibility factor (m), which has a value between 0 and 1. The stress life relation obtained by Venkataraman et al. is

$$(\Delta\tau - 2k)\ N_i^a = 0.37\left(\frac{\mu d}{mh}\right)\left(\frac{\gamma_s}{\mu d}\right)^{1/2} \qquad (5\text{-}5)$$

which predicts a grain size dependence that is contradictory to Eq. 5-4 and experimental data. The scaling law for fatigue crack initiation proposed by Chan [41] is an extension of the Coffin-Manson LCF equation to include a microstructure size parameter. The modified strain life equation gives a grain size dependence of fatigue life initiation that is similar to that described in Eq. 5-4. The statistical model by Ihara and Tanaka [14] considers the accumulation of stochastic damage within the dislocation cell structure formed during the fatigue process. Harvey et al. [42] proposed a fatigue crack initiation based on the deepening of slip bands into a fatigue crack during strain cycling. Fatigue crack initiation was assumed to occur when the cumulative slip height displacement. K.S. Chan [43] gave a microstructure based fatigue crack initiation model. They presented results on the development of a microstructure based fatigue crack initiation model which includes explicit crack size and microstructure scale parameters.

All the models mentioned above either assume a specific sequence of slip events or assume that a PSB has already formed, which will then nucleate a crack. Additionally, none of the models explains the channel-vein or the ladder-like structure in PSBs. Tanaka and Mura model is one of the most classical models for the fatigue crack initiation. Thus, in this study, the calculation of delaying effect on the fatigue crack initiation is based on the Tanaka and Mura model, and the detail was addressed in the

next section.

5.2.2 Dislocation density model

The essence of the fatigue crack initiation process by the dislocation dipole mechanism, operating in a surface grain, is depicted in Fig. 5-1 [6-14]. During fatigue loading, irreversible slip occurs in a favorably oriented surface grain, leading to dislocation motion on a slip plane and dislocation pile-ups at grain boundaries. Here, h is the width of slip band, $2a$ is the grain size. Upon unloading, dislocations with opposite signs are activated on an adjacent plane, producing reverse slip and the formation of vacancy and interstitial dislocation dipoles at the ends of the double pile-ups.

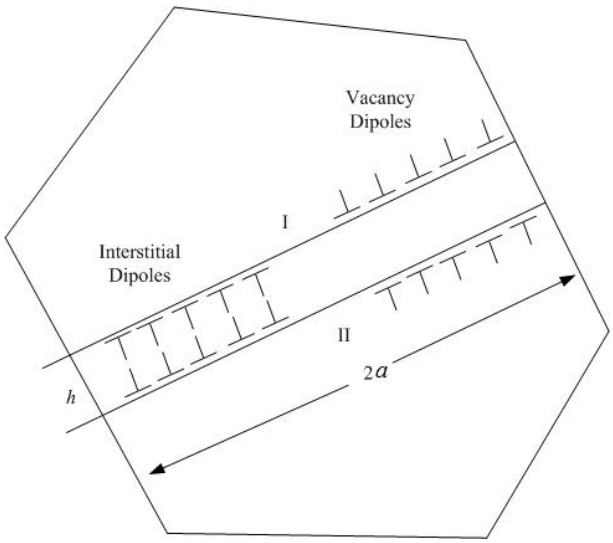

Fig. 5-1 A schematic showing the accumulation of dislocation dipoles generated by

irreversible slip during fatigue loading.

In order to investigate the delaying effect of HDPC on crack initiation, it is essential to investigate the mechanism of fatigue crack initiation due to dislocation. Irreversible slip leads to dislocation motion on a slip plane and dislocation pile–ups. Dislocation density increased with the accumulation of dislocation pile-ups. Representing the dislocation pile-ups in terms of continuum dislocations, Tanaka and Mura [6] showed the dislocation accumulation for the case of double pile-ups.

After cyclic loading of *n* cycles, the total density of dislocation, *D*, is given by

$$D_n = \frac{\pi(1-\nu)}{Ga}\left[(\tau_1 - k) + n(\Delta\tau - 2k)\right], \tag{5-6}$$

where

$$\Delta\tau = \tau_1 - \tau_2, \tag{5-7}$$

τ_1 is the maximum shear stress and τ_2 the minimum shear stress in one cycle. *k* is the frictional stress, *G* is the shear modulus, *v* is Poisson's ratio and *n* is the number of fatigue cycles. The stored strain energy of dislocation can be expressed with the function of dislocation density by [6]

$$W = \frac{\int_{-a}^{a} \pi D\, x\, d}{2}, \tag{5-8}$$

where, x is the glide distance of dislocation within the grain, $0<x<2a$. When the strain energy due to dislocation accumulates at the plastic zone reaches a critical value, microcracks at notch tip will occur. Therefore, the increase of dislocation density represented the accumulation of strain energy stored by dislocation. When dislocation density reaches a critical value, D_f, the number of fatigue cycles leading to crack initiation was obtained by equating the stored energy in the dislocation dipoles to the specific fracture energy (W_s). Mura and Nakasone [12] postulated that the onset of fatigue crack initiation occurs when the fracture energy change reaches a maximum, and the number of cycles to reach the maximum free energy change is taken to be the number of cycles to fatigue crack initiation. The energy barrier can easily be provided by the stored strain energy of the dislocation dipoles, since the dipole structure is unstable with respect to the fatigue crack configuration.

5.3 Evaluation of the delaying effect of fatigue crack initiation due to the application of high-density pulse current

According to the theories of fatigue crack initiation mentioned earlier, there are criteria for crack initiation that are based on the accumulation of dislocations [7, 8]. From Eq. 5-6 and Eq. 5-9, we can obtain the relationship between dislocation density, D, and fatigue cycles, n, as shown in Fig. 5-2. Consequently, the damage parameter, P, can be readily evaluated in terms of the variation of dislocation density.

$$P = \frac{D_n - D_I}{D_F - D_I}, \tag{5-9}$$

where, D_I is the dislocation density of a non-damaged material, D_F is the dislocation density of a damaged material reaching crack initiation, and D_n is the dislocation density of a damaged material at any loading cycle before the crack initiation.

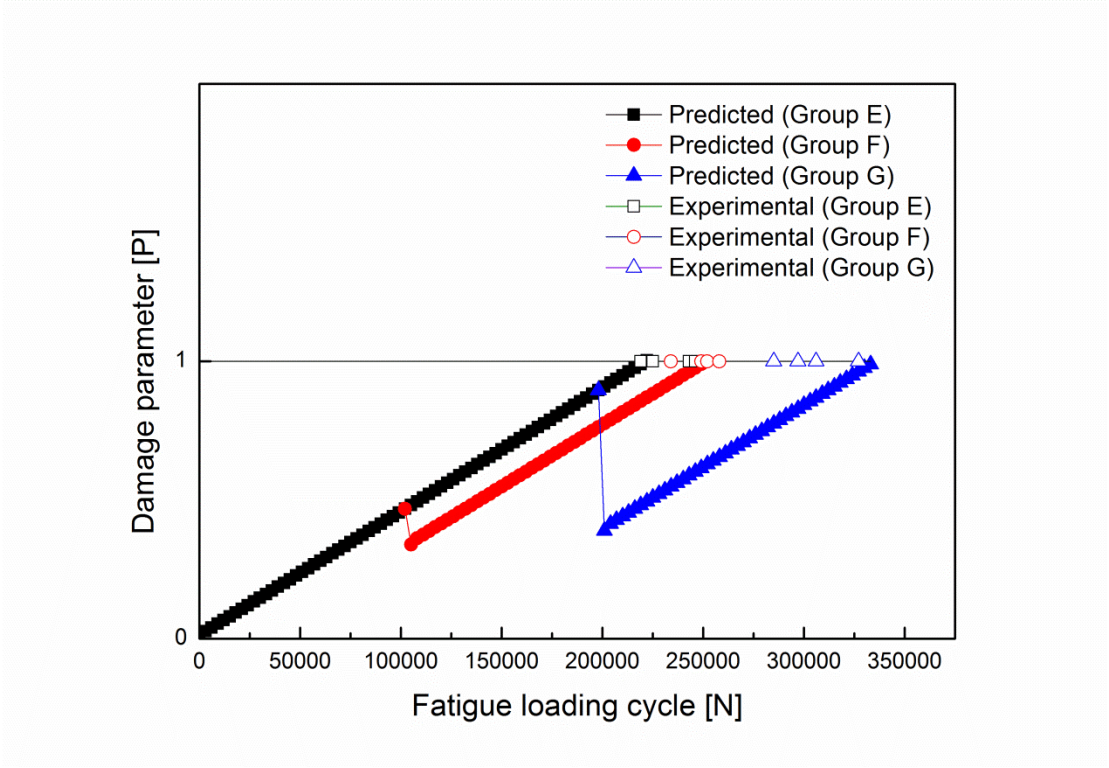

Fig. 5-2 Calculated damage parameter *vs* fatigue loading cycle under the conditions with and without the application of HDPC.

The delaying effect of HDPC on crack initiation was evaluated using the decrease of damage parameter as shown in Fig. 5-2. The dislocation density of the original

state was measured to be $D_I = 1.38 \times 10^9$ m^{-2} in average as described in section 4.3.2. Moreover, according to the experimental results that fatigue crack initiation occurs at 2.34×10^5 cycles under the condition without the application of HDPC, the value of dislocation density was measured to be $D_F = 1.21 \times 10^{13}$ m^{-2} in average. Therefore, the relationship between the damage parameter and fatigue loading cycle for Group E can be obtained from Eq. 5-6 and Eq. 5-9 as shown in Fig. 5-2, where considering c=2.025mm (crack length) and ω=1 mm (plastic width), τ_1 and τ_2 were determined to be 64.92 MPa and 3.25 MPa, respectively. k=25 MPa [38], v=0.25, G=77 GPa [43], a = 37.5 μm.

On the other hand, the dislocation density at 2.0×10^5 cycles before the application of HDPC was measured to be $D_{nM} = 1.08 \times 10^{13}$ m^{-2} in average (see section 4.3.2). Thus, according to the Eq. 5-9, the damage parameter of Group G was obtained to be P=0.90 at 2.0×10^5 cycles. After the application of HDPC, the measured dislocation density decreased to 4.67×10^{12} m^{-2}, and the damage parameter was calculated to be P=0.38 with Eq. 5-9. For the material without the application of HDPC (e.g. Group E), P=0.38 (i.e. D_{nM}=4.67×10^{12} m^{-2}, see section 4.3.2) is corresponding to the loading cycle of 0.94×10^5 from Eq. 5-6 and Eq. 5-9. Therefore, it can be considered that the loading cycle was delayed 1.06×10^5 (2.0×10^5-0.94×10^5) cycles to reach the same dislocation density after the application of HDPC. Since the measured dislocation density of the materials at the crack initiation after the application of HDPC at 2.0×10^5 cycles (i.e. $D_F = 1.18 \times 10^{13}$ m^{-2}, see section 4.3.2) , is similar as the case of without the application of HDPC (i.e. $D_F = 1.21 \times 10^{13}$ m^{-2}), we assume that the

increase of dislocation density with loading cycle is still corresponding to the Eq. 5-6 after the application of HDPC, and the damage parameters for fatigue crack initiation based on the dislocation density are the same under the conditions with and without the application of HDPC. The relationship between the damage parameter and fatigue loading cycle for Group G after the application of HDPC at 2.0×10^5 cycles, can be obtained by adding the delayed cycles of 1.06×10^5 to the relationship of Group E directly as shown in Fig.5-2. Consequently, the total number of cycles to reach the crack initiation was predicted to be 3.40 $\times10^5$ cycles. Although the actual average crack initiation cycle of 2.93×10^5 cycles (section 3.3) is less than the predicted cycle, the predicted number of cycles is within the scatter of experimental results.

Table 5-1 Experimental and calculated average number of cycles for crack initiation

	Group E	**Group F**	**Group G**
Experimental average number of cycles for initiation, *N*[cycle]	2.34×10^5	2.47×10^5	2.93×10^5
Calculated average number of cycles for initiation, *N*[cycle]		2.50×10^5	3.40×10^5

However, when electric current was applied at 1.0×10^5 cycles, the damage parameter, *P*, was decreased from 0.47 to 0.34. The number of cycles for crack initiation was predicted to be 2.50×10^5 cycles which is in agreement well with the experimental result of 2.47×10^5 cycles (section 3.3). The delaying effect of current

application depends on the healing effect of fatigue damage. Therefore, after the application of HDPC, the decrease of dislocation density can be used to predict the delaying of crack initiation. The comparison of the model calculation and experimental data was summarized in Table 5-1.

5.4 Multi-application of high-density pulse current

To improve the delaying effect on fatigue crack initiation by the application of HDPC, the delaying effect was investigated by multi-application of HDPC at a maximum net stress of σ_{max}=115 MPa. Furthermore, the delaying effect was analyzed by the fatigue damage parameter proposed in section 5.3. Here, the high-density pulse current was applied by increasing every 5.0×10^4 cycles from 2.0×10^5 cycles until real crack initiation occurs.

The delaying effect of multi-application of HDPC on fatigue crack initiation was evaluated using the decrease of damage parameter as shown in Fig. 5-3. After the high-density pulse current was applied at 2.0×10^5 cycles, 2.5×10^5 cycles and 3.0×10^5 cycles, respectively, it was found the loading cycles for crack initiation increased experimently to be 3.44×10^5 cycles in average. According to Eq. 5-6, 5-7 and 5-9, the fatigue damage parameters were obtained to be P=0.38 (i.e. $D_{nM}=4.67\times10^{12}$ m^{-2}, see section 4.3.2), P=0.55 (i.e. $D_{nM}=6.65\times10^{12}$ m^{-2}, see section 4.3.2) and P=0.69 (i.e. $D_{nM}=8.35\times10^{12}$ m^{-2}, see section 4.3.2) when the high-density pulse current was applied at 2.0×10^5 cycles, 2.5×10^5 cycles and 3.0×10^5 cycles, respectively.

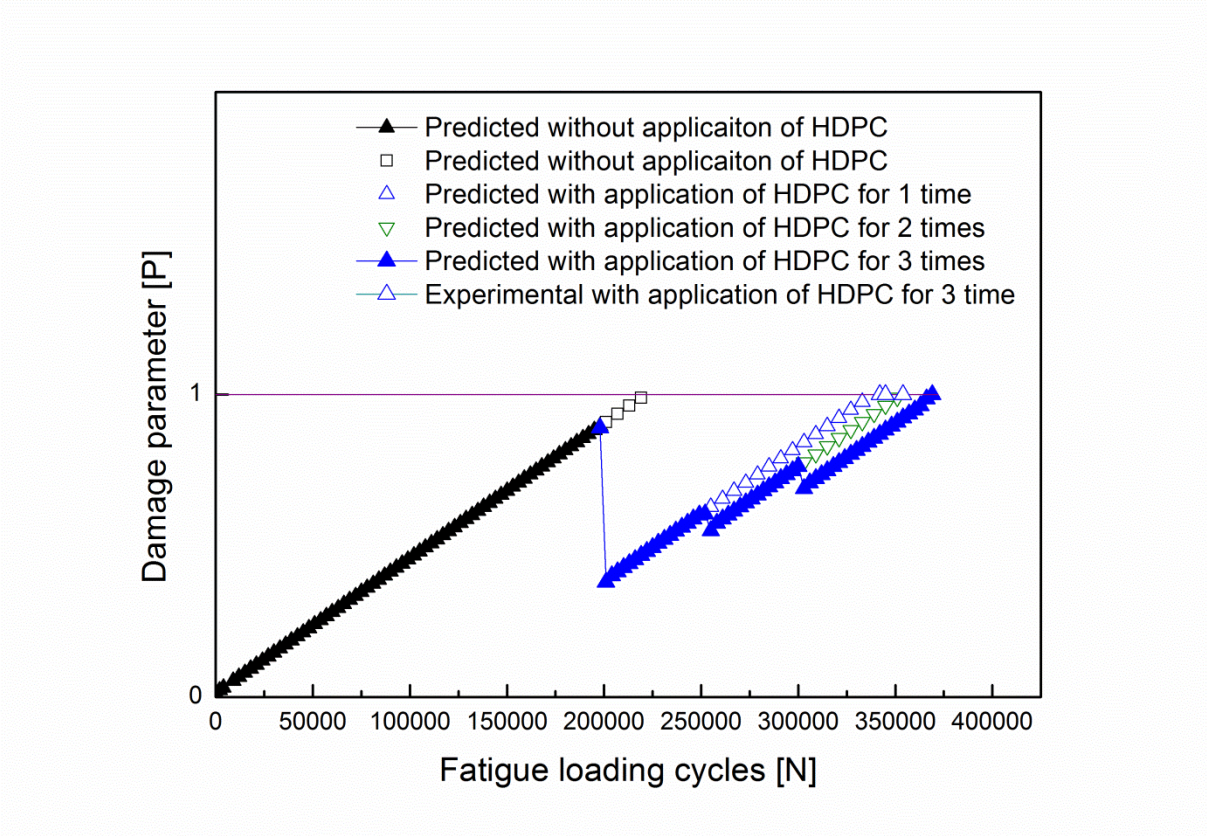

Fig. 5-3 Calculated damage parameter *vs* fatigue loading cycle under the conditions with multi and without the multi-application of HDPC.

Similar as that described in section 5.3. The relationship between the damage parameter and fatigue loading cycle after the application of HDPC at 2.5×10^5 cycles and 3.0×10^5 cycles can be evaluated. Consequently, the total number of cycles to reach the crack initiation was predicted to be 3.74×10^5 cycles. After the three times application of HDPC，it was found that multi-application of HDPC can further improve the delaying fatigue crack initiation, although the delaying effects of the second and third times are small comparing with the first time application of HDPC.

As described in section 4.2, the healing effect on the dislocation depends on the dislocation density. Hence, one reason for the decreased delaying effect at the second time of HDPC application was due to the low dislocation density. On the other hand, according the analysis in the section 4.4.2, it was found that partial dislocation was easy to be recovered, but the remained dislocation was difficult to be recovered. After the first time application of HDPC, with the recovery of dislocation, the remained dislocation was difficult to be recovered in the second time application of HDPC. Only partial new generated dislocation can be recovered. Therefore, the delaying effects of the second and third time applications are small comparing with the first time application of HDPC.

5.5 Analysis of the relationship between the reversed dislocation density and the delaying crack initiation

In Tanaka and Mura model on the fatigue crack initiation, the reversibility of dislocations was discussed [44]. They proposed the reverse of dislocation during the unloaded. The retardation of crack initiation affected by the reverse process of dislocation in inert environments and at low temperatures has been demonstrated by Sriram et al. [45] and Kwon et al. [46], respectively. The increased reverse of dislocation has been proved to extend the number of cycles for fatigue crack initiation.

Upon unloading, the total strain energy of dislocation is minimized in the system.

Hence, dislocations with opposite signs are activated to reverse slip on an adjacent plane. Annihilation also occurs when two dislocations of opposite sign from different dislocation pairs approach each other. The movement and annihilation of dislocations is an important mechanism of recovery. The annihilation of dislocations reduced the dislocation density. When electric current was applied upon unloading, the electric current can exert a drag on dislocations as the electrons collide with atoms. Therefore the electron wind force is one of the important reasons for the improved reverse of dislocation. In this study, the retardation of crack initiation affected by the reverse process of dislocation in inert environments and at low temperatures was demonstrated. The increased reverse of dislocation has been proved to extend the number of cycles for crack initiation. On the basis of experimental results, the reverse of dislocation leads to uniform distribution and low density of dislocations. After the application of HDPC, dislocation density was decreased due to the annihilation of dislocation dipoles.

5.6 Summary

The relationship between the delaying fatigue crack initiation and the decrease of dislocation density due to the application of HDPC has been established. According to the comparison of the model calculation and experimental data, the delaying fatigue crack initiation can be predicted by the decrease of dislocation density due to the application of HDPC. Furthermore, the delaying fatigue crack initiation was due to

the improved the reverse of dislocation.

References:

[1] C. Gaudin, X. Feaugas, Cyclic creep process in AISI 316L stainless steel in terms of dislocation patterns and internal stresses, Acta Mater., 52 (2004) 3097-3110.

[2] O.B. Pedersen, Overview No. 89 Mechanism maps for cyclic plasticity and fatigue of single phase materials, Acta Mater., 38 (1990) 1221-1239.

[3] X. Feaugas, On the origin of the tensile flow stress in the stainless steel AISI 316L at 300 K: back stress and effective stress, Acta Mater., 47 (1999) 3617-3632.

[4] M.D. Sangid, H.J. Maier, H. Sehitoglu, A physically based fatigue model for prediction of crack initiation from persistent slip bands in polycrystals, Acta Mater., 59 (2011) 328-341.

[5] V. Ya. Kravchenko, Effect of directed electron beam on moving dislocations, Soviet Phys. Jetp., 24 (1967) 1135-1142.

[6] K. Tanaka, T. Mura, A dislocation model for fatigue crack initiation, J. Appl. Mech., 48 (1981) 97-102.

[7] K. Tanaka, T. Mura, A theory of fatigue crack initiation at inclusions, Metall. Trans., 13 (1982) 117-123.

[8] K. Tanaka, T. Mura, A micromechanical theory of crack initiation from notches, Mech. Mater., 1 (1981) 63-73.

[9] G. Venkataraan, Y. W. Chung, T. Mura, Application of minimum energy formalism

in a multiple slip band model for fatigue crack nucleation and derivation of a generalized Coffin-Manson law, Acta Metall. Mater., 39 (1991) 2621-2629.

[10] M.R. Lin, M.E. Fine, T. Mura, Fatigue crack initiation on slip bands: theory and experiment, Acta Metall., 34 (1986) 619-628.

[11] G. Venkataraman, Y.W. Chung, Y. Nakasone, T. Mura, Free energy formulation of fatigue crack initiation along persistent slip bands: calculation of S-N curves and crack depths, Acta Metall. Mater., 38 (1990) 31-40.

[12] T. Mura, Y. Nakasone, A theory of fatigue crack initiation in solids, J. Appl. Mech., 57 (1990) 1-6.

[13] T. Mura, A theory of fatigue crack initiation, Mater. Sci. Eng. A, 176 (1994) 61-70.

[14] C. Ihara, T. Tanaka, A stochastic damage accumulation model for crack initiation in high-cycle fatigue, Fatigue Fract. Eng. Mater. Struct., 23 (2000) 375-380.

[15] M.R. Mitchell, Fundamentals of modern fatigue analysis for design in Fatigue and Microstructure, American Society for Metals, (1978).

[16] S.S. Manson, M.H. Hirschberg, An inter disciplinary approach, Syracuse University Press, (1964).

[17] L.F. Coffin, A study of the effects of cyclic thermal stresses on a ductile metal, trans. ASME, 76 (1954) 931-950.

[18] S. Brinckmann, On the role of dislocations in fatigue crack initiation, (1974).

[19] J. Kratochvil, Self-organization model of localization of cyclic strain into PSBs and the formation of dislocation wall structures, Mater. Sci. Eng. A, 309 (2001)

331-335.

[20] P. Neumann, Coarse slip model of fatigue, Acta Metall., 17 (1969) 1219-1225.

[21] N.F. Mott, A theory of the origin of fatigue cracks, Acta Metall., 6 (1958) 195-197.

[22] J.G. Antonopoulos, L.M. Brown, A.T. Winter, Vacancy dipoles in fatigued copper, Phil. Mag., 34 (1976) 549-563.

[23] U. Essmann, U. Gosele, H. Mughrabi, A model of extrusions and intrusions in fatigued metals-I. point-defect production and the growth of extrusions, Phil. Mag. A, 44 (1981) 405-426.

[24] E.A. Repetto, M. Ortiz, A micromechanical model of cyclic deformation and fatigue-crack nucleation on f.c.c. single crystals, Acta Mater., 45 (1997) 2577-2595.

[25] K. Differt, U. Essmann, H. Mughrabi, A model of extrusions and intrusions in fatigued metals - II. surface roughening by random irreversible slip, Phil. Mag. A, 54 (1986) 237-258.

[26] W. Bilby, Miller, Fundamentals of deformation and fracture, Eshelby Memorial Symposium, (1984).

[27] P. Neumann, Coarse slip model of fatigue, Acta Metall., 17 (1969) 1219-1225.

[28] E.W. Johnson, H.H. Johnson, Imperfection density of fatigued and annealed copper via electrical-resistivity measurements, Tran. Metal. Soci. AIME, 233 (1965) 1333-1339.

[29] O. Helgeland, Resistivity studies of defect concentrations resulting from cyclic

stressing of copper single crystals at room temperature, Tran. Metal. Soci. AIME, 239 (1967) 2001-2002.

[30] A.K. Eikum, I. Holwech, Recovery on copper after fatigue at 78K, Scripta Metall., 2 (1968) 605-610.

[31] J. Polak, The effect of intermediate annealing on the electrical resistivity and shear stress of fatigued copper, Scripta Metall., 4 (1970) 761-764.

[32] W. Kromp, B. Weiss, Electrical resistivity of copper after high frequency fatigue, Scripta Metall., 5 (1971) 499-504.

[33] W. Kromp, B. Weiss, Recovery of electrical resistivity of copper after high frequency fatigue, Scripta Metall., 5 (1971) 505-510.

[34] N. Thompson, N.J. Wadsworth, N. Louat, The origin of fatigue fracture in copper, Phil. Mag., 1 (1956) 113-126.

[35] S.S. Manson, ASTM, Philadelphia, (1971).

[36] M. Meshii, Fatigue and microstructure, American Society for Metals, (1978).

[37] L. Remy, C.J. Beevers, International conference on fatigue and fatigue Thresholds, Engineering Materials Advisory Services, (1984).

[38] A.S. Cheng, C. Laird, Fatigue life behavior of copper single crystals. Part II: Model for crack nucleation in persistent slip bands, Fatigue Fract. Eng. Mater. Struct., 4 (1981) 343-353.

[39] G. Venkataraan, Y.W. Chung, T. Mura, Application of minimum energy formalism in a multiple slip band model for fatigue crack nucleation and derivation of a generalized Coffin-Manson law, Acta Metall. Mater., 39 (1991)

2631-2638.

[40] A. Saxena, S.D. Antolovich, Low cycle fatigue, fatigue crack propagation and substructures in a series of polycrystalline Cu-Al alloys, Metall. Trans. A, 6 (1975) 1809-1828.

[41] K.S. Chan, Theorical analysis of grain size effects on tensible ductility, Scripta Metall. Mater., 32 (1994) 235-240.

[42] S.E. Harvey, P.G. Marsh, W.W. Gerberich, Atomic force microscopy and modeling of fatigue crack initiation in metals, Acta Metall. Mater., 42 (1994) 3493-3502.

[43] K.S. Chan, A microstructure based fatigue crack initiation model, Metall. Mater. Trans., 34 (2003) 43-58.

[44] T. Mura, Y. Nakasone, A theory of fatigue crack initiation in solids, J. App. Mech., 57 (1990) 1-6.

[45] T.S. Sriram, M.E. Fine, Y.W. Chung, STM and surface analytical study of the effect of environment on fatigue crack initiation in silver single crystals I: Surface chemical effects, Scripta metall., 24 (1990) 279-284.

[46] G. Venkataraman, Y.W. Chung, Y. Nakasone, T. Mura, Free energy formulation of fatigue crack initiation along persistent slip bands: calculation of S-N curves and crack depths, Acta Metall. Mater., 38 (1990) 31-40.

Chapter 6 Conclusions

The improvement of long-term durability and reliability of material is a critical issue to extend the safe service-life of metal material. This dissertation aims to establish an effective method to delay the fatigue failure. In this study, the application of high-density pulse current was carried out to delay the fatigue crack initiation by the restoration of the fatigue damage.

The fatigue crack initiation was delayed successfully by the application of HDPC. The delaying effect was different depending on the timing of the application of HDPC. The reason of the delaying fatigue crack initiation was due to the restoration of fatigue damage.

To clarify the effect of HDPC on the healing of fatigue damage, the residual strain and microhardness at the root of the notch tip were evaluated. On the surface of specimen, the locally disappear of slip bands and the decrease of the height of slip bands were found. The interfaces between the PSBs and the matrix serve as preferential sites for fatigue crack initiation. The locally vanishing of the slip bands can decrease of the possibility of the fatigue crack initiation. It is the important reason for the delaying effect on fatigue crack initiation. In addition, it was found that the residual strain was recovered after the application of HDPC. The strain hardening was also recovered. The recovery of residual strain and strain hardening represent the

decrease of the fatigue damage. The recovery of residual strain has an effect on the temporary retardation of fatigue crack initiation. Moreover, it is thought that the stress concentration factor will also affect the delaying effect of crack initiation and the lower K_t may have a high delaying effect. Meanwhile, for specimens with different thicknesses, it may possible to realize the delaying crack initiation by application of HDPC with different electric current density.

In the microstructure, the recovery of dislocation due to the effect of HDPC was observed to elucidate the mechanism of healing effect on fatigue damage. After the application of HDPC, the dislocation pile-ups disappeared and the dislocation density decreased. The motion and annihilation of dislocations is an important mechanism of damage recovery. It was analyzed that the decrease of dislocation density was due to the dislocation annihilation. When the high-density pulse current was applied upon unloading, the reverse motion of dislocation was improved due to the effect of electron wind force. In addition, the application of HDPC causes a high-rate heating. It is thought that joule heating is a side effect.

To establish the relation between the delaying fatigue crack initiation and the dislocation structure, a model of fatigue damage parameter is proposed based on the fatigue crack initiation model in which the accumulation of the dislocation density was considered. The proposed model was evaluated against experimental data. The predication of the delaying effect on the fatigue crack initiation can be carried out by the decrease of dislocation density caused by the application of HDPC. According to the physics of the fatigue crack initiation, the delaying fatigue crack initiation is due

to the improved reverse of dislocation. Moreover, it was found that multi-application of HDPC can further improve the delaying fatigue crack initiation.

Acknowledgments

I would like to express my sincerely gratitude to my supervisor, Professor Yang Ju, for giving me an opportunity to study in Ju laboratory. I had a great time being in his group. Thank him for his supervision and his insight in science. Also, thank him for sharing his non-science-related ideas. Thank him for having an open ear for all problems of my life. Specially, thank him for confidence and trust and his encouragement. His invaluable support and care made it is possible to complete this study.

I want to thank deeply Professor Nobutada Ohno for his irreplaceable suggestions on this thesis and his incomparable kindness in Pusan during the APCFS-MM2012. Sincerely thank Professor Tetsuya Tagawa for his invaluable help to prepare this thesis.

I am also grateful to Associate Professor Yasuyuki Morita for the valuable suggestions and enjoyable discussions on the application of Digital Image Correlation method. Furthermore, thank him for his kind encouragement.

I further extend my appreciations to Assistant Professor Atsushi Hosoi for his help. As the expert on the fatigue strength of material, he gives me many valuable suggestions on the study of fatigue fracture.

Here, I must thanks to Technical assistant Dr. Teruaki Mikuriya and Mr. Kiyoshi Minagawa. They help me to prepare the specimen for the fatigue test and TEM

samples. Their good work supplies to prepare me the precise specimen with wire cutting in time.

Thanks all members of the fatigue group of Ju Lab. for the support. The cultural diversity of the group always gave refreshing support. Special thanks to: the graduated students Mr. Takatane Nagahama who teach me the basic experimental method on the fatigue test; Mr. TakahiroYano who help finish the fatigue test in Japan Fine Ceramics Center (JFCC); Tomoya Kishi and the graduate student Mr. Yuichi Iwase, Mr. Yukiyasu Asaoka who teach me Japanese, discuss the life and friendship.

Many thanks also to all my friends and colleagues who made my life so full and happy by their warm friendship and understanding during those past years. They always give me the confidence and encouragement.

I also gratefully acknowledge that the scholarship provided by National construction high level university government-sponsored graduate student project China supported my study in Japan.

My special thanks to my parents for their loving support and encouragement. Furthermore, I want to thank my wife Qing Wang for her support all the time.

Finally, I will thanks to all of you who have contributed to this study.

Yongpeng Tang

Nagoya University

September, 2013